Dissertation

submitted to the
Combined Faculties for the Natural Sciences and for Mathematics of the Ruperto-Carola University of Heidelberg, Germany

for the degree of
Doctor of Natural Sciences

Presented by
Dipl.-Ing. Biotechnologie Dorothee Alatorre
Born in Offenburg

Oral examination:

Analysis of *Cis*-acting Replication Elements in Enteroviruses: The Multi-Functional Roles of the Cloverleaf Structure and the *cre*(2C) RNA.

Referees: **Prof. Dr. Hans-Georg Kräusslich**
Prof. Dr. Ralf Bartenschlager

Für meine Großmutter

Anna Pfrang

Acknowledgments

I am very excited to finally write this page to express my gratitude to the people who contributed in many different ways to the accomplishment of this thesis, and without them this work would not have been possible.

The work for this thesis was carried out at Raul Andino's laboratory at UCSF, San Francisco, USA. I am extremely grateful to Raul for giving me the opportunity to pursue my PhD under his supervision and introducing me to virology and the subtleties of RNA replication. Raul is a wonderful scientist who never gets tired of sharing his endless ideas and enthusiasm. He was always willing to discuss experiments but gave me enough independence to mature as a scientist.

Many thanks go to Prof. Kräusslich who supported my work in Raul's lab, and thus made this work possible. My thanks also go to Prof. Bartenschlager who immediately agreed to be second referee.

The beginning of my work started with a four weeks crash course in poliovirus replication by Jens Herold. It is hard to believe how much I learned from him in such a short period of time. Jens is a great and inspiring scientist who made a long lasting impression.

Thanks to all members in the Andino Lab, past and present, who make this lab a wonderful place to do science. I really feel honored that I worked side by side with them: Liz, who established the tea-times in the lab and always had an open ear to talk. Chanti, the Super-Swede, who is the friendliest person on earth. I really missed the "old" replication crew when you left. Ronald, who doesn't say a lot but has a lot to say. Dwight, who makes every place a happier place and is always willing to help with anything. Arabinda, with whom I finally had someone to talk "*cre*" with. Thanks for all your help with the 2C work. Marco, the great virologist from whom I learned so much, and who brings so much fun to the lab with his unique personality. Thank you also for the critical reading of my thesis. Armin, who taught me that patience with experiments can greatly increase the beauty of the results. He loves taking on technical challenges and is always willing to help. Thanks also for all your help with the "Zusammenfassung"! Many thanks go to Leonid for all his help in the lab and for being a wonderful friend. Our late night talks often kept me going especially when things didn't work. And then there is Carla, a wonderful scientist and friend. Working in the lab will never be the same without you around, but I am glad to have found a friend for life in you! Then there is the "new crew": Thanks to Adam for proof reading my thesis, and Michelle who always makes time for a quick chat. Amethyst and Cecily, I wish you both a successful and interesting PhD time.

Many thanks go to JJ Miranda for all his help with the protein work, for proof reading my thesis and for being a friend. Thanks for your "Just do it" mentality", which really helped me in the end to get to the finish line.

Ich möchte mich gerne bei meiner ganzen Familie bedanken, die mich immer in allem unterstützt hat. Vor allem bei meiner Patin, Evmarie, die mir gezeigt hat, wie wichtig es ist, als unabhängige Frau im Leben zu stehen, und bei meinem Bruder, Steffen, der mich von klein auf immer zu neuen Herausforderungen angespornt hat.

Ich widme diese Arbeit meiner Oma, Anna Pfrang, die viele Jahre vor mir wusste, dass ich eines Tages promovieren werde. Leider kann sie dies nicht mehr selbst miterleben.

Mein ganz besonderer Dank geht an meine Eltern, für alle ihre Liebe und Unterstützung. Ihr habt mir die Augen zu so vielen Möglichkeiten im Leben geöffnet und mich immer dazu ermutigt, meinen eigenen Weg zu gehen und meine eigenen Ziele zu verfolgen, und habt somit die Grundlage zu meinem Erfolg im Leben gelegt. Vielen Dank!

Last but not least, I would like to thank my husband, Eric, for all his love, support, patience, and belief in me! I could not have asked for a better partner in life! My PhD time will be forever linked with the time when we started our life together.

Contributions

The work described in part 4.2 of this thesis was conducted in collaboration with the group of Willem Melchers in Nijmegen, the Netherlands. The contributions are as follows: Mark van Ooij carried out the MFOLD predictions of the *cre*(2C) element, the cloning of all coxsackievirus constructs, the *in vitro* VPg-uridylylation assays and the transfections into BGM cells. All other work was performed by Dorothee Alatorre.

Table of Contents

Abstract

Enteroviruses, such as polio- and coxsackievirus, are positive-stranded RNA viruses, and belong to the family of Picornaviruses. Positive-stranded RNA viruses follow a common mechanism to replicate their RNA genomes. First, the viral genome is transcribed into a minus-strand intermediate, which then acts as a template for the synthesis of new plus-strands. The same viral RNA-dependent RNA polymerase synthesizes both RNA strands using viral and host factors to initiate synthesis. Enteroviruses make very efficient use of their small genomes. Several *cis*-acting replication elements can be found throughout their genome, including one within the coding region. Most of these elements consist of RNA regions, which fold into secondary structures that can form complexes with viral and cellular proteins. Such complex formations are often required to initiate a new step in replication, and thus, function as key players in regulation of the viral life cycle. Some of the *cis*-acting replication elements have overlapping functions and play a role in several steps in RNA synthesis.

In this thesis, two *cis*-acting replication elements in enteroviruses were analyzed for their roles in RNA synthesis: the cloverleaf structure in poliovirus and the *cre*(2C) hairpin RNA in coxsackievirus B3 (CVB3).

A cloverleaf-like RNA structure formed at the 5'-end of the poliovirus plus-strand is required for negative-strand RNA synthesis but has also been implicated in positive-strand RNA synthesis. Analyzing the precise role of the cloverleaf RNA element in positive-strand RNA synthesis has been hindered by its role in negative-strand synthesis, as mutations disrupting the structure and/or functions on the cloverleaf disrupt minus-strand RNA synthesis. To overcome this limitation, we have developed a novel approach to analyze *cis*-acting elements with multiple roles in virus replication. Poliovirus replicons were engineered to contain two tandem cloverleaf structures to separate multiple functions. Thus, a downstream cloverleaf, which only supports minus-strand RNA synthesis, allowed the genetic analysis of a 5'-terminal cloverleaf dedicated to promote plus-strand RNA synthesis. Our results reveal that the cloverleaf structure in the plus-strand functions as a promoter for both positive- and negative-strand RNA synthesis. We could show that *stem a* sequences within the cloverleaf structure are essential for plus-strand RNA synthesis. Also required to initiate plus-strand RNA synthesis are the binding sites for the viral polymerase precursor 3CD and the host factor PCBP2 located within the cloverleaf structure. Furthermore, in a functional assay we could demonstrate that the viral 2C protein is directly involved in plus-strand RNA synthesis. Based on our results, we propose a new model for the initiation of positive-strand RNA synthesis in poliovirus.

In the second part of this thesis, the *cre*(2C) RNA of coxsackievirus B3 and its role in RNA replication was analyzed. A stem-loop element located within the 2C coding region of CVB3 has been proposed to function as a *cis*-acting replication element. The MFOLD program was used to predict the structure and the precise location of the *cre*(2C) hairpin. Characterization of the *cre*(2C) loop showed that a proposed entero- and rhinoviral consensus sequence is also applicable to the CVB3 *cre*(2C) loop sequence, and that the *cre*(2C) element functions as a template for VPg-uridylylation *in vitro*. Even though previous studies of the *cre(*2C) in poliovirus have shown that the *cre* RNA is not required for initiation of negative-strand RNA synthesis, we were able to demonstrate that the CVB3 *cre*(2C) is required for the imitation of both, negative- and positive-strand RNA synthesis.

Zusammenfassung

Enteroviren, wie zum Beispiel Polio- und Coxsackieviren, sind positivsträngige RNA-Viren und gehören zur Familie der Picornaviren. Positivsträngige RNA-Viren replizieren ihre Genome auf sehr ähnliche Art und Weise, indem das Virusgenom zunächst in einen Minusstrang umgeschrieben wird, welcher im nächsten Schritt als Vorlage zur Synthese von neuen Plussträngen dient. Dieselbe virale RNA-abhängige RNA Polymerase synthetisiert, unter Mithilfe von viralen und Wirtsproteinen bei der Initiierung der Synthese, beide RNA-Stränge. Im Genom von Enteroviren finden sich mehrere *cis*-aktive Replikationselemente, von denen sogar eines innerhalb des kodierenden Bereichs liegt. Die meisten solcher Elemente bestehen aus RNA-Bereichen, die sich in Sekundärstrukturen falten und dann Komplexe mit viralen und zellulären Proteinen eingehen können. Solche Komplexformationen sind häufig Vorraussetzung zur Initiierung eines neuen Replikationsschrittes und stellen daher Schlüsselereignisse in der Regulation des Lebenszyklus der Viren dar. Einige der *cis*-aktiven Replikationselemente haben mehrere überlappende Funktionen und spielen eine Rolle in mehreren Schritten der RNA-Synthese. In der vorliegenden Dissertation wurden zwei *cis*-aktive Replikationselemente von Enteroviren auf ihre Rolle in der RNA-Synthese analysiert: die Kleeblatt-Struktur in Poliovirus und die *cre*(2C) Haarnadelstruktur in Coxsackievirus B3 (CVB3).

Eine Kleeblatt-ähnliche Sekundärstruktur am 5'-Ende des Positivstrangs von Poliovirus ist essentiell für die Negativstrangsynthese, wurde aber auch mit der Positivstrangsynthese in Verbindung gebracht. Die Analyse der präzisen Rolle der Kleeblatt RNA-Struktur in der Positivstrangsynthese wurde bisher durch ihre Rolle in der Negativstrangsynthese behindert, da Mutationen, die die Struktur und/oder die Funktion der Kleeblatt-Struktur zerstören, die Negativstrangsynthese behindern. Um diese Einschränkung zu umgehen, haben wir ein neues System entwickelt, das die Analyse *cis*-aktiver Elemente mit mehreren Rollen in der Virusreplikation erlaubt. Poliovirus-Replikons mit zwei direkt aufeinander folgenden Kleeblatt-Strukturen ermöglichten die genetische Analyse der 5'-terminalen Kleeblatt-Struktur, die die Positivstrangsynthese unterstützt, während die nachgeschaltete Kleeblatt-Struktur nur für die Negativstrangsynthese zur Verfügung stand. Unsere Ergebnisse zeigen, dass die Kleeblatt-Struktur im Positivstrang als Promoter sowohl für die Negativ- als auch die Positivstrangsynthese dient. Die Sequenzen des *Stem a* der Kleeblatt-Struktur waren für die Positivstrangsynthese unentbehrlich. Zwei weitere Bindungsstellen innerhalb der Kleeblatt-Struktur, für 3CD, die Proteinvorstufe der viralen Polymerase, und das Wirtsprotein, PCBP, sind ebenfalls für die Positivstrangsynthese erforderlich. Auβerdem konnten wir nachweisen, dass das virale Protein 2C direkt an der Positivstrangsynthese beteiligt ist. Basierend auf unseren Ergebnissen stellen wir ein neues Modell für die Initiierung der Positivstrangsynthese in Poliovirus vor.

Im zweiten Teil dieser Dissertation wurde die Rolle der *cre*(2C) RNA in der RNA-Replikation von Coxsackievirus B3 untersucht. Eine Haarnadelstruktur innerhalb des 2C Kodierungsbereichs von CVB3 wurde als *cis*-aktives Replikationselement vorhergesagt. Mit Hilfe von MFOLD wurden die Struktur und die präzise Lage der *cre*(2C) Haarnadelstruktur berechnet. Die Charakterisierung der Schleifensequenzen von *cre*(2C) zeigte, dass eine vorhergesagte Entero- und Rhinovirus Konsensussequenz auch auf das CVB3 *cre*(2C) zutrifft, und dass das *cre*(2C) als Kopiervorlage zur VPg-Uridylylierung *in vitro* dient. Im Gegensatz zu früheren Untersuchungen, die gezeigt haben, dass das Poliovirus *cre*(2C) nicht an der Negativstrangsynthese beteiligt ist, konnten wir nachweisen, dass das CVB3 *cre*(2C) sowohl für die Initiierung der Negativ- als auch der Positivstrangsynthese notwendig ist.

Abbreviations

aa	amino acid
ATP	adenosine triphosphate
CTP	cytidine triphosphate
cDNA	complementary desoxyribonucleic acid
cpm	counts per minute
DNA	desoxyribonucleic acid
dNTP	deoxyribonucleotides
DTT	dithiothreitol
EDTA	ethylene diamine tetraacetic acid
EGTA	ethylene glycol tetraacetic acid
ER	endoplasmic reticulum
FPLC	fast protein liquid chromatography
GTP	guanosine triphosphate
HEPES	N-2-hydroxyethylpiperazine-N'-2-ethanesulfonic acid
hnRNP	heterogeneous nuclear ribonucleoprotein
Ig	immunoglobulin
IPTG	Isopropyl β-D-1-thiogalactopyranoside
kb	kilobase
kDa	kilo Dalton
min	minute
mRNA	messenger RNA
nt	nucleotide
NTP	ribonucleotides
PAGE	polyacrylamide gel electrophorese
PCR	polymerase chain reaction
RNA	ribonucleic acid
RNP	ribonucleoprotein
rRNA	ribosomal ribonucleic acid
SDS	sodium dodecyl sulphate
tRNA	transfer ribonucleic acid
UMP	uridine monophosphate
UTP	uridine triphosphate

1. Introduction

1. Introduction

Since the first discovery of poliovirus as the causative agent of paralytic poliomyelitis in 1909 by Landsteiner & Popper (Landsteiner, 1909), the studies to understand the life cycle and pathogenesis of this virus have ultimately led to a new field of science called “Molecular Virology”. The revolutionary development of new genetic techniques paved the way for numerous viral research milestones achieved by polio- and picornavirologists during the last 50 years. The *Picornaviridae* family includes many animal and human pathogens such as rhinovirus, the most important cause of the common cold; foot-and-mouth disease virus, an important agricultural pathogen; hepatitis A virus, which causes acute liver infections; and enteroviruses such as poliovirus or coxsackie A and B virus, which have been associated with a variety of clinical manifestations. Research on picornaviruses has had an impact on virology and even biology in general. Such research highlights include growth of these viruses in cell culture (Colter et al., 1957; Alexander et al., 1958), the development of inactivated and attenuated vaccines (Salk, 1953c, a, b; Sabin et al., 1954; Sabin, 1955a, b), the discovery of receptor families (Holland & McLaren, 1959), the demonstration of the first RNA-dependent RNA polymerase activity of an animal virus (Franklin & Baltimore, 1962; Baltimore et al., 1963), polyproteins as precursors for viral polypeptides and their proteolytic cleavage (Jacobson & Baltimore, 1968; Summers & Maizel, 1968), the first full sequence analysis of a virus (Kitamura et al., 1981; Racaniello & Baltimore, 1981b), demonstration that a cDNA copy produced virus progeny after transfection into cells (Racaniello & Baltimore, 1981a), the first resolution of the three-dimensional structures of animal viruses at the atomic level (Hogle et al., 1985), the discovery of internal ribosomal entry sites (IRES) to initiate translation in a cap-independent mechanism (Jang et al., 1988; Pelletier & Sonenberg, 1988), and the production of infectious virus in cell-free extracts programmed with purified viral RNA (Molla et al., 1991). However, the precise details of molecular events of picornavirus replication, such as virion uncoating, translation initiation, viral RNA replication, virus assembly, and virus-host interactions remain to be elucidated.

Poliovirus in particular has proven a good model system that has helped to shed light on mechanisms of the viral life cycle common not only to picornaviruses, but to many positive-strand RNA viruses. The eradication of poliovirus as an agent of human

disease is just around the corner. Nevertheless, with human picornaviruses alone causing an estimated 6 billion infections per year, continued detailed research remains critical to learn as much as possible about the life cycles of these viruses.

1.1 Vaccines

Fifty years ago, polio was endemic throughout the world (Paul, 1971). In 2001, the total number of polio cases worldwide was estimated to be <1000 (World Health Organization, 2002). The widespread immunization with both the inactivated (IPV) and the oral attenuated live (OPV) poliovirus vaccine has made this near eradication success possible (Plotkin, 1999; Sutter, 1999). There are three serotypes of poliovirus (type 1, 2, and 3) that are defined by their gross serological properties and the cross protection induced, such that infection with one type does not give solid protection against the other two (Rueckert, 1997). The main site of replication of poliovirus is in the intestine, and transmission of infection is normally by the fecal-oral route. Disease occurs when the virus escapes its normal intestinal replication site and infects the central nervous system (Bodian, 1955, 1958). Both the IPV and OPV vaccines induce protection through a strong serotype specific humoral neutralizing antibody response and immunity is thought to persist for life. Several studies suggest that immunization protects from disease rather than reinfection by the virus (Modlin, 1995). Using the OPV for immunization provides advantages in ease of administration by oral route, lower costs in production and administration, and the ability to induce intestinal immunity that is capable of effectively blocking person-to-person transmission of wild-type poliovirus in an immune population. The OPV also results in shedding of the attenuated vaccine strains by vaccinees, with the potential advantage of conferring herd immunity. However, this shedding carries the risk of propagating acquired mutations (revertants, for example) in the transmitted vaccine strains, which can result in increased pathogenesis and a neurovirulent phenotype. The calculated risk for contracting paralytic poliomyelitis from an OPV infection is 1 in 2.5 million individuals, with the risk increasing in immunocompromised persons (Modlin, 1995). Unlike the live OPV strains, the IPV consists of a formalin-killed preparation of wild-type viruses (Plotkin, 1999). This provides the advantage of being non-replicative, and thus unable to revert to a neurovirulent phenotype. The efficacy rate of IPV is similar to that of OPV. The disadvantages of IPV are that it does not induce intestinal immunity, and since

there is no shedding of live viruses it does not lead to herd immunity. However, with the eradication efforts closing in on their goal, IPV will be the vaccine of choice for the future to avoid circulation of new potentially neurovirulent polioviruses.

Table 1: Current classification of *Picornaviridae* (Stanway, 2002)

Genus	Species
Enterovirus	*Poliovirus*
	Human enterovirus A (HEV-A)
	Human enterovirus B (HEV-B)
	Human enterovirus C (HEV-C)
	Human enterovirus D (HEV-D)
	Bovine enterovirus (BEV)
	Porcine enterovirus A (PEV-A)
	Porcine enterovirus B (PEV-B)
Rhinovirus	*Human rhinovirus A* (HRV-A)
	Human rhinovirus B (HRV-B)
Cardiovirus	*Encephalomyocarditis virus* (EMCV)
	Theilovirus (ThV)
Aphtovirus	*Foot-and-mouth disease virus* (FMDV)
	Equine rhinitis A virus
Hepatovirus	*Hepatitis A virus*
	Avian encephalomyelitis-like virus (AEV)
Parechovirus	*Human parechovirus* (HPeV)
Erbovirus	*Equine rhinitis B virus* (ERBV)
Kobuvirus	*Aichi virus* (AiV)
Teschovirus	*Porcine teschovirus* (PTV)

1.2 Genetics of poliovirus

1.21 Classification

The viral family *Picornaviridae* was originally divided into four genera. This classification was based on shared pathogenic properties in humans and animals, and biophysical properties such as density, sedimentation coefficient, virion weight, absence of lipid envelope, ether resistance and stability over a certain pH-range (Melnick et al., 1974). The fast accumulation of new information such as a large amount of sequence data, structural analysis and receptor identification called for a

new classification of this virus family. Classification is now based on phylogenetic properties that more accurately reflect evolutionary history and the details of the virus replication mechanisms (Stanway, 2002). Traditionally, picornaviruses have been defined in terms of serotypes, grouped into genera. Recently, a radical change has been introduced: the concept of picornavirus species, generally consisting of several serotypes (King, 2000). To date, the *Picornaviridae* family is divided into nine genera with most of them consisting of several species (see table 1).

The conditions for a picornavirus to be classified as a species of the genus Enterovirus are the following (King, 2000):

- a 5'untranslated region (UTR) of a particular general form and function
- a 2A protein that is related to the chymotrypsin group of proteases
- no leader protein
- a 3'UTR containing at least two stem-loops that interact to form a tertiary structure

1.22 Genetic organization of poliovirus

Picornaviruses are positive-stranded RNA viruses, whose genome and mRNA are of the same polarity. Poliovirus genomic RNA and mRNA are identical molecules except that the viral protein, VPg, is absent from mRNA. Following infection and uncoating of the virus, VPg is removed by a cellular enzyme that cleaves the phosphodiester bond (Ambros et al., 1978; Ambros & Baltimore, 1980; Wimmer, 1982)

The poliovirus RNA genome is 7433 nucleotides long and includes a 5'UTR followed by a single open reading frame (ORF) of 6528 nt and a polyadenylated 3'UTR. The 5'-end of the genome is covalently linked to a viral peptide of 22 amino acids, VPg (Yogo & Wimmer, 1972; Flanegan et al., 1977; Lee et al., 1977; Racaniello & Baltimore, 1981b). The 5' UTR is 743 nt long and contains a high degree of secondary structure as predicted both by computer modeling and biochemical analysis. The ORF is translated into one polyprotein that is co-translationally processed by the virally encoded proteases 2A, 3CD and 3C into several precursors and 12 final peptides (Kräusslich & Wimmer, 1988). An overview of the genomic organization and protein processing is shown in Figure 1.1. The N-terminal portion of the polyprotein (P1 region) encodes the structural proteins, none of which are required for genomic replication. The P2 and P3 regions encode the non-structural proteins required for replication. The

first cleavage event is mediated by the 2A protease and leads to the release of the P1 region from the rest of the polyprotein (Toyoda et al., 1986). The remaining cleavage events are mediated by the 3C or 3CD proteases (Hanecak et al., 1982; Hanecak et al., 1984). Picornaviruses make very efficient use of their small genomes in that protein precursors, in addition to fully processed, peptides have very distinct and often multiple functions within the virus life cycle.

.

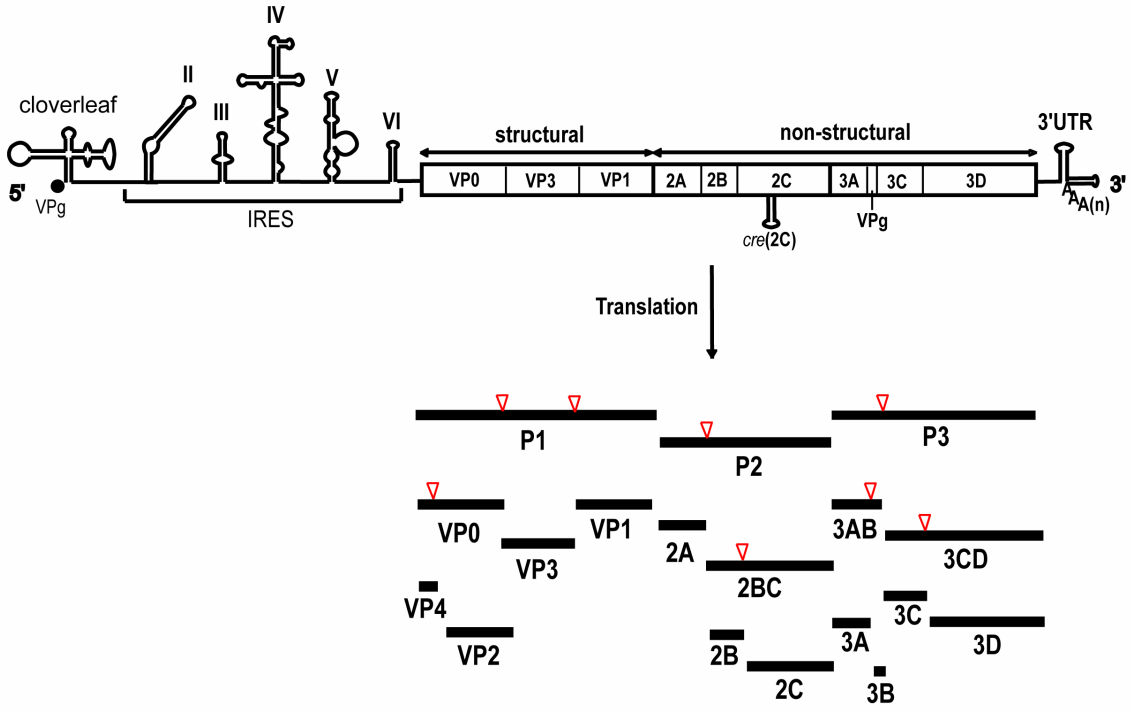

Figure 1.1: Structure of poliovirus genomic RNA and processing of the polyprotein. The single-stranded RNA of poliovirus is shown with the terminal protein VPg at its 5'-end and the 3'-UTR with the poly(A) tail at its 3'-end. The 5'UTR consists of the cloverleaf and the large IRES element. The location of the *cre*(2C) hairpin in the coding region of 2C is indicated. The polyprotein contains structural (P1) and non-structural (P2, P3) domains. The single ORF as well as the gene products are represented by open boxes. The final proteins that result after proteolytic cleavage by viral proteases are indicated; the cleavage sites are represented by red triangles.

1.3 Effects of poliovirus infection in the host cell

1.31 Host cell translation shutoff

Picornaviruses have developed subtle strategies to interfere with the host cell metabolism and to simultaneously promote the expression of their own genome. Infected cells lose the capability of synthesizing cellular proteins within 2 to 3 hours after infection, a phenomenon called “host cell shutoff”, while translation of viral proteins increases progressively (Sonenberg, 1990, 1996; Ehrenfeld, 1997). Poliovirus translation is initiated from an IRES located within the long 5’UTR region, whereas cellular mRNA translation occurs by a cap-dependent mechanism (Kitamura et al., 1981; Racaniello & Baltimore, 1981b). There is overwhelming evidence that the viral protein $2A^{pro}$ mediates cleavage of the translation initiation factor eIF4GI (formerly known as p220, then called eIF4G before being renamed eIF4GI) (Kräusslich et al., 1987; Lloyd et al., 1988; Sun & Baltimore, 1989; Davies et al., 1991; Aldabe et al., 1995). eIF4GI constitutes an ideal target, as it acts as a central scaffold in the assembly of a complex between the capped mRNA and the ribosome during initiation of cap-dependent protein synthesis. The interaction of these various players results in the circularization of the functional mRNA in the state of translation and reinitiation (Michel et al., 2000). Thus, cleavage of eIF4GI leads to the inactivation of cap-dependent translation and consequently to the shutoff of cellular protein synthesis.

The cleavage of eIF4GI is the main, but not the only, strategy of the virus for the shutoff of host cell translation. During an infection in the presence of 2 mM guanidine hydrochloride (GuHCl), which inhibits replication, complete cleavage of eIF4GI is observed yet cap-dependent translation is blocked by only 40-50% (Leibowitz & Penman, 1971; Nielsen & McConkey, 1980). What is responsible for the inhibition of the other 50%? Several other cleavage events of cellular proteins are observed in such virus infections that are blocked by treatment with GuHCl. eIF4GII, a functional homologue of eIF4GI, is also cleaved during poliovirus infection, albeit at a slower rate than 4GI (Gradi et al., 1998). Another viral protease, $3C^{pro}$, is responsible for the cleavage of the TATA-binding protein (TBP) (Das & Dasgupta, 1993), the transcription factors CREP (cyclic AMP-responsive element-binding protein required for activation of cAMP-regulated genes) and Oct-I (octamer-binding protein that activates SnRNA transcription) (Yalamanchili et al., 1997b; Yalamanchili et al., 1997c), the poly(A)binding protein (PABP) (Joachims et al., 1999; Kuyumcu-Martinez et al., 2002),

and the microtubule-associated protein 4 (MAP-4) (Joachims et al., 1995). Similar events are promoted by the other viral protease $2A^{pro}$, which also cleaves TBP (Yalamanchili et al., 1997a) and PABP, (Joachims et al., 1999), in addition to both forms of eIF4G (Kräusslich et al., 1987; Gradi et al., 1998). With the exception of eIF4GI these cleavages all occur later in infection when the expression levels of $2A^{pro}$ and $3C^{pro}$ are higher. One study indicates that $3C^{pro}$ preferentially cleaves ribosome-associated PABP (Kuyumcu-Martinez et al., 2002). This would specifically target PABP, which is involved in the circularization of mRNAs, and therefore supporting translation and reinitiation of cellular protein synthesis. This cleavage event results in the cleavage of only 70% of cellular PABP. Recently, PABP was identified to play a role in poliovirus replication. Here, it is part of an RNA-protein-protein-RNA bridge that results in the circularization of the viral genome and leads to initiation of negative-strand RNA synthesis (Herold & Andino, 2001). This could explain why the virus might target only specific PABP, which is involved in cellular translation, and why cleavage is not 100% efficient. The rest of the PABP in the cell remains available to poliovirus to recruit into its replication complex. To which extent the individual cleavage events contribute to the host shutoff needs to be elucidated but in sum they could account for the complete shutoff of cellular protein synthesis during poliovirus infection.

1.32 Host cell transcription shutoff

Many viruses are known to shut off transcription and/or translation of host cell genes to increase expression of their own genes (Kaariainen & Ranki, 1984). Poliovirus first shuts off RNA Pol I-mediated transcription in the host cell at the early stage of infection, followed by Pol II- and Pol III-mediated transcription at the mid-stage of infection. This strategy is believed to increase the pool of free ribonucleotides that the poliovirus-encoded RNA-dependent-RNA polymerase (RdRP) uses to transcribe and replicate the viral genomic RNA.

RNA Pol I is responsible for transcription of a single class of genes, the rRNA genes. In humans, Pol I transcription requires the cooperative binding of UBF (upstream binding factor) and SL1 (species-specific factor) to the rRNA promoter (Learned et al., 1985; Learned et al., 1986). SL1 consists of TBP and three TBP-associated factors (TAFs). The viral protease $3C^{pro}$ targets SL1 by cleavage of one of the TAFs, which appears to

be the cause for inactivation of Pol I transcription (Rubinstein & Dasgupta, 1989; Rubinstein et al., 1992).

A crucial basal factor for Pol II transcription is TBP, which interacts with the TATA-box (Zawel & Reinberg, 1992). $3C^{pro}$ is responsible for cleavage of TBP, which in return is unable to form the TBP-TATA-box complex, and hence prevents further recruitment of transcription factors and Pol II (Clark et al., 1993). This inactivation of TBP seems to be the major cause of Pol II transcription shutoff (Yalamanchili et al., 1996). In addition, $3C^{pro}$ also cleaves three activator proteins that are involved in activator-dependent transcription mediated by Pol II: cleavage of CREP and Oct-1, resulting in altered binding of these factors to their target sequence, and cleavage of the tumor suppressor p53, seemingly affecting interaction of this factor to some cellular protein (Yalamanchili et al., 1997b; Yalamanchili et al., 1997c; Weidman et al., 2001). As a result, poliovirus infection inhibits both basal and activator-dependent transcription by Pol II promoters.

RNA Pol III transcribes a set of genes giving rise to small RNAs, including 5SRNA and tRNA (Segall et al., 1980). Pol III transcription requires binding of TFIIIC to the B-box internal promoter, and recruitment of TFIIIB and Pol III. During poliovirus infection, a subunit of TFIIIC is cleaved by $3C^{pro}$, affecting DNA-binding properties, and consequently leads to shutoff of Pol III transcription (Clark & Dasgupta, 1990; Clark et al., 1991; Shen et al., 1996).

1.33 Effects on cellular membrane metabolism and function

As is typical of cytolytic animal viruses, poliovirus infection leads to profound alterations in cellular membranes (Carrasco et al., 1989; Carrasco, 1995). Both morphology and functioning of cell membranes are modified upon infection. The events taking place can be divided into effects at early and at late stages of infection. During viral entry, early membrane permeabilization is directed to locate the virus genome in the cytoplasm (Carrasco, 1981; Belnap et al., 2000a). Later in infection, three types of changes are observed in cellular membranes: (i) proliferation of intracellular membranous vesicles, (ii) inhibition of vesicular trafficking with the consequent blockage of protein glycosylation, and (iii) enhanced membrane permeability that requires viral gene expression and involves the diffusion of ions and small molecules through the plasma membrane.

Electron microscopic study revealed the existence of a large number of membrane vesicles in the perinuclear region of poliovirus infected cells (Dales et al., 1965). These structures are apparent 3 h post infection and proliferate extensively, occupying almost all of the cytoplasm by 7 h post infection. Recent studies have shown that these vesicles have a double lipid bilayer, suggesting a double-budding mechanism or a wrapping of the cytosol by membranous compartments (Schlegel et al., 1996). Their origins are not completely clear. Markers from the ER, golgi apparatus and lysosomes were found (Bienz et al., 1994; Schlegel et al., 1996). High-resolution autoradiography indicated that viral RNA replication is associated with these vesicles (Bienz et al., 1983; Bienz et al., 1992; Troxler et al., 1992; Egger et al., 1996). Studies suggest that the viral proteins 2B, 2C and 3AB could mediate the association between the membranous vesicles and the replication complexes that consist of viral RNA, and viral and host proteins required for replication (Bienz et al., 1987; Johnson & Sarnow, 1991; Heinz & Vance, 1995).

In addition to these vesicles, a complete change in the morphology of poliovirus infected cells can be observed. This includes rearrangement of the intracellular membranous organelles of the secretory pathway, the disappearance of the Golgi complex, and a swelling of the ER together with the reorganization of the cytoskeletal framework (Lenk & Penman, 1979; Joachims & Etchison, 1992). This change is associated with the viral proteins 2B, 2BC and 3A, since they are able to block glycoprotein transport when they are expressed individually in mammalian cells (Doedens & Kirkegaard, 1995; Doedens et al., 1997; Sandoval & Carrasco, 1997). 3A blocks transport from the ER to the Golgi apparatus, whereas 2B and 2BC act on a later step in the secretory pathway. Several recent studies have elucidated the mechanism how 3A interferes with the secretory pathway (Belov et al., 2005; Wessels et al., 2006; Belov et al., 2007). 3A inhibits the activation of the GTPase ADP-ribosylation factor (ArfI), which regulates the recruitment of the COP-I coat complex to membranes. 3A specifically inhibits the function of GBFI (a guanidine nucleotide exchange factor (GEF)) for ArfI, by interacting with its N-terminus (Wessels et al., 2006). A study by Belov et al. has shown that the viral proteins 3A and 3CD independently recruit different Arf GEFs (GBFI and BIG1/2) to the new virus-induced membrane structures. The recruitment of these GEFs explain the sensitivity of virus growth to brefeldin A, which can be rescued by the overexpression of GBFI (Belov et al., 2005; Wessels et al., 2006; Belov et al., 2007). Inhibition of protein secretion might

help the virus evade the host immune response by interfering with secretion of interferon and other cytokines, and by blocking antigen presentation in the context of major histocompatibility complex class I molecules (Doedens & Kirkegaard, 1995).
Late membrane permeability alters the internal milieu and has important consequences for both cellular and viral macromolecular synthesis. This membrane damage is reflected in parameters such as intracellular change in monovalent cations, membrane potential, pH, divalent cations, and leak of metabolites and enzymes out of the cells and diffusion of low-molecular weight inhibitors into the cells (Carrasco, 2002). The viral proteins 2BC and 2B have been identified as major factors responsible for these changes at late time of infection (Doedens & Kirkegaard, 1995; Aldabe et al., 1996). All the cellular changes occurring at late stage of infection ultimately lead to cytopathic effect (CPE), and thus, cell lysis and release of new progeny (Carrasco, 2002).

1.4 Viral life cycle of poliovirus

For an overview of the life cycle of poliovirus see Figure 1.2.

1.41 Entry & uncoating

Picornaviruses use a variety of cell receptors for their entry into the host cell. Poliovirus recognizes CD155 (also called Pvr) on the cell surface. CD155 is a transmembrane glycoprotein with three extracellular Ig-like domains (Mendelsohn et al., 1989). Its cellular function is not well understood. With respects to poliovirus, several studies suggest that the first (N-terminal) Ig-like domain of Pvr is responsible for virus-binding and infection (Koike et al., 1991a; Selinka et al., 1991; Morrison & Racaniello, 1992; Selinka et al., 1992). Binding of the virion to the receptor triggers a conformational change in the virus which results in formation of the altered or A particle (Joklik & Darnell, 1961; Fenwick & Cooper, 1962). The A particle differs from the native particle in sedimentation (135S versus 160S for native) and antigenicity (De Sena & Mandel, 1977). The A particle is sensitive to proteases and highly hydrophobic, whereas the virion is soluble and stable to proteases (Fricks & Hogle, 1990). The next step is not well understood. It has been proposed that the N-terminus of VP1 and possibly the myristoyl group of VP4, which are external in the A particle but internal in the virion, may facilitate cell entry by disrupting the cell membrane or by forming a pore through which the RNA is extruded (Fricks & Hogle, 1990; Moscufo & Chow, 1992). Indeed, the change in VP1 leads to an increase in its hydrophobicity, and results in the ability of the

A particle to bind to liposomes which might direct the entry of the viral RNA (Fricks & Hogle, 1990). Following this interaction, a second altered form of the virus can be observed that has lost its RNA (80S), which is the empty A particle after the RNA is released into the cell (Ketterlinus & Wiegers, 1994). It has been shown that infection is not dependent on either low pH or clathrin-mediated endocytosis, and thus, supports the proposed models of RNA entry into the cell (Perez & Carrasco, 1993; DeTulleo & Kirchhausen, 1998).

Cell receptors are one of the most important determinants of tissue tropisms for viruses. Humans are the only natural hosts for poliovirus. The presence of the receptor is enough to confer susceptibility to infection in mice, effectively changing the host range of poliovirus (Selinka et al., 1992). However, studies of the expression of Pvr show that tissue tropism does not necessarily correlate with the receptor expression (Mendelsohn et al., 1989; Ren & Racaniello, 1992). This indicates that the cell receptor is not the only determinant of tissue tropism, and that other factors contribute to it.

1.42 Translation

After release of the viral VPg-linked RNA into the cell, VPg is removed by a cellular enzyme that cleaves the phosphodiester bond (Ambros et al., 1978; Ambros & Baltimore, 1980; Wimmer, 1982). Next, the viral RNA immediately functions as mRNA and is translated into the polyprotein. Early studies of poliovirus showed that cellular translation was shut-off during infection (see section 1.31). However, viral translation still occurred, suggesting that poliovirus mRNAs initiate translation by a unique and novel mechanism different from the known cap-dependent translation mechanism of cellular mRNAs. In 1981, with the complete sequence of poliovirus available, it was shown that the 5'-end of the viral genome was not capped and the 5'UTR was extremely long and highly structured (Kitamura et al., 1981; Pelletier & Sonenberg, 1988). The 5'UTR precedes the initiating AUG codon, and numerous AUG triplets in context apparently favorable for initiation were present, yet not utilized. The initiation of translation at a specific AUG in a cap-independent fashion uncovered the function of an IRES element, demonstrated for the first time for poliovirus and EMCV (Jang et al., 1988; Pelletier & Sonenberg, 1988). Since then, several other positive-strand RNA viruses, as well as a subset of cellular mRNAs, have also been shown to contain an IRES element (Martinez-Salas et al., 2001).

Three types of picornavirus IRES elements have now been defined, with enteroviruses containing type I (Wimmer et al., 1993). The three types of IRES elements differ by sequence and secondary structure, and their definition was based on sequence comparison and biochemical or enzymatic probing. Between members of the same IRES type, sequence identity is moderate; but predicted secondary structures are highly conserved. In poliovirus, the IRES element spans over a region of five stem-loop structures (II-VI) within the 5'UTR (Pilipenko et al., 1989; Skinner et al., 1989). The 3' boundary of the IRES is an AUG triplet which is not used for initiation. Rather, translation initiation occurs 150 nt downstream at the next AUG (Agol, 1991). Despite great differences in sequence and structure between the different IRES types, some sequence motifs that are key elements in translation initiation are conserved among all picornavirus IRES elements:

(i) the Yn-Xm-AUG motif, in which Yn is a pyrimidine-rich region (also called A box), Xm is a spacer of 15-25nt, and the AUG box (box B) marks the 3'-boundary of the IRES (Pilipenko et al., 1992a)

(ii) the GNRA tetraloop (N is any nt, and R is a purine) is present within the stem-loop IV of the type I IRES and has been shown to be important for IRES function (Kaminski et al., 1994; Lopez de Quinto & Martinez-Salas, 1997; Robertson et al., 1999). RNA tetraloops with GNRA consensus are often found within large RNAs with stable tertiary structures and are believed to mediate interactions between RNA that contain the motif and other RNA or protein targets

(iii) an A/C-rich sequence, which is present in stem-loop IV and V in type I IRES structures. The functional importance of this motif has been confirmed by mutational analysis (Nicholson et al., 1991; Lopez de Quinto & Martinez-Salas, 1997) and it has been suggested that the A/C-rich loop in domain V of the poliovirus IRES participates in the formation of a pseudoknot formation (Le et al., 1992).

Despite a vast amount of structural and mutational studies of IRES elements, the precise mechanism by which ribosomes are recruited to the RNA, and thus how translation is initiated in a cap-independent way, is still unknown. Cap-dependent translation is initiated by binding of eIF4E to the m^7G cap group at the 5'-end of the mRNA. This binding event triggers further recruitment of translation initiation factors, the initiator tRNA and the ribosomal unit to form a multicomponent complex, which subsequently initiates protein synthesis (Jackson, 2002). eIF4G functions as the key component in organizing all necessary components and as a scaffold for this complex.

The IRES element on the other hand, initiates translation internally and not through the cap group. It has been shown that a complete set of canonical initiation factors, except the cap binding-protein, is also required for poliovirus IRES-dependent translation (Scheper et al., 1992; Pause et al., 1994; Ohlmann et al., 1996; Pestova et al., 1996). Here, eIF4G is an essential player in anchoring the initiation complex to the RNA (De Gregorio et al., 1999). The ultimate goal of translation initiation is to direct the ribosomes to the mRNA. The most likely location for ribosome binding is at the 3'-end of the IRES element, but other parts of the IRES element structure could be also involved.

In addition to canonical translation factors, cellular proteins have been shown to play a role in IRES-mediated translation. The protein synthesis of poliovirus in rabbit reticulocyte lysate (RRL) is inefficient unless HeLa cell fractions are added (Dorner et al., 1984; Phillips & Emmert, 1986). The same was shown for translation in *Xenopus* oocytes where coinjection of HeLa cell cytoplasmic extract rescued translation efficiency, indicating the requirement of mammalian cellular factors for translation (Gamarnik & Andino, 1996). Proteins identified in participating in viral translation initiation include the pyrimidine tract binding protein (PTB, a nuclear protein presumably involved in RNA splicing) (Hunt & Jackson, 1999) and the La autoantigen (Meerovitch et al., 1993; Svitkin et al., 1994). These factors seem to stimulate viral protein synthesis in RRL. Binding of these proteins to the IRES might help in stabilizing the three-dimensional structure of the IRES; however, their precise role is not known.

Another cellular protein with a role in IRES-mediated translation in poliovirus is poly(rC) binding protein 2 (PCBP2; also known as hnRNP E or –αCP). PCBP2 is a cytoplasmic RNA-binding protein with three KH domains. Originally, it was found to bind to stem-loop IV of the IRES (Blyn et al., 1996). When HeLa cell extracts were depleted of PCBP2 by an affinity column procedure, the extract lost its capacity to support poliovirus translation, an effect which could be rescued by addition of recombinant PCBP2 (Gamarnik & Andino, 1997). However, the role of PCBP2 is more complex than just supporting translation. A molecular mechanism has been proposed that involves the cloverleaf structure (stem-loop I) of the poliovirus 5'UTR and describes the switch from translation to replication (Parsley et al., 1997; Gamarnik & Andino, 1998, 2000). PCBP2 binds two specific sites in poliovirus, the above mentioned stem-loop IV of the IRES structure and the cloverleaf structure. Translation generates the viral protein 3CD, which binds to the cloverleaf structure forming a complex that binds PCBP2 more

tightly, which down regulates translation and is required for initiation of viral RNA synthesis. Several mutations within the cloverleaf or deletion of the entire cloverleaf structure resulted in reduced translation levels, indicating a role of the cloverleaf structure in viral translation (Simoes & Sarnow, 1991; Gamarnik & Andino, 1998).

Finally, the IRES element is not only important for translation but also seems to be a major determinant for virulence. This is supported by several studies. Mutations within the IRES are a defining factor for the attenuated phenotype of all three Sabin vaccine strains (Minor, 1992), and disruptions of a region in stem-loop II generated viruses that were highly attenuated in poliovirus-sensitive mice, transgenic for the poliovirus receptor (Shiroki et al., 1997). Further evidence comes from studies using chimeric viruses where part of the IRES of one enterovirus was substituted by the equivalent region of another (Gromeier et al., 1999; Chapman et al., 2000). Those substitutions led to attenuation of the chimeric virus in cell culture or even in mice.

1.43 RNA replication

1.431 The switch from translation to replication

Positive-stranded RNA viruses face several obstacles when it comes to replication of their own genome. In a unique reaction they need to synthesize new RNA genomes using RNA as a template. This process is carried out by the viral RNA-dependent RNA polymerase (RdRP, $3D^{pol}$ in poliovirus) which is generated during translation. For the specificity of this reaction, the RdRP needs to distinguish between the viral RNA and cellular mRNAs, which also contain a poly(A) tail at the 3'-end . This requires *cis*-acting replication elements within the viral RNA that can guide the polymerase either directly or through cofactors, to the right location in the genome to initiate RNA synthesis. Another problem is the switch from translation to replication, since the ribosomes move from 5' to 3' along the viral genome for translation. However, the viral polymerase starts synthesizing RNA at the 3'-end of the RNA molecule and moves towards the 5'-end. Without any regulation of these processes, this could lead to collision of the ribosomes and the RdRP.

Several studies suggest that the switch from translation to replication is regulated. Using *in vitro* translation reactions of poliovirus replicons and purified $3D^{pol}$, Gamarnik & Andino (1998) showed that the polymerase is unable to replicate the input RNA templates while it is undergoing translation. They proposed that the switch from translation to RNA synthesis is achieved when a critical concentration of $3CD^{pro}$

accumulates in the infected cell. Without the presence of $3CD^{pro}$, PCBP2 binds with high affinity to the IRES structure and promotes translation. With the generation of $3CD^{pro}$ during protein synthesis, the viral protein binds to the cloverleaf and increases the binding affinity of PCBP2 to this structure, which in return represses translation. Another study demonstrated that, using poliovirus in a cell-free translation replication system, translating ribosomes inhibit negative-strand RNA synthesis (Barton et al., 1999).

1.432 A common replication mechanism

It is generally accepted that all picornavirus replication follows a common mechanism. The positive-strand is used as a template to synthesize a complementary negative-strand, which results in a double-stranded intermediate, called replicative form (RF) (see Figure 1.2). The negative-strand is then used to generate several new positive-strands, which produces an intermediate that is partially single- and partially double-stranded, called replicative intermediate (RI) (Wimmer et al., 1993; Agol et al., 1999). RNA synthesis results in asymmetry in the production of positive- and negative-strands, such that the ratio of plus- to minus-strands is approximately 50:1 in poliovirus infected cells (Novak & Kirkegaard, 1991). Consistent with these data, negative-strands can only be found in association with RF or RI and free minus strands are not detectable in cells. It is believed that RF is a true replication intermediate rather than an artifact (Wimmer et al., 1993; Agol et al., 1999). Both newly synthesized positive- and negative-strands are VPg-linked at their 5'-end (Lee et al., 1977; Ambros & Baltimore, 1978). The new positive-strands are then used either as mRNA, and after translation subsequently start a new round of RNA synthesis, or as genomic RNA for encapsidation into new virions later in infection (see Figure 1.2).

1.433 Viral proteins involved in replication

Picornaviruses utilize their small genomes very efficiently. All non-structural proteins are involved in RNA synthesis, and a number of their precursors in addition to the mature polypeptides carry out several different functions (Wimmer et al., 1993). Proteins of the P2 region are the least understood, but they are strongly associated with the biochemical and structural changes that are induced in the host cell following infection. The P3 proteins are most directly involved in the process of RNA synthesis, with 3B, also called VPg, functioning as the primer for the viral polymerase; $3CD^{pro}$, the

uncleaved precursor of the polymerase, acting as a co-factor in several steps of RNA replication; as well as $3D^{pol}$, the polymerase and thus the key player in RNA synthesis.

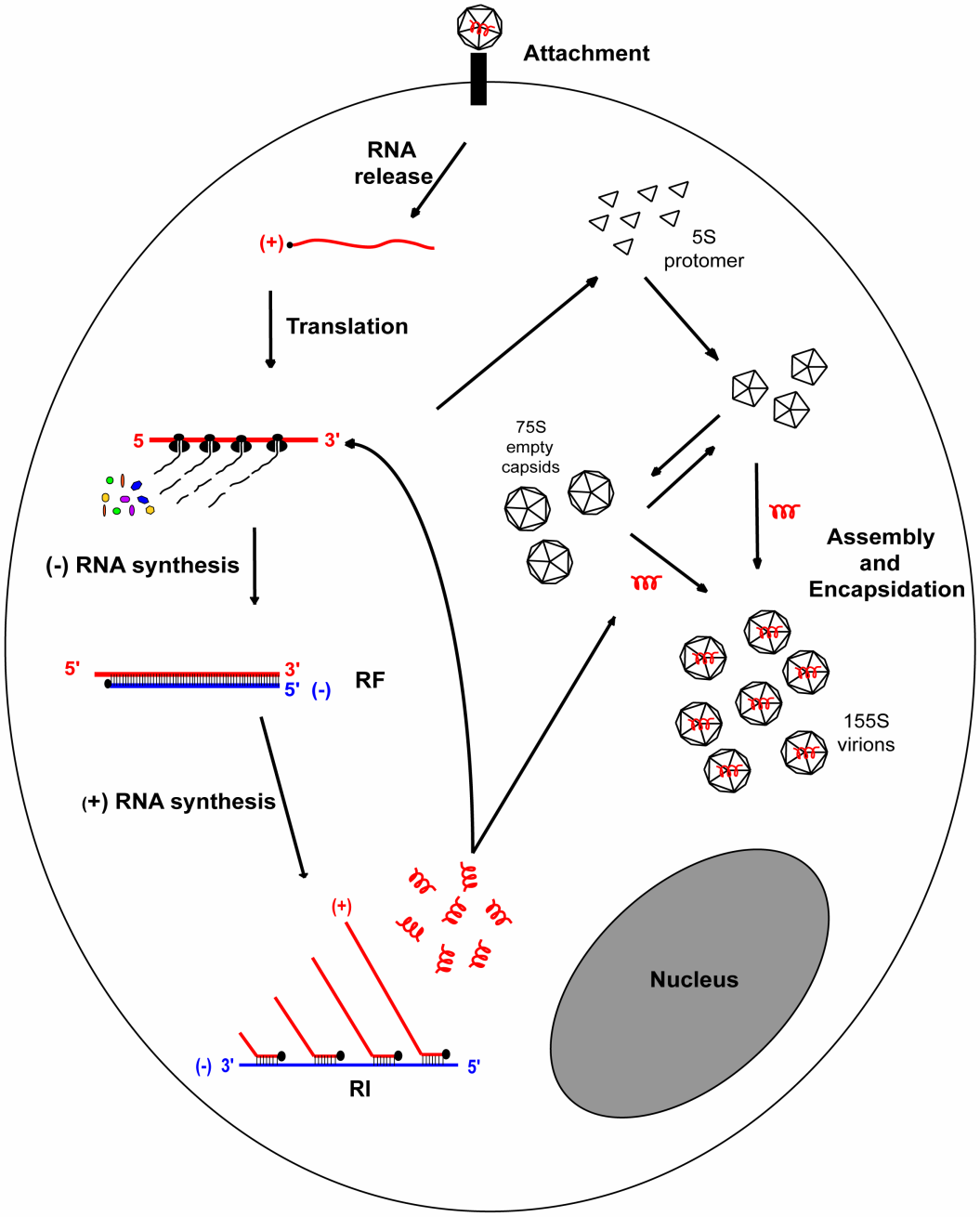

Figure 1.2: Poliovirus life cycle. Shown are the steps leading to infection and replication of poliovirus. The viral RNA is delivered into the host cell after interaction with the cognate receptor. The genomic RNA is then translated to yield the structural proteins (that go on to participate in assembly of new virions) and the non-structural proteins (which participate in the synthesis of negative and positive polarity RNA). Newly synthesized VPg linked genomic sense RNA is either recycled and used for the translation of more viral polypeptides, or packaged into new infectious particles. Virus particles are released upon lysis of the infected cell.

1.434 Cis-acting replication elements

The cloverleaf-structure

Negative-strand RNA synthesis starts at the poly(A) tail at the 3'-end of the viral genome. However, as mentioned above, cellular mRNAs also contain poly(A) tails, and hence, other more specific *cis*-acting replication elements must be involved in initiation of RNA synthesis. One essential replication element is the cloverleaf structure at the 5'-end of poliovirus, an element which is present in all enteroviruses. This 5'-end RNA structure of 94 nt was originally predicted by computer-modeling and verified by site-directed mutagenesis and by chemical and RNAse probing (Andino et al., 1990). The cloverleaf RNA was identified to form a ternary complex with the viral protein $3CD^{pro}$ and a cellular protein (Andino et al., 1990; Andino et al., 1993), later identified as PCBP2 (Parsley et al., 1997). Mutational analysis demonstrated that $3CD^{pro}$ interacts with the stem-loop d and PCBP2 interacts with stem-loop b of the cloverleaf structure (Andino et al., 1993; Parsley et al., 1997; Gamarnik & Andino, 2000). Mutations disrupting the formation of the ternary complex affected the accumulation of positive-strands in cells, suggesting a role for the cloverleaf in positive-strand RNA synthesis (Andino et al., 1990).

More recent data identified the cloverleaf structure as a key *cis*-acting element for initiation of negative-strand RNA synthesis. The ternary complex formed around the cloverleaf structure can interact with the cellular factor, poly(A) binding protein (PABP), which binds to the poly(A) tail at the 3'-end of the genome (see Figure 1.3). This leads to circularization of the viral genome and initiation of negative-strand RNA synthesis (Barton et al., 2001; Herold & Andino, 2001). The interaction between the 5'- and the 3'-end of the viral genome might be a common mechanism for positive-strand RNA viruses to initiate negative-strand RNA synthesis. Indeed, flaviviruses have complementary sequences within their 5' and 3'UTR that can promote direct RNA-RNA interaction without using any proteins to form a bridge (Khromykh et al., 2001; Corver et al., 2003; Lo et al., 2003; Alvarez et al., 2005). Data is also accumulating for coronaviruses and brome mosaic viruses, that support the RNA-protein-protein-RNA bridge as a way for both ends to communicate (Diez et al., 2000; Spagnolo & Hogue, 2000). In all these viruses, circularization of the genome brings a replication initiation complex, formed at the 5'-end of the genome, in close proximity to the 3'-end where the polymerase initiates negative-strand synthesis. It has also been shown that 3AB and $3CD^{pro}$ can form a ribonucleoprotein complex with the cloverleaf structure that

plays a role in replication (Harris et al., 1994; Xiang et al., 1995). Its significance, however, remains unclear.

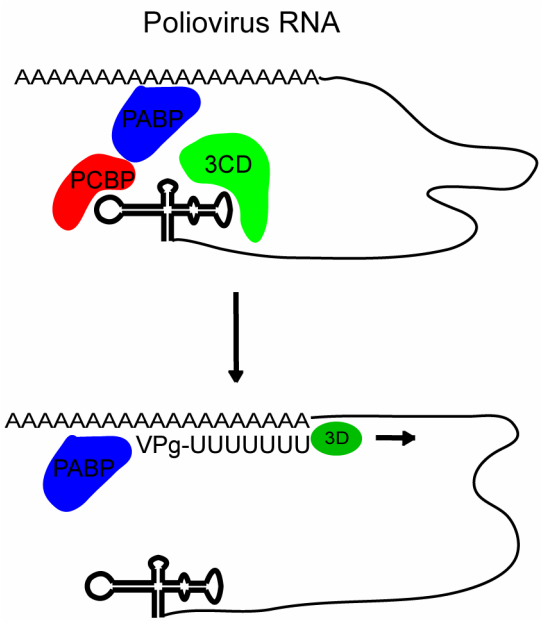

Figure 1.3: A model for initiation of negative-strand RNA synthesis during poliovirus replication. After translation of the poliovirus polyprotein, the viral polymerase containing polypeptide 3CD binds, together with the cellular PCBP, to the 5' cloverleaf, thus down regulating translation. Interactions between 3CD, PCBP, and PAPB hold the 5'- and the 3'-end of the poliovirus RNA in a noncovalent juxtaposition that leads to the circularization of the genomic RNA. These interactions bring the viral polymerase in close proximity of the 3' poly(A) tail and allow for the initiation of negative-strand RNA synthesis (Herold & Andino, 2001)

The 3'UTR and the poly(A) tail

Poliovirus has a highly structured 3'UTR, consisting of two stem-loop structures. A model has been proposed in which both stem-loops interact with each other, resulting in a "kissing" interaction (Pilipenko et al., 1996; Melchers et al., 1997). This model has been supported by mutational analysis of this structure in poliovirus and coxsackievirus B. Mutations disrupting this interaction negatively affect replication, indicating its importance as a *cis*-acting replication element (Pilipenko et al., 1996; Melchers et al., 1997). Surprisingly, viral RNAs completely lacking the 3'UTR showed impaired replication, but produced viable viruses (Todd et al., 1997).

The poly(A) tail at the 3'-end of the viral genome is a common *cis*-acting replication element for positive-strand RNA viruses. Although not unique to viral RNAs, as cellular mRNAs also bear poly(A) tails, it is the location where the polymerase binds to start

negative-strand RNA synthesis. In teamwork with other *cis*- and *trans*-acting factors, the polymerase can specifically be directed to it. The poly(A) tail of poliovirus consists of approximately 90 nt (Yogo & Wimmer, 1972). It has been shown that viruses with poly(A) tails of less than 20 A's retain only 5% of wild-type infectivity (Spector & Baltimore, 1974) . Other studies have shown that at least 8-12 A's are required in poliovirus for efficient replication, a length that enables PABP to bind (Sarnow, 1989; Herold & Andino, 2001). New data have shown that negative-strand RNA synthesis in poliovirus is initiated at A_8 which results in negative-strands with 8 U's at its 5'-end (Polacek, C. & Andino, R, unpublished date). These negative-strands are then used as a template to generate new positive-strands with only 8 A's. However, new plus-strands isolated from infected cells have again acquired a long poly(A) tail. A cellular poly(A) polymerase might be responsible for extending the short poly(A) tail to its final length (Polacek, C. & Andino, R, unpublished date).

The *cre* RNA

In 1986, the first *cis*-acting replication element within the coding region of a picornavirus was discovered by McKnight & Lemon (1986, 1988). The small hairpin within the VP1 coding region of *human rhinovirus 14* was named *cre* (***c****is*-acting-**r**eplication **e**lement). Similar *cre* hairpins were also found in other picornaviruses (Lobert et al., 1999; Gerber et al., 2001a), including in the 2C-coding region of poliovirus (*cre*(2C)) (Goodfellow et al., 2000). The hairpin structures in the different viruses differ in sequence and structure but seem to have similar function *in vivo*, since disruption of the hairpin structure results in inhibition of replication. Studies of the *cre* RNAs of poliovirus and HRV2 indicated at least two possible roles for the hairpin (Paul et al., 2000; Rieder et al., 2000; Gerber et al., 2001a): (i) that it functions as a site of recognition and binding of $3CD^{pro}$ prior to the *in vitro* uridylylation of VPg by $3CD^{pol}$, (ii) that it serves as specific template *in vitro* for the protein priming reaction.

The viral polymerase is strictly primer-dependent (Flanegan & Baltimore, 1977), and both positive- and negative-strands of poliovirus are VPg-linked (Nomoto et al., 1977a). Subsequently, uridylylated VPg was discovered in poliovirus infected cells (Crawford & Baltimore, 1983). Eventually a model evolved that VPg serves as a primer for the polymerase (Paul et al., 1998). VPg-uridylylation can be accomplished in different ways in an *in vitro* reaction using purified proteins. In a reaction containing poliovirus RNA, $3D^{pol}$, and oligo(U), full-length minus-strand is synthesized (Baron & Baltimore, 1982).

This elongation reaction also proceeds efficiently on a poly(A) template (Flanegan & Baltimore, 1977). *In vitro*, it has been shown that poly(A) can serve as a template for uridylylation of VPg, which generates VPg-poly(U) as a final product (Paul et al., 1998; Paul et al., 2000; Gerber et al., 2001b), and which also resembles the 5'-end of negative-strands (Nomoto et al., 1977a). *In vitro* studies demonstrated that in reactions where full-length poliovirus or HRV2 RNAs were used as templates, *cre*(2C) in case of poliovirus or *cre*(2A) in HRV2 was used as the primary template for the synthesis of VPgpUpU (Paul et al., 1998; Goodfellow et al., 2000; Paul et al., 2000; Gerber et al., 2001a). This reaction was stimulated by addition of $3CD^{pro}$.

It was initially observed that all picornavirus *cre* RNAs contain a common conserved sequence of AAACA that is located either in the loop or bulge of the hairpin and is required for replication (McKnight & Lemon, 1998; Goodfellow et al., 2000; Rieder et al., 2000). More recently, Yang et al. (2002) postulated a common $R_1NNNAAR_2NNNNNNR_3$ motif (R, A/G; N, any nucleotide) for the loop of rhinovirus and enterovirus *cre'*s, an observation that was confirmed for poliovirus (Yin et al., 2003). Biochemical studies of the *cre* demonstrated the importance of the A's within this motif (Paul et al., 2003). The data are consistent with a slide-back mechanism in which the first A is used as a template for the linkage of UMP to VPg. This is followed by the slide-back of VPgpU to hydrogen bond with A_2. The second UMP is then added again by $3D^{pol}$ on the A_1 template nucleotide, resulting in VPgpUpU (Paul et al., 2003). This has been proposed to be the primer for both negative- and positive-strand RNA synthesis (Paul et al., 2000; Rieder et al., 2000; Gerber et al., 2001a). Recent reports, however, showed that a structurally disrupted *cre* mutant retained the capacity to induce negative-strand RNA synthesis in a cell-free translation replication system, suggesting that the *cre*-generated VPgpUpU is only required for positive-strand RNA synthesis (Goodfellow et al., 2003b; Morasco et al., 2003; Murray & Barton, 2003). It has been proposed that the poly(A) tail functions as a template for VPg-poly(U), which is then used as a primer for negative-strand RNA synthesis, and the *cre*-mediated VPgpUpU as a primer for positive-strand RNA synthesis.

1.435 Positive-strand RNA synthesis

As mentioned before, replication is a highly asymmetric process, as many more positive- than negative-strands are produced, suggesting different regulation mechanisms for each synthesis. However, most replication mechanisms remain poorly

understood and the least is known about how positive-strand RNA synthesis occurs. Two recent studies demonstrated the importance of precise 5'-end sequences of the viral genome for efficient positive-strand RNA synthesis. Herold & Andino have shown that additional non-viral sequences at the 5'-end of poliovirus RNA lead to defects in positive-strand RNA synthesis in a cell-free system and to a two hour delay in replication in cells, where the non-viral sequences get eventually deleted (Herold & Andino, 2000). A study by Sharma et al. (2005) highlighted the importance of the 5'-terminal 9 nucleotides for efficient plus-strand synthesis. Since the 5'-end of the positive-strand is the template for the 3'-end of the negative-strand, which is the location where the primer and the polymerase bind for plus-strand RNA synthesis; it has been proposed in both reports (Herold & Andino, 2000; Sharma et al., 2005) that these precise end-sequences are required on the level of the negative-strand. The 5'-end sequence of the positive-strand is highly conserved among enteroviruses and rhinoviruses and starts with UU (Klump et al., 1990; Zell & Stelzner, 1997; Zell et al., 2002). This results in AA at the 3'-end of the negative-strand. This sequence is consistent with a *cre*-generated primer VPgpUpU that binds to the two A's and initiates positive-strand RNA synthesis.

The remaining question is: What other *cis*-acting replication elements and *trans*-acting factors are involved in plus-strand RNA synthesis? The cloverleaf structure was found to be involved in positive-strand RNA synthesis (Andino et al., 1990). However, the precise mechanism of how the cloverleaf promotes positive-strand RNA synthesis was not identified in the initial study. Proteins that are involved in positive-strand RNA synthesis might have specific binding-affinities to the 3'-end of the minus-strand, since positive-strand RNA synthesis starts at this location. Two proteins have been identified with such binding properties. These proteins are the viral protein $2C^{ATPase}$ (Banerjee et al., 2001) and a cellular protein that was recently identified as hnRNP C1 (Roehl & Semler, 1995; Roehl et al., 1997; Brunner et al., 2005). However, evidence for their role in positive-strand RNA synthesis has yet to be demonstrated.

1.436 The role of membranous vesicles in replication

All RNA synthesis events take place in the cytoplasm as part of replication complexes that are associated with membranous vesicles (see section 1.33). 3AB interacts with the membrane through the hydrophobic domain of its 3A moiety (Giachetti et al., 1992; Towner et al., 1996). It is generally assumed that 3AB, through its binding to $3D^{pol}$ and

$3CD^{pro}$, recruits these proteins to the replication complex, which by themselves are unable to associate with membranes (Hope et al., 1997; Xiang et al., 1998). Membranous vesicles isolated from infected cells were shown to contain not only single-stranded RNA but also double-stranded intermediates, RF and RI, indicating that both negative- and positive-strand RNA synthesis occurs in the same replication complexes attached to membranes (Bienz et al., 1992). The role of membranes in replication is still not clear. It was suggested that membranes act either as scaffold for the assembly of the replication complex and/or to protect the viral RNA from degradation by cellular enzymes. Alternatively, they serve to concentrate the viral proteins at the site of RNA synthesis or to physically separate viral RNA template from other cellular mRNAs. A recent study suggests that the formation of poliovirus replication complexes requires coupled translation, vesicle production and viral RNA synthesis (Egger et al., 2000). However, the main question regarding the role of the membranes in viral RNA synthesis is still open.

1.44 Assembly & encapsidation

The poliovirus virion is composed of 60 copies each of VP1, VP2, VP3, and VP4, forming an icosahedral surface around a single copy of the VPg linked genomic RNA. The particles are approximately 30 nm in diameter, and have a sedimentation coefficient of 155S. The crystal structure of poliovirus has been solved in different conditions: poliovirus alone, bound to the receptor, or the empty virion intermediate during assembly (Hogle et al., 1985; Basavappa et al., 1994; Belnap et al., 2000b; Bubeck et al., 2005). Despite differences in primary sequence, the major capsid proteins VP1, VP2, and VP3 share a high degree of structural similarity, forming a β-barrel structure domain found in a variety of icosahedral viruses. These proteins display structural differences within the loop that connects the elements that form the β-barrel core. The outer surface of the virus is dominated by star-shaped mesas at the five-fold axes and three-fold propeller-like structures (see Figure 1.4). These prominent surface features are punctuated by depressions surrounding the five-fold axes and crossing the two-fold axes. The depressions surrounding the five-fold axes are joined to form a canyon, which is the site of receptor attachment. At the five-fold axes of symmetry cluster five copies of VP1, while VP2 and VP3 are found alternating around

the 20 three-fold axes of symmetry. VP4 appears as an N-terminal extension of VP2 (Hogle & Racaniello, 2002).

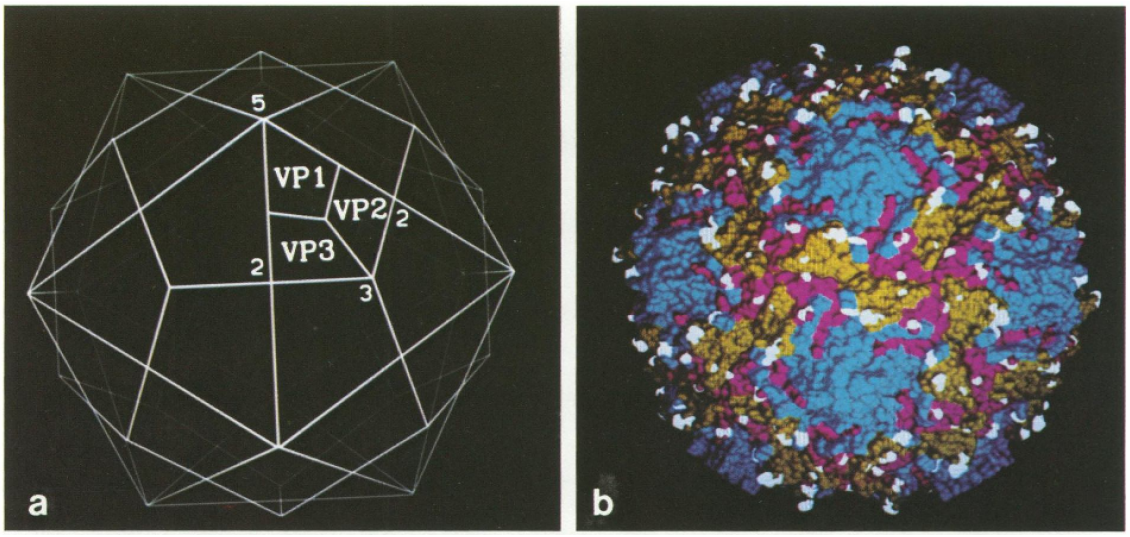

Figure 1.4: The structure of the poliovirus virion. a) A simple geometric figure showing the symmetry and approximate shape of the poliovirus particle. The positions of VP1, VP2 and VP3 that forms a single protomer are indicated in relation to the two-fold, three-fold and five-fold axes of symmetry of the particle. Vertices of the geometric figure correspond to the prominent protusions which occur at the five-fold and three-fold axes of the virion. b) Space-filling representation of the outer surface of the poliovirion. VP1 is blue, VP2 is yellow, and VP3 is red. Antigenic sites are highlighted in white (Page et al., 1988).

Early co-translational cleavage of the polyprotein by $2A^{pro}$ releases a precursor protein P1 from the N-terminus of the polyprotein. Further processing of the P1 protein by the viral protease $3CD^{pro}$ generates the capsid proteins VP0 (uncleaved VP4 and VP2), VP3 and VP1, and is dependent on a cellular factor (Harris et al., 1992; Blair et al., 1993). This cleavage event is associated with the formation of VP0, VP3, and VP1, which assemble into a 5S protomer. Next, five protomers assemble to form the 14S pentamer. Twelve 14S pentamers then either assemble around an RNA molecule or form the 80S procapsid structure into which an RNA molecule is threaded. In either case, this assembly process results in the formation of a short-lived 150S provirion (Compton et al., 1990). Processing of the immature protein VP0 to yield VP4 and VP2 is associated with encapsidation of the RNA (Arnold et al., 1987; Basavappa et al., 1994; Ansardi et al., 1996). There is no known protease requirement for this cleavage and it is thought to be autocatalytic, depending only on the capsid proteins themselves and perhaps the viral RNA. Cleavage of VP0 to form the mature virion is associated with a significant increase in the stability of the particle. Proper capsid assembly and

RNA encapsidation are essential for virus infectivity, and cellular chaperones associate with newly synthesized virus particles and possibly contribute to virus particle assembly (Macejak & Sarnow, 1992).

The amino-terminus of the poliovirus polyprotein is myristylated. This fatty-acid modification is thought to occur co-translationally after the removal of the initiator methionine to yield an exposed glycine. Thus, N-terminal cleavage of the P1 protein precursor yields myristoyl-VP0, which further cleavage then releases as myristoyl-VP4. Mutant viruses defective in myristylation are not viable in cell culture. This modification could not be associated with targeting of the structural proteins or the assembly intermediates to the membranous replication complexes (Lee & Chow, 1992). However, myristylation of P1 seems to be required for proteolytic cleavage by $3C^{pro}$ (Marc et al., 1989; Kräusslich et al., 1990). Several studies have shown that the modification is required for the proper assembly of viral particles (Ansardi et al., 1996). The myristate moiety makes several contacts with amino acids from VP3 and VP4 located at the five-fold axis of symmetry in the β-tube, which is thought to be important for the nucleation of pentamer assembly intermediates. This proposal is supported by findings that viruses mutant in myristylation have defects in accumulation of assembly intermediates and mature viral particles. It has been shown that mutants defective in myristylation also display a decrease in infectivity as measured by the particle to PFU (plaque-forming units) ratio, which led to the proposal that the fatty acid molecule plays a role earlier in infection, possibly in the cell entry of the virus (Marc et al., 1990; Moscufo et al., 1991).

One of the least understood processes in the life cycle of poliovirus and other picornaviruses is the mechanism of RNA encapsidation. Studies to define encapsidation signals within the viral RNA could only narrow down the RNA regions containing them. Defective interfering (DI) genomes lacking the capsid-coding region are efficiently packaged, indicating that major encapsidation signals of poliovirus lie somewhere outside this region (Kuge et al., 1986). There is evidence that unidentified signals in the 5'UTR stimulate poliovirus RNA packaging (Johansen & Morrow, 2000). It has also been proposed that packaging signals are most likely located within the 2B or 3D coding regions (Barclay et al., 1998) In addition, mutations in the 2C-coding region of poliovirus may affect the assembly pathway (Li & Baltimore, 1990; Vance et al., 1997).

However, there might not be any clear encapsidation signals within the viral RNA at all, but packaging could be linked to certain events occurring during the infectious cycle. Encapsidation is associated with viral RNA synthesis, since VPg-lacking genomes, which function as mRNA for translation, are not efficiently packaged (Nomoto et al., 1977b; Nugent et al., 1999). Virion assembly seems to be another determinant for RNA packaging. There is evidence that each protein component of the pentamer (VP0, VP3, and VP1) contacts the viral RNA in the poliovirus replication complex (Nugent & Kirkegaard, 1995; Pfister et al., 1995). Therefore, encapsidation may start at the pentamer level rather than at the empty particle step.

1.5 Model systems of poliovirus replication

The methods of reverse genetics facilitated the successful reconstruction of a positive-stranded RNA virus genome as an infectious cDNA clone (Racaniello & Baltimore, 1981b). Viral RNA can be synthesized *in vitro* by DNA-dependent RNA polymerases using cDNA clones as templates (Ahlquist et al., 1984; van der Werf et al., 1986). Both, the cDNA (Racaniello & Baltimore, 1981a) as well as *in vitro* synthesized RNA (van der Werf et al., 1986), are infectious when introduced into cells, providing a powerful tool for the genetic manipulation and analysis of the viral replication cycle.

In 1991, Molla and colleagues developed the synthesis of infectious poliovirus from cell-free systems, containing uninfected human HeLa cell extracts. Barton and colleagues (1995) demonstrated the formation of RNA replication complexes, which contained membranous vesicles, viral RNA and cellular proteins, and catalyzed the replication of poliovirus RNA. During the course of the infection cycle, a significant overlap develops between the translation and replication steps because of their mutual interdependence. Therefore, the amplification of viral RNA in infected cells occurs in a circular pathway involving iterative steps of translation and RNA replication. The inhibition of either step significantly affects the other and complicates the analysis of the regulatory mechanisms controlling virus replication. By using a reversible inhibitor of poliovirus RNA replication, it is possible to synchronize viral RNA replication in the cell-free system. Pre-initiation complexes are formed when replication is inhibited by guanidine hydrochloride (GuHCl). These complexes, when sedimented by centrifugation, initiate RNA replication upon their resuspension in reaction mixes

lacking GuHCl (Barton et al., 1995). This enables the direct measurement of the sequential synthesis of negative- and positive-strand RNA (Barton & Flanegan, 1997).
Poliovirus RNA *in vitro* transcripts with extra nucleotides at the 5'-end are able to initiate RNA replication but lack efficient positive-strand RNA synthesis in a cell-free translation replication system (Herold & Andino, 2000). Transcription of DNA clones containing a hammerhead ribozyme 5' of the poliovirus genome permitted the generation of RNA transcripts with authentic 5'-ends *in vitro*, which not only replicated in a cell-free replication system comparably to virion RNA, but showed improved kinetics in tissue culture cells (Herold & Andino, 2000). Using these improved transcripts in the *in vitro* system is of significant practical importance since conditional and lethal mutations of the virus can be tested for their specific effect on individual steps in the RNA replication cycle.
An alternative and complementary system using *Xenopus Laevis* oocytes has been developed in our laboratory for the study of viral replication (Gamarnik & Andino, 1996). Microinjection of poliovirus RNA into *Xenopus* oocytes leads to the production of viral particles, provided that a HeLa cell extract is coinjected. The fact that the oocyte is an intact cell is advantageous since it more faithfully recreates the environment that the virus encounters in an infected cell.
The only natural hosts of poliovirus are humans. Until recently only monkeys and chimpanzees provided an experimental animal model for the study of immunology and pathogenesis, since they express a homologue to the human poliovirus receptor, which makes them susceptible to the virus (Koike et al., 1990). The identification of the receptor for poliovirus (Pvr) allowed for the generation of transgenic mouse lines susceptible to poliovirus infection (Ren et al., 1990; Koike et al., 1991b). Mice infected with poliovirus develop a polio-like paralytic disease, opening up the possibility to study the mechanism of pathogenesis of poliovirus in a reproducible manner. In addition, these mice have proven to be useful in the study of the immune responses generated by poliovirus recombinant vectors (Andino et al., 1994; Morrow et al., 1994; Mandl et al., 1998).

1.6 Coxsackievirus B3

With the eradication campaign of poliovirus moving into an advanced stage, poliovirus will soon be banned from research labs. Virologists who use poliovirus as a model to

study the life cycle of picornaviruses will have to rely on other model systems. Because of its research restriction in Europe, poliovirus has already been replaced by other enteroviruses such as coxsackie- and rhinovirus as the focus of research. Since these pathogens are still a major threat to our society, it makes sense to study them in more detail, both as models and as pathogens.

Coxsackievirus B3 is classified as a serotype of the species *Human enterovirus B* (HEV-B) and belongs, like poliovirus, to the genus Enterovirus. Enteroviruses were originally classified as poliovirus (PV), coxsackievirus A (CVA), coxsackievirus B (CVB), and echovirus on the basis of their pathogenicity in experimental animals (Melnick, 1996). Coxsackieviruses are mouse pathogens, and they were discriminated into A and B subgroups on the basis of the disease observed in newborn mice: CVAs cause flaccid paralysis while CVBs cause spastic paralysis (Hyypiä et al., 1993). This is due to the involvement of the central nervous system by the CVB infection whereas CVAs replicate in the muscle tissue. In humans, the members of the large HEV-B group cause a great variety of diseases varying from exanthemas to carditis and infections of the central nervous system, but the most frequent consequence of infection is mild respiratory infection (Grist et al., 1978). Coxsackievirus B3 uses CAR (the coxsackievirus B and adenovirus 2 receptor) for cell entry (Bergelson et al., 1997). Unlike CD155, the receptor used by poliovirus, CAR has been reported to have cell adhesion function (Honda et al., 2000). The precise physiological function of CAR that is highly conserved between primates and rodents remains obscure. However, DAF (decay accelerating factor) can also function as a receptor for a large number of B-, C-, and D-cluster enteroviruses (Shafren et al., 1995).

The current classification of enteroviruses based on phylogenetic properties and genome organization (see section 1.21) underscores the similarities between CVB3 and poliovirus in genomic structure, although some notable differences exist. In CVB3, the 5'UTR also contains a cloverleaf structure at the very 5'-end and a large higher order structure that functions as a type I IRES. The 3'UTR contains three stem-loop structures (X, Y, Z) rather than two as in poliovirus (X, Y) (Pilipenko et al., 1992b), but mutational analysis of the 3'UTR in CVB3 and poliovirus supports a "kissing" interaction between X and Y for both of them (Pilipenko et al., 1996; Melchers et al., 1997). Based on homology with poliovirus, it has been suggested that a *cre* RNA is also located in the 2C coding region of coxsackievirus B3 (Goodfellow et al., 2000; Paul et al., 2000; Rieder et al., 2000; Witwer et al., 2001)

2. Aims of this thesis

Enteroviruses make very efficient use of their small RNA genomes. Several *cis*-acting replication elements can be found throughout the genome. Most of these elements consist of RNA regions which fold into secondary structures that can form complexes with viral and cellular proteins. Such complex formations are often required to initiate a new step in replication, and thus function as key players in regulation of the viral life cycle. Some of the *cis*-acting replication elements have overlapping functions and play a role in several steps in RNA synthesis. It is not clear how the same RNA element regulates different events.

One of the key players in RNA replication is the small cloverleaf structure at the 5'-end of the enterovirus genome. When originally described, this RNA element was found to be involved in positive-strand RNA synthesis, which is initiated at the 3'-end of the opposite strand. However, more recent studies identified the cloverleaf as a key element in initiation of negative-strand RNA synthesis, which starts at the 3'-end of the genome. The question about the role of the cloverleaf in positive-strand RNA synthesis remains. Does it form the same complex to initiate both, positive- and negative-strand RNA synthesis? Is the cloverleaf structure that can form on the negative-strand important? What proteins are involved in positive-strand RNA synthesis?

Another *cis*-acting replication element is the recently identified *cre*-element which lies within the coding region of most enteroviruses. It has been shown that this RNA hairpin functions as a template for VPgpUpU formation, which was thought to be the primer for both negative- and positive-strand RNA synthesis. Recently, it has been demonstrated that it is required for positive- but not negative-strand RNA synthesis. It has been proposed that the poly(A) tail functions as a template for the synthesis of VPg-poly(U), which then serves as a primer for minus-strand synthesis. This opens the question: is poly(A) tail mediated VPg-uridylylation the common mechanism by which the virus generates the primer for negative-strand RNA synthesis, or is there an alternative mechanism the virus can use in case the *cre*-mediated VPg-uridylylation is inhibited?

In the first part of this thesis, poliovirus was used to analyze the role of the cloverleaf structure in positive-strand RNA synthesis. Analyzing the precise role of the RNA cloverleaf element in positive-strand RNA synthesis has been hindered by its role in negative-strand RNA synthesis, as mutations disrupting the structure and/or functions of the cloverleaf disrupt minus-strand synthesis. The first aim of this thesis was to

overcome this limitation by developing a system that enabled us to separate the cloverleaf function in negative- and positive-strand RNA synthesis. Once this system was in place, the structural and sequence requirements of the RNA element to support positive-strand RNA synthesis were identified by mutational analysis. Replication phenotypes of cloverleaf mutants were characterized in a cell-free translation replication system and after transfection into HeLa cells. Additional analysis focused on possible roles of proteins involved in positive-strand RNA synthesis either through binding to the RNA structure itself or through a different mechanism.

The second part of this thesis focused on *cre*(2C) in coxsackievirus B3 (CVB3). A stem-loop element located within the 2C coding region of CVB3 has been proposed to function as a *cis*-acting replication element. The MFOLD program was used to predict the structure and the precise location of the *cre*(2C), and its structure and sequence was then compared to a recently published enteroviral *cre* consensus loop sequence. The aim of this study was to examine the structural and functional requirements of the CVB3 *cre*(2C) in RNA replication. *Cre*(2C) loop mutants were analyzed for their capacity to serve as a template for VPg-uridylylation and to induce negative- and positive-strand RNA synthesis using HeLa S10 extract.

3. Materials & Methods

3. Materials & Methods

3.1 Equipment

PTC-200, Peltier Thermal Cycler, MJ Research	GMI, Ramsey, MI
Luminometer: Optocomp	MGM Instruments, Hamden, CT
Spectrometer: BioSpec-1601	Shimadzu, Columbia, MD
Electro cell manipulator 600	BTX, Holliston, MA
Centrifuge 5415C	Eppendorf, Westbury, NY
Tabletop centrifuge: MTX-150	TOMY, Fremont, CA
Sorvall RC 3B plus	Sorvall, New Castle, DE
Gel dryer: Model 583	Bio-Rad, Hercules, CA
Gel-imaging system: FluorChem^{TM}8900	Alpha Innotech, San Leandro, CA
Sonicator 3000	Misonix, Farmingdale, NY
Scintillation counter S6500	Beckman Coulter, Fullerton, CA
Typhoon 9400, Amersham Biosciences	GE Healthcare, Piscataway, NJ
Äkta FPLC system, Amersham Biosciences	GE Healthcare, Piscataway, NJ

3.2 Molecular Biology

3.21 Plasmids and cloning

3.211 Primers used for cloning of the poliovirus plasmids:
(purchased from Elim Biopharmaceuticals, Hayward, CA)

1. 5'-GCAGAGGCCGAGGCCGCCTCGGCCTCTGAGCTATT-3'
2. 5'-TTAAAGAGCTCGTTACGGGAAGGGAGTA-3'
3. 5'- GGTATCCCGGGTTCTTAAAACAGGAGCTCTTAAAACAGCTCTGGGGTTG-3'
4. 5'-GAGTGCTGAGCGCAACGCATCG-3'
5. 5'-GGGTTCTTAAAACACACGTTGTTTTAGAGCT-3'
6. 5'-CTAAAACAACGTGTGTTTTAAGAACCC-3'
7. 5'-GGGTTCTTAAAACAGCCCACGTGGCTGTTTTAGAGCT-3'
8. 5'-CTAAAACAGCCACGTGGGCTGTTTTAAGAACCC-3'
9. 5'-GAGGCCCACGTGGCGGCTAGTACTCCGGTATTGCGGTACCCTTGTACGCCACAAAAATACTCCCTTCC CGTAAC-3'
10. 5'-TATATCCCGGGTTCTTCCGGCAGCTCTGGGGTTGTACC-3'
11. 5'-GGGAGTATGGCCCAGGCGTACAAGGGTACCGCAATACCGGA-3'
12. 5'-GTACGCCTGCCGGATACTCCCTTCCCGTAACTTAGACGCAC-3'
13. 5'-TTTTGGAGGCCTAATACGACTCACTATAGGGTGCCGGAACTGATGAGGCGCTT-3'
14. 5'-AATTAAGAGCTCTTCCGGCAGCTCTGGGGTTGTACC-3'
15. 5'-GGGTTCTTAAAACAGCTCTAAAGTTGTACCCACCCCAGAGGCCCAC-3'
16. 5'-GTGGGCCTCTGGGGTGGGTACAACTTTAGAGCTGTTTTAAGAACCC-3'
17. 5'-GGGTTCTTAAAACAGCTCTGGGGTTGTACCCACTTTAGAGGCCCAC-3'
18. 5'-GTGGGCCTCTAAAGTGGGTACAACCCCAGAGCTGTTTTAAGAACCC-3'
19. 5'-CCGGGTTCTTAAAACAGGAGACCCCATGTACCCTGGGGTCTCGCCCAC-3'
20. 5'-GTGGGCGAGACCCCAGGGTACATGGGGTCTCCTGTTTTAAGAAC-3'
21. 5'-CCGGGTTCTTAAAACAGGCTGTCTGCTGTACCCGCAGACAGCGCCCAC-3'
22. 5'-GTGGGCGCTGTCTGCGGGTACAGCAGACAGCCTGTTTTAAGAAC-3'
23. 5'-TTAATTCACGTGGGCCTCTGGGGTAAGCTTAACCCCAGAGCTGTTTTAAG-3'

24. 5’- GAGGCCCACGTGGCGGCTAGTACTCCGGcATTGCGGcACCCTTGTACG-3’
25. 5’-GAGGCCCACGTGGCGGCTAGTACTCCGGTgTTGCGGTgCCCTTGTACG-3’
26. 5’-GAGGCCCACGTGGCGGCTAGTACTCCGGTATTGCGgtacGTACCCTTGTACG-3’
27. 5’-TTAATTAAGAGCTCGTATAAAACAGGCGTACAAGCCATCCGCAAATGGGGAGTACTAGC-3’
28. 5’-TTAATTAAGAGCTCGTATAAAACAGGCGTACAAGCCATCCGCAATACCGGAG-3’
29. 5’-TTAATTAAGAGCTCGTATAAAACAGGCGTACAAGGCGCAATACCGGAGTAC-3’
30. 5’-TTAATTAAGAGCTCGTATAAAACAGGCGTACAAGGGTACGAACCTACCGGAGTACTAGC-3’
31. 5’-TATATCCCGGGTTCTTTTTTCAGCTCTGGGGTTGTACC-3’
32. 5’-GGGAGTATTTTTCAGGCGTACAAGGGTACCGCAATACCGGA-3’
33. 5’-GTACGCCTGAAAAATACTCCCTTCCCGTAACTTAGACGCAC-3’
34. 5’- TTTTGGAGGCCTAATACGACTCACTATAGGGTGAAAAAACTGATGAGGCGCTT-3’
35. 5’- AATTAAGAGCTCTTTTTTCAGCTCTGGGGTTGTACC-3’
36. 5’-CCTAATACGACTCACTATAGGGTGTTAAAACTGATGAGGCCGAAAGGCCGAAAACCCGGTATC-3’
37. 5’-CCGGGATACCGGGTTTTCGGCCTTTCGGCCTCATCAGTTTTAACACCCTATAGTGAGTCGTATTAGG-3’
38. 5’-TATATCCCGGTATCCCGGGTTCTTTTAACAGCTCTGGGGTTGTACC-3’
39. 5’-GGGAGTATTTAACAGGCGTACAAGGGTACCGCAATACCGGA-3’
40. 5’-GTACGCCTGTTAAATACTCCCTTCCCGTAACTTAGACGCAC-3’
41. 5’-CCTAATACGACTCACTATAGGGTGAATTAACTGATGAGGCCGAAAGGCCGAAAACCCGGTATC-3’
42. 5’-CCGGGATACCGGGTTTTCGGCCTTTCGGCCTCATCAGTTAATTCACCCTATAGTGAGTCGTATTAGG-3’
43. 5’-TATATCCCGGTATCCCGGGTTCTTAATTCAGCTCTGGGGTTGTACC-3’
44. 5’- GGGAGTATAATTCAGGCGTACAAGGGTACCGCAGCGATACCGGA-3’
45. 5’-GTACGCCTGAATTATACTCCCTTCCCGTAACTTAGACGCAC-3’
46. 5’-CCTAATACGACTCACTATAGGGTGTTTCAACTGATGAGGCCGAAAGGCCGAAAACCCGGTATC-3’
47. 5’-CCGGGATACCGGGTTTTCGGCCTTTCGGCCTCATCAGTTGAAACACCCTATAGTGAGTCGTATTAGG-3’
48. 5’-TATATCCCGGTATCCCGGGTTCTTGAAACAGCTCTGGGGTTGTACC-3’
49. 5’-GGGAGTATGAAACAGGCGTACAAGGGTACCGCAATACCGGA-3’
50. 5’-GTACGCCTGTTTCATACTCCC-3’
51. 5’-CCTAATACGACTCACTATAGGGTGTTCTAACTGATGAGGCCGAAAGGCCGAAAACCCGGTATC-3’
52. 5’-CCGGGATACCGGGTTTTCGGCCTTTCGGCCTCATCAGTTAGAACACCCTATAGTGAGTCGTATTAGG-3’
53. 5’-TATATCCCGGTATCCCGGGTTCTTAGAACAGCTCTGGGGTTGTACC-3’
54. 5’-GGGAGTATAGAACAGGCGTACAAGGGTACCGCAATACCGGA-3’
55. 5’-GTACGCCTGTTCTATACTCCCTTCCCGTAACTTAGACGCAC-3’
56. 5’-CCTAATACGACTCACTATAGGGTGTCTTAACTGATGAGGCCGAAAGGCCGAAAACCCGGTATC-3’
57. 5’-CCGGCATACCGGGTTTTCGGCCTTTCGGCCTCATCAGTTAAGACACCCTATAGTGAGTCGTATTAGG-3’
58. 5’-TATATCCCGGTATCCCGGGTTCTTAAGACAGCTCTGGGGTTGTACC-3’
59. 5’-GGGAGTATAAGACAGGCGTACAAGGGTACCGCAATACCGGA-3’
60. 5’-GTACGCCTGTCTTATACTCCCTTCCCGTAACTTAGACGCAC-3’
61. 5’-CCTAATACGACTCACTATAGGGTGCTTTAACTGATGAGGCCGAAAGGCCGAAAACCCGGTATC-3’
62. 5’-CCGGGATACCGGGTTTTCGGCCTTTCGGCCTCATCAGTTAAAGCACCCTATAGTGAGTCGTATTAGG-3’
63. 5’-TATATCCCGGTATCCCGGGTTCTTAAAGCAGCTCTGGGGTTGTACC-3’
64. 5’-GGGAGTATAAAGCAGGCGTACAAGGGTACCGCAATACCGGA-3’
65. 5’-GTACGCCTGCTTTATACTCCCTTCCCGTAACTTAGACGCAC-3’
66. 5’-CCTAATACGACTCACTATAGGGTGTTCCAACTGATGAGGCCGAAAGGCCGAAAACCCGGTATC-3’
67. 5’-CCGGGATACCGGGTTTTCGGCCTTTCGGCCTCATCAGTTGGAACACCCTATAGTGAGTCGTATTAGG-3’
68. 5’-TATATCCCGGTATCCCGGGTTCTTGGAACAGCTCTGGGGTTGTACC-3’
69. 5’-GGGAGTATGGAACAGGCGTACAAGGGTACCGCAATACCGGA-3’
70. 5’-GTACGCCTGTTCCATACTCCCTTCCCGTAACTTAGACGCAC-3’
71. 5’-CCTAATACGACTCACTATAGGGTGTTCCTTCTGATGAGGCCGAAAGGCCGAAAACCCGGTATC-3’
72. 5’-CCGGGATACCGGGTTTTCGGCCTTTCGGCCTCATCAGTTAAGGCACCCTATAGTGAGTCGTATTAGG-3’
73. 5’-TATATCCCGGTATCCCGGGTTCTTAAGGCAGCTCTGGGGTTGTACC-3’
74. 5’-GGGAGTATAAGGCAGGCGTACAAGGGTACCGCAATACCGGA-3’
75. 5’-GTACGCCTGCCTTATACTCCCTTCCCGTAACTTAGACGCAC-3’
76. 5’-GCCAACGCAGCCTGGACCA-3’
77. 5’-GGGTTCTTAAAACAGCTCTAAAGTTGTACCCACTTTAGAGGCCCAC-3’
78. 5’-GTGGGCCTCTAAAGTGGGTACAACTTTAGAGCTGTTTTAAGAACCC-3’
79. 5’-GGGTTCTTAAAACAGCTCTAAAGTTGTACCCACTTTATAGGCCCAC-3’
80. 5’-GTGGGCCTATAAAGTGGGTACAACTTTAGAGCTGTTTTAAGAACCC-3’
81. 5’-GGGTTCTTAAAACAGCTTTAAAGTTGTACCCACTTTAGAGGCCCAC-3’
82. 5’-GTGGGCCTCTAAAGTGGGTACAACTTTAAAGCTGTTTTAAGAACCC-3’
83. 5’-GGTATCCCGGGTTGTTAAAACAGC-3’

3.212 Poliovirus plasmid design

prib(+)Luc-Wt: The luciferase-expressing poliovirus-derived replicon plasmid, containing a 5’-end hammerhead ribozyme to generate precise 5’-ends of the viral RNA transcripts, has been described before (Herold & Andino, 2000).

prib(-)Luc-Wt: The same as prib(+)Luc-Wt but contains a point mutation that inactives the hammerhead ribozyme, thus, the viral transcripts contain about 50 additional non-viral nt at their 5'-end (Herold & Andino, 2000)

prib(+)Xpa: containing the cDNA of the Mahoney strain of poliovirus as well as the hammerhead ribozyme, as described before (Herold & Andino, 2000).

prib(+)Luc-SacI: 5'-TTAAAACAG in addition to a SacI site was introduced 5' of the poliovirus sequence using prib(+)Luc-Wt as the parental plasmid for easier cloning of tandem cloverleaf constructs containing the wild-type cloverleaf at the downstream position.
A PCR was performed using prib(+)Luc-Wt as a template and the primers #3+4. The PCR product was cut with SmaI and BlpI and ligated to the vector prib(+)Luc-Wt, cut with the same enzymes.

pG-Cpair-cloverleaf: The four A-U pairs in *stem a* of the cloverleaf were replaced by four G-C pairs using prib(+)Luc-Wt as the parental plasmid. The complementary sequence of the hammerhead ribozyme was also altered to ensure sufficient cleavage.
Two PCRs were performed using prib(+)Luc-Wt as the template and the two primer sets: #10+11; #4+12. The two resulting fragments were used as a template in an overlapping PCR with the primers #4+10. The final PCR product was cut with XmaI and BlpI and ligated with the vector prib(+)Luc-Wt, cut with the same enzymes; resulting in pG-Cpair-cloverleaf A.
pG-Cpair-cloverleaf A was used as a template in a fourth PCR using primers #4+13. The resulting PCR product was cut with StuI and BlpI and ligated with vector pG-Cpair-cloverleaf A, cut with the same enzymes.

Single cloverleaf mutations:

pStemB-mut(+): Poliovirus replicon containing *stem b* mutation in cloverleaf, that disrupts the *stem b* structure in the plus-strand.
Anneal primers #15+16, then ligate with vector prib(+)Luc-Wt, cut with SmaI and PmlI.

pStemB-mut(-): Poliovirus replicon containing *stem b* mutation in cloverleaf, that disrupts the *stem b* structure in the minus-strand.

Anneal primers #17+18, then ligate with vector prib(+)Luc-Wt, cut with SmaI and PmlI.

pStemB-DNC1: Poliovirus replicon containing *stem b* mutation in cloverleaf, that maintains the structure on both strands.
Anneal primers #77+78, then ligate with vector prib(+)Luc-Wt, cut with SmaI and PmlI.

pStemB-DNC8: Poliovirus replicon containing *stem b* mutation in cloverleaf, that disrupts the structure on the plus-strand.
Anneal primers #79+80, then ligate with vector prib(+)Luc-Wt, cut with SmaI and PmlI.

pStemB-DNC81: Poliovirus replicon containing *stem b* mutation in cloverleaf, that disrupts the structure on the minus-strand.
Anneal primers #81+82, then ligate with vector prib(+)Luc-Wt, cut with SmaI and PmlI.

pStemD-mut(+): Poliovirus replicon containing *stem d* mutation in cloverleaf, that disrupts the structure on the plus-strand.
A PCR was performed using prib(+)Luc-Wt as a template and the primers #24+4. The PCR product was cut with PmlI and BlpI, and then ligated with vector prib(+)Luc-Wt, cut with the same enzymes.

pStemD-mut(-): Poliovirus replicon containing *stem d* mutation in cloverleaf, that disrupts the structure on the minus-strand.
A PCR was performed using prib(+)Luc-Wt as a template and the primers #25+4. The PCR product was cut with PmlI and BlpI, and then ligated with vector prib(+)Luc-Wt, cut with the same enzymes.

pStemD-insert: Poliovirus replicon containing an insertion in stem-loop d that increases the loop.
A PCR was performed using prib(+)Luc-Wt as a template and the primers #26+4. The PCR product was cut with PmlI and BlpI, and then ligated with vector prib(+)Luc-Wt, cut with the same enzymes.

ribozyme(-)constructs: To generate poliovirus replicons with the single cloverleaf mutation in the ribozyme(-) context, a PCR was performed using the respective

ribozyme(+) single cloverleaf mutant plasmid as the template and primers #83+4. The resulting PCR product was cut with PmlI and BlpI, and then ligated with vector prib(-) Luc-Wt, cut with the same enzymes.

Tandem cloverleaf constructs with wild-type cloverleaf downstream

pWt-Wt: Tandem cloverleaf construct with two wild-type cloverleaves next to each other.
A PCR was performed using prib(+)Luc-Wt as a template and the primers # 1+2. The PCR product was cut with SfiI and SacI, and ligated with the vector prib(+)Luc-SacI, cut with the same enzymes.

pStemD-mut(+)-Wt: Tandem cloverleaf construct with a wild-type cloverleaf downstream and a StemD-mut(+) cloverleaf at the 5'-end.
A PCR was performed using pStemD-mut(+) as a template and the primers #1+2. The PCR product was cut with SfiI and SacI, and ligated with the vector prib(+)Luc-SacI, cut with the same enzymes.

pStemD-mut(-)-Wt: Tandem cloverleaf construct with a wild-type cloverleaf downstream and a StemD-mut(-) cloverleaf at the 5'-end.
A PCR was performed using pStemD-mut(-) as a template and the primers #1+2. The PCR product was cut with SfiI and SacI, and ligated with the vector prib(+)Luc-SacI, cut with the same enzymes.

pStemD-insert-Wt: Tandem cloverleaf construct with a wild-type cloverleaf downstream and a StemD-insert cloverleaf at the 5'-end
A PCR was performed using pStemD-insert as a template and the primers #1+2. The PCR product was cut with SfiI and SacI, and ligated with the vector prib(+)Luc-SacI, cut with the same enzymes.

Tandem cloverleaf constructs with G-C pair cloverleaf downstream

pPlus 9: The G-C pair cloverleaf sequence was introduced into the cloverleaf of prib(+)Luc-SacI, resulting in a G-C pair cloverleaf with wild-type 5'-end sequence in addition to a SacI site between the 5'-end sequence and the G-C pair cloverleaf. This

plasmid was used as the parental plasmid for all tandem cloverleaf constructs containing a G-C pair cloverleaf downstream. The SacI-site was used for easier cloning to the tandem construct.
Two PCRs were performed using prib(+)Luc-SacI as the template and the two primer sets: #11+14; #4+12. The two resulting fragments were annealed and used as the template in an overlapping PCR with the primers #4+14. The final PCR product was cut with SacI and BlpI and ligated with the vector prib(+)Luc-SacI, cut with the same enzymes.

pdouble-Luc-Wt: Tandem cloverleaf construct with G-C-pair cloverleaf downstream and wild-type cloverleaf at the 5'-end.
A PCR was performed using prib(+)Luc-Wt as a template and the primers #1+2. The PCR product was cut with SfiI and SacI, and ligated with the vector pPlus9, cut with the same enzymes.

pPlus 20: G-C pair cloverleaf with wild-type *stem a* at the 5'-end.
Anneal primer #5+6, and anneal with vector pPlus9, cut with SmaI and SacI.

pPlus 27: GC-pair cloverleaf with wild-type *stem a* and *stem c* at the 5'-end.
Anneal primer #7+8, and anneal with vector pPlus9, cut with SmaI and SacI.

pdble-StemA-disr: G-C pair cloverleaf downstream and a disrupted *stem a* at the 5'-end.
A PCR was performed using prib(+)Luc-Wt as a template and the primers #9+4. The PCR product was cut with PmlI and BlpI, and annealed with vector prib(+)Luc-Wt, cut with the same enzymes, resulting in prib(+)Luc-StemA-disr.
A second PCR was performed using prib(+)Luc-StemA-disr as a template and the primers #1+2. The PCR product was cut with SfiI and SacI, and annealed with the vector pPlus9, cut with the same enzymes.

pdble-StemB-mut(+): G-C pair cloverleaf downstream and a StemB-mut(+) cloverleaf at the 5'-end.

A PCR was performed using pStemB-mut(+) as a template and the primers #1+2. The PCR product was cut with SfiI and SacI, and ligated with vector pPlus9, cut with the same enzymes.

pdbl-StemB-mut(-): G-C pair cloverleaf downstream and a StemB-mut(-) cloverleaf at the 5'-end.
A PCR was performed using pStemB-mut(-) as a template and the primers #1+2. The PCR product was cut with SfiI and SacI, and ligated with the vector pPlus9, cut with the same enzymes.

pdbl-StemB-swap: G-C pair cloverleaf downstream and StemB-swap cloverleaf (sequences of *stem b* are swapped) at the 5'-end.
Primers #19+20 were annealed, and then ligated with the vector prib(+)Luc-Wt, cut with XmaI and PmlI, resulting in pStemB-swap.
A PCR was performed using pStemB-swap as a template and the primers #1+2. The PCR product was cut with SfiI and SacI, and then ligated with the vector pPlus9, cut with the same enzymes.

pdbl-StemB-shuffle: G-C pair cloverleaf downstream and StemB-shuffle cloverleaf (sequences of *stem b* are randomly shuffled) at the 5'-end.
Primers #21+22 were annealed, and then ligated with the vector prib(+)Luc-Wt, cut with XmaI and PmlI, resulting in pStemB-shuffle.
A PCR was performed using pStemB-shuffle as a template and the primers #1+2. The PCR product was cut with SfiI and SacI, and then ligated with the vector pPlus9, cut with the same enzymes.

pdbl-StemB-ΔPCBP: G-C pair cloverleaf downstream and a cloverleaf with mutation in PCBP-binding site at the 5'-end.
A PCR was performed using prib(+)Luc-Wt as a template and the primers #1+23. The PCR product was cut with PmlI and SfiI, and then ligated with the vector prib(+)Luc-Wt, cut with the same enzymes, resulting in pStemBΔPCBP.
A second PCR was performed using pStemB-ΔPCBP as a template and the primers #1+2. The PCR product was cut with SfiI and SacI, and then ligated with the vector pPlus9, cut with the same enzymes.

pdbl-StemD-mut(+): G-C pair cloverleaf downstream and a StemD-mut(+) cloverleaf at the 5'-end.
A PCR was performed using pStemD-mut(+) as a template and the primers #1+2. The PCR product was cut with SfiI and SacI, and ligated with the vector pPlus9, cut with the same enzymes.

pdbl-StemD-mut(-): G-C pair cloverleaf downstream and a StemD-mut(-) cloverleaf at the 5'-end.
A PCR was performed using pStemD-mut(-) as a template and the primers #1+2. The PCR product was cut with SfiI and SacI, and ligated with the vector pPlus9, cut with the same enzymes.

pdbl-StemD-insert: G-C pair cloverleaf downstream and a StemD-insert cloverleaf at the 5'-end.
A PCR was performed using pStemD-insert as a template and the primers #1+2. The PCR product was cut with SfiI and SacI, and ligated with the vector pPlus9, cut with the same enzymes.

pdbl-StemD-swap: G-C pair cloverleaf downstream and a StemD-swap cloverleaf (sequences of *stem d* are swapped) the 5'-end.
A PCR was performed using prib(+)Luc-Wt as a template and the primers #27+1. The PCR product was cut with SfiI and SacI, and then ligated with the vector pPlus9, cut with the same enzymes.

pdbl-StemD-disr: G-C pair cloverleaf downstream and a StemD-disr cloverleaf (mutation that disrupts the structure on both strands) at the 5'-end.
A PCR was performed using prib(+)Luc-Wt as a template and the primers #28+1. The PCR product was cut with SfiI and SacI, and then ligated with the vector pPlus9, cut with the same enzymes.

pdbl-StemD-Δ3CD: G-C pair cloverleaf downstream and a cloverleaf with mutation in 3CD-binding site at the 5'-end.

A PCR was performed using prib(+)Luc-Wt as a template and the primers #29+1. The PCR product was cut with SfiI and SacI, and then ligated with the vector pPlus9, cut with the same enzymes.

pdbl-StemD-loop: G-C pair cloverleaf downstream and a StemD-loop cloverleaf (mutations in loop sequences) at the 5'-end.
A PCR was performed using prib(+)Luc-Wt as a template and the primers #30+1. The PCR product was cut with SfiI and SacI, and then ligated with the vector pPlus9, cut with the same enzymes.

Tandem cloverleaf constructs with *stem a* mutations:

To introduce mutations in *stem a* of the cloverleaf, three areas needed to be mutated; the two parts of the stem, as well as the complementary sequence of the hammerhead ribozyme had to be altered to ensure sufficient cleavage.
The common cloning strategy if not mentioned otherwise was the following:

1. Perform two PCRs with the primer pair C+D and the primer pair E+#4 with prib(+)Luc-Wt as the template.
2. Overlapping PCR with PCR products from (1) as the template, using the primers C+#4, resulting product was cut with XmaI and BlpI, then anneal with annealed primers A+B. The resulting long product is ligated with the vector prib(+)Luc-Wt, cut with StuI and BlpI. The resulting plasmid is called: prib(+)Luc-stemA-mut.
3. Perform PCR on prib(+)Luc-StemA-mut as the template and the primers #1+2. The PCR product is cut with SfiI and SacI, and then ligated with the vector pPlus9, cut with the same enzymes.

pdbl-StemA-mut1: Primer A: #36; B: #37; C: #38; D: #39; E: #40
pdbl-StemA-mut2: Primer A: #41; B: #42; C: #43; D: #44; E: #45

pdbl-StemA-mut3:

1. Perform two PCRs with the primers #31+32 and the primers #33+4 with prib(+)Luc-Wt as the template.
2. Overlapping PCR with PCR products from (1) as the template, using primers #31+4, cut resulting product with XmaI and BlpI, then ligate with the vector

prib(+)Luc-Wt, cut with the same enzymes. The resulting plasmid is called: prib(+)Luc-StemA-mut3A.

3. Perform PCR on prib(+)Luc-StemA-mut3A as the template and the primers #34+4. The PCR product is cut with StuI and BlpI, and then ligated with the vector prib(+)Luc-StemA-mut3A, cut with the enzymes. The resulting plasmid is called: prib(+)Luc-StemA-mut3.
4. Perform PCR on prib(+)Luc-StemA-mut3 as the template and the primers #1+2. The PCR product is cut with SfiI and SacI, and then ligated with the vector pPlus9, cut with the same enzymes.

pdbl-StemA-mut4: Primer A: #46; B: #47; C: #48; D: #49; E: #50
pdbl-StemA-mut5: Primer A: #51; B: #52; C: #53; D: #54; E: #55
pdbl-StemA-mut6: Primer A: #56; B: #57; C: #58; D: #59; E: #60
pdbl-StemA-mut7: Primer A: #61; B: #62; C: #63; D: #64; E: #65
pdbl-StemA-mut8: Primer A: #66; B: #67; C: #68; D: #69; E: #70
pdbl-StemA-mut9: Primer A: #71; B: #72; C: #73; D: #74; E: #75

pdbl-StemA-mut10: Perform PCR on pG-Cpair-cloverleaf as the template and the primers #1+2. The PCR product is cut with SfiI and SacI, and then ligated with the vector pPlus9, cut with the same enzymes.

pdbl-StemA-disr-virus: Perform PCR on pdbl-StemA-disr as the template and the primers #1+76. The PCR product is cut with AgeI and SfiI, and ligated with vector rib(+)Xpa, cut with the same enzymes.

pdbl-StemA-mut3-virus: Perform PCR on pdbl-StemA-mut3 as the template and the primers #1+76. The PCR product is cut with AgeI and SfiI, and ligated with vector rib(+)Xpa, cut with the same enzymes.

pdbl-StemA-mut8-virus: Perform PCR on pdbl-StemA-mut8 as the template and primers #1+76. The PCR product is cut with AgeI and SfiI, and ligated with vector rib(+)Xpa, cut with the same enzymes.

pdbl-StemA-mut10-virus: Perform PCR on pdbl-StemA-mut10 as the template and the primers #1+76. The PCR product is cut with AgeI and SfiI, and ligated with vector rib(+)Xpa, cut with the same enzymes.

3.213 Expression vector for MBP-2C

An expression vector for the expression of the fusion protein MBP-2C was cloned, using the pMAL-c2E vector from New England Biolabs (NEB, Ipswich, MA) as the parental plasmid. A PCR was performed using prib(+)Luc-Wt as a template and the following primers (to amplify the 2C sequence):

1) 5'-AATTAA**GAATTC***GGTGACAGTTGGTTGAAGAAG*-3' (bold: EcoRI-site; italics: N-terminal of 2C)

2) 5'-TTAATTAAGC**TTACTA***TTGAAACAAAGCCTCCATAC*-3' (bold: stop codon; italics: C-terminal of 2C)

The PCR product was cut with EcoRI and HindIII, and ligated with vector: pMAL-c2E, cut with the same enzymes. The resulting plasmid was called: pMBP-2C. The expression of this plasmid results in a fusion protein of MBP-2C, with MBP at the N-terminal of 2C.

3.214 Coxsackievirus B3 plasmid design

Construction of *cre* mutants. All *cre* mutations were introduced into the CVB3 infectious clone (Klump et al., 1990) by using the Altered Sites in vitro mutagenesis system (Promega, Madison. MA). Selected clones were verified for the correct mutation by using sequence analysis and a BssHII/XbaI digestion was used to ligate the mutated *cre*s into pRibCB3/T7.

pHR-CRE(Art)

Silent mutations disrupting the CRE structure [distortion mutant (DM)] were introduced into p53CB3/T7-Luc, making use of unique BssHII and BstEII restriction sites. The insert was ligated into the luciferase gene-containing vector, creating p53CB3/T7-Luc-DMCRE. A PCR-derived cloning cassette, containing unique restriction sites, was introduced between the luciferase gene and 2A junction by using forward primer 5′-GCCCGGAGCGGCCGCGAAGACGCCAAAAACATA-3′, containing a NotI site (underlined), and reverse primer 5′-GGGGGGGGGTTTAAA*CCGCGG* **CCCGGG** GGCGATCGCAGATCTCAATTTGGACTTTCCGCCCTTCTTGGA-3′, containing five

additional unique sites (DraI, underlined; BglII, dotted line; SgfI, double underlined; XmaI, bold type; SacII, italic type). The PCR product, digested with NotI and DraI, was ligated into p53CB3/T7-Luc-DMCRE digested with NotI and HpaI, generating p53CB3/T7-Luc-linker DMCRE. By using infectious clones containing wild-type or CRE loop point mutants as a template, CRE-containing PCR products were generated with forward primer 5′GGGGGGGGGAGATCTGCGATCGCC*GCACTTTTCCAAGGA* GAGAAGAAGATGAGCAATTACATACAGTTCAA-3′ and reverse primer 5′-GGGGGGGGGCCGCGGCCCGGGGCTCCCGTGCAGGAGCAAACATACAGGTTCAA -3′, and inserted into p53CB3/T7-Luc-linker-DMCRE by using BglII and SacII (underlined)-digested fragments, creating pGG-CRE(Art). The PCR product contained an additional $3CD^{pro}$ cleavage sequence (italic type) to cleave off appending protein sequences at the carboxy-terminal end of the luciferase enzyme, due to translation of translocated CRE sequences that might affect luciferase activity. Subsequently, by using a SalI and ApaI digestion of constructs p53CB3/T7-Luc-linker-DMCRE and pRibCB3/T7, the hammerhead ribozyme sequence was ligated into the p53CB3/T7-Luclinker vector rendering pHR-CRE(Art).

Oligonucleotide site-directed mutagenesis. Oligonucleotide-directed mutagenesis was performed by using phagemid pALTER-1 as described previously (Melchers et al., 1997). Synthetic oligonucleotides (Biolegio, see 3.215) were used to introduce site-specific mutations. The mutated fragments were cloned into the infectious cDNA clone (pRibCB3/T7) and sequence analysis was used to verify the mutated nucleotide sequence.

3.215 Primers used for mutagenesis of *cre*-mutants

Underlined nucleotides indicate mutations from the wild-type sequence.

DM	5’-AGGGCTCCCGTGCAGGAGCAAGCAAACCGGTTCTATCCTACACTTACTTTTAAATTGAA TATAATTGCTCATCTTCTTCTC-3’
DM+A_5G	5’-AGGGCTCCCGTGCAGGAGCAAGCAAACCGGTTCTATCCTACACTCACTTTTAAATTG AATATAATTGCTCATCTTCTTCTC-3’
CRE PM1	5’-AATACGGCATTTGGAGTTGAACTGTATGTAATTGC-3’
CRE PM2	5’-AATACGGCATTTGGATTTGAACTGTATGTAATTGC-3’
CRE PM3	5’-ACAGGTTCAATACGGCATTGGGACTTGAACTGTATG-3’
CRE PM4	5’-ACAGGTTCAATACGGCATTCGGACTTGAACTGTATG-3’
CRE PM5	5’-ACAGGTTCAATACGGCATTAGGACTTGAACTGTATG-3’
CRE PM6	5’-ACAGGTTCAATACGGCATCTGGACTTGAACTGTATG-3’
CRE PM7	5’-ACAGGTTCAATACGGCATGTGGACTTGAACTGTATG-3’
CRE PM8	5’-ACAGGTTCAATACGGCATATGGACTTGAACTGTATG-3’

CRE PM9 5'-ACAGGTTCAATACGGCACTTGGACTTGAACTGTATG-3'
CRE PM10 5'-ACAGGTTCAATACGGCAGTTGGACTTGAACTGTATG-3'
CRE PM11 5'-ACAGGTTCAATACGGCAATTGGACTTGAACTGTATG-3'
CRE PM12 5'-ACAGGTTCAATACGGCGTTTGGACTTGAACTGTATG-3'
CRE PM13 5'-ACAGGTTCAATACGGCTTTTGGACTTGAACTGTATG-3'
CRE PM14 5'-CAAACATACAGGTTCAACACGGCATTTGGACTTG-3'
CRE PM15 5'-CAAACATACAGGTTCAAGACGGCATTTGGACTTG-3'
CRE PM16 5'-CAAACATACAGGTTCAAAACGGCATTTGGACTTG-3'
CM 5'-ACAGGTTCAATACGGTGTTTGGACTTGAACTGTATG-3'

3.22 PCR protocols

Standard PCR protocol: Using the primers described for the cloning of the different plasmids, the desired region was amplified in a standard PCR reaction using 10-50 ng of template DNA, 1 x PCR reaction buffer (Stratagene, Cedar Creek, TX), 0.4 µM forward and reverse primer, 200 µM dNTP, 2.5 U Pfu Turbo DNA polymerase (Stratagene) and H_2O to 50 µl. The DNA was amplified with the following program:

- Denaturing for 2 min at 94°
- 30-33 cycles of : 30 seconds at 94°, annealing for 30 seconds at 50-60°C (depending on the annealing temperature of the used primers), elongation for 1 min per 1000 bp at 72°C
- Elongation for 8 min at 72°C

Overlapping PCR:

For an overlapping PCR, two PCR reactions were performed using two different sets of primers. The resulting PCR products had overlapping regions and were used in equal molar ratios as the template in a third PCR. Here, 3 cycles were performed without primers. The overlapping regions of the two DNA fragments should anneal and the annealed regions function as the primers to fill up the single-stranded regions, resulting in one long double-stranded template. After 3 cycles, the PCR is paused, and two primers binding to the two ends of the long template are added, and then 30 more cycles following the standard PCR protocol is performed.

The amplified DNA fragments were then analyzed on a 0.8 -1% agarose 0.5 x TBE gel containing ethidium bromide (50 ng/ml), using 0.5 x TBE as running buffer. The DNA was mixed with DNA loading buffer (NEB). The bands were visualized under UV light.

10 x TBE buffer:
108 g Tris base
55 g Boric acid
40 ml 0.5 M EDTA (pH 8.0)
add H_2O to 1 l

3.23 Restriction digest

Restriction enzymes used for restriction digests were usually purchased from NEB, and the reactions were set up in the manufacturer's recommended buffer and incubated at the recommended temperature. When possible, double digests were set up. The resulting DNA fragments were either gel purified using the QIAquick gel extraction kit (Qiagen, Valencia, CA) or purified using the QIAquick PCR purification kit (Qiagen).

3.24 Ligation and transformations

Ligation reactions were done in a 10 µl reaction containing about 3-5 molar excess of insert to vector (using about 50 ng vector DNA), 400 U T4 DNA Ligase (NEB) and 1x Ligase buffer (NEB). The reaction was incubated over night at 16°C. The reaction was dialyzed against H_2O by incubating 5 µl of the reaction on top of a nitrocellulose membrane that was floating on the surface of a beaker filled with H_2O for 10 min. The ligation reaction was then transformed into 10 µl ElectroMAX™ DH5α-E™ Cells (Invitrogen, Carlsbad, CA) in 0.1 cm cuvettes in a total volume of 40 µl using an Electro Cell Manipulator 600 (BTX, Holliston, MA) with the following settings: 1.4 kV, 129 Ω. 460 µl of LB medium was added and 100 µl of the bacteria was plated on an LB plus ampicillin (100 µg/ml) plate and incubated at 37°C over night to allow for single colony formation. Individual colonies were picked and transferred into 5 ml of LB medium containing 100 µg/ml ampicillin, and incubated shaking over night at 37°C. The DNA was purified using the QIAprep spin mini prep kit (Qiagen). All plasmids were sequenced on an ABI 3730xl sequencer (by Elim Biopharmaceuticals, Hayward, CA), using plasmid specific primers.

3.25 DNA preparations

To achieve higher yields of plasmid DNA, single bacterial colonies (transfected with a plasmid) were grown in 100-200 ml of LB medium supplemented with ampicillin over night at 37°C. Plasmid DNA was then purified using either the PureYield Midiprep System (Promega) or the QIAfilter plasmid midi kit (Qiagen).

3.26 Transcription of viral RNA

Poliovirus-specific plasmid DNA was linearized with ApaI. Coxsackievirus B3-specific plasmid DNA was linerarized with MluI. RNAs were transcribed *in vitro* in reactions

containing bacteriophage T7 RNA polymerase, 1 x transcription buffer (80 mM HEPES-KOH (pH 7.5), 24 mM $MgCl_2$, 2 mM spermidine, 40 mM DTT) and 7.5 mM NTP-mix. After incubation at 37°C for 3 h, 2 U DNaseI (Roche, Indianapolis, IL) was added and reactions incubated at 37°C for 15 min. RNA was precipitated by adding 50% (in volume) of $LiCl_2$-solution (7.5mM LiCl2; 50 mM EDTA, pH 8.0) and incubation over night at -20°C. After centrifugation at 12,000 g for 20 min, the pellet was washed once with 70% ethanol. The RNA was then resuspended in RNA storage solution (Ambion), and stored in aliquots at -80°C. The RNA was analyzed on a 0.8% agarose gel, 0.5 x TBE, and quantified measuring A_{260} and A_{280}.

3.27 *In vitro* translation replication system

3.271 HeLa S10 extract

3 liters of HeLa S3 spinner culture was harvested by centrifugation at 300 g for 12 min at 4°C. The supernatant was removed and the cells washed three times in 40 ml of isotonic buffer (35 mM HEPES, pH 7.4; 146 mM NaCl; 11 mM glucose). After the last wash, the cells were resuspended in 1 volume of ice-cold hypotonic buffer (20 mM HEPES, pH 7.4; 10 mM KCl; 1.5 mM magnesium acetate; 1 mM DTT) and incubated for 10 min on ice. The cells were disrupted by 25 strokes in a pre-chilled dounce homogenizer (Bellco, Vineland, NJ), using pestle B. 0.1 volume of ice-cold 10 x resuspension buffer (200 mM HEPES, pH 7.4; 1200 mM potassium acetate; 40 mM magnesium acetate; 50 mM DTT) was added and immediately placed on ice. The lysate was centrifuged at 2000 rpm for 10 min at 4°C (TOMY MTX-150). The supernatant was transferred into a new tube and both tubes were then again centrifuged at 9000 rpm for 10 min at 4°C. The supernatant of both tubes were combined and dialyzed for 2 x 1 h (with a buffer change after 1 h) against 500 volumes of dialysis buffer (40 mM HEPES, pH 8.0; 120 mM potassium acetate; 5.5 mM magnesium acete; 10 mM potassium chloride; 6 mM DTT), using the Slide-A-Lyzer cassettes (10,000; Pierce, Rockford, IL). After dialysis, 1/1000 volume 1 M $CaCl_2$, and 75 U/ml S7 Micrococcal Nuclease (resuspended in 1 mM Tris, pH 7.5; Roche) were added, and the extract was incubated for 15 min at room temperature. To quench the reaction, 1/100 volume 200 mM EGTA was added. After centrifugation at 9000 rpm for 10 min at 4°C (TOMY MTX-150), the supernatant was frozen in aliquots at -80°C.

3.272 Initiation factor

Uninfected HeLa cells were harvested and homogenized as described above for the preparation of the S10 extract. After homogenization, the nuclei were removed by centrifugation without the addition of any buffer or salt. The postnuclear supernatant was centrifuged for 15 min at 10,000 rpm at 4°C in a JA-20 rotor. The S10 supernatant was centrifuged at 60,000 rpm for 1 h at 4°C in a Beckman 70 Ti rotor to pellet the ribosomes. The supernatant was discarded, and the ribosomal pellet was resuspended in hypotonic buffer at 240 A_{260} U/ml. The ribosomes were adjusted to a concentration of 0.5 M KCl by the addition of 4 M KCl and stirred for 15 min on ice. The salt-washed ribosomes were centrifuged at 60,000 rpm for 1 h in a 70 Ti rotor at 4°C, and the supernatant was removed and dialyzed for 2 h at 4°C against solution containing 5 mM Tris-HCl (pH 7.5), 100 mM KCl, 0.05 mM EDTA, 1 mM DTT, and 5% glycerol. This ribosomal salt wash IF preparation was frozen in aliquots at -80°C.

3.273 Translation replication assay

1 µg RNA transcripts were mixed with 25 µl HeLa S10 cell extract, 2 µl initiation factors, 5 µl 10 x NTP/energy mix (10 mM ATP, 2.5 mM CTP, 2.5 mM GTP, 600 mM potassium acetate, 300 mM creatine phosphate, 155 mM HEPES (pH 7.0), 0.4 mg Creatine Kinase / 100µl), and 1 µl 100 mM guanidine hydrochloride in a total volume of 50 µl. After incubation at 30°C for 4 h, 1 µl was removed and added to 50 µl cell culture lysis reagent (Promega, Madison, WI) of which 10 µl was then used to measure luciferase activity to monitor translation. The rest of the original translation reaction was centrifuged at 12,000 g for 15 min, the supernatant was carefully removed, and the preinitiation complexes were resuspended in 25 µl labelling mix, containing 15 µl HeLa S10 cell extract, 2.5 µl 10 x NTP/energy mix, 2.5 µl of puromycin (1mg/ml) and 30 µCi [α-^{32}P]-UTP (3000Ci/mmol) (Perkin Elmer, Waltham, MA). After incubation at 30°C for 2 h (if not indicated otherwise), the samples were mixed with 175 µl TENSK buffer (50 mM Tris/HCl (pH7.5), 5 mM EDTA, 100 mM NaCl, 1% (v/v) SDS, 200 µg/ml proteinase K) to stop the reaction. After incubation at 37°C for 2 h, RNA was extracted by using 1 volume phenol/chloroform (1:1, v/v), and RNA was precipitated by using ethanol. The pellet was resuspended in RNA-storage solution (Ambion) and gel-loading buffer (New England Biolabs, Ipswich, MA) was added prior to loading on a 0.8% agarose gel (0.5 x TBE). The gel was run at 20 V constant current over night. After drying the gel,

products were visualized by using autoradiography. Bands were quantified using a phosphorimager (Typhoon 9400; GE Healthcare, Piscataway, NJ)

Coxsackie virus B3 *in vitro* assay:

For replication of coxsackievirus B3 RNA transcripts *in vitro*, 2 µg rather than 1 µg of RNA transcripts were used to program the HeLa S10 extract.

In order to quantify the accumulated replicative form (RF) bands, irrespective of loading and RNA-extraction efficiency, the amount of [^{32}P]UMP incorporated in both the RF and the 28S rRNA was determined by using a phosphorimager (Storm 860; Molecular Dynamics). The amount of 28S rRNA in each lane represents the amount of RNA loaded on the gel and was normalized to wild-type. Subsequently, the accumulated RF was corrected for the amount loaded on the gel.

3.274 VPg-uridylylation assay with poliovirus replicons

HeLa S10 cell extract was programmed with replicon RNA as described in 3.282. Pre-initiation complexes were resuspended as decribed above with incubation for 1 h rather than 2 at 30°C. The synthesis of VPgpUpU was then detected by the two methods described below:

(i) Method 1: After centrifugation of the reactions at 12,000 g for 15 min, the supernatant was removed and the replication-complexes were resuspended in 40 µl Tricine-sample buffer (Bio-Rad, Hercules, CA). The samples were heated at 94°C for 5 min, and then analyzed on a 20% Tris-Tricine gel (see below) at 75 mA for 1 h and then for 72 h at 11 mA at 4°C. After drying the gel, products were visualized by using autoradiography using a phosphorimager (Typhoon 9400; GE Healthcare, Piscataway, NJ).

(ii) Method 2: 500 µl Dynabeads®ProteinA (Invitrogen, Carlsbad, CA) were washed twice with 0.1 M NaPhosphate buffer (pH8.0) and then resuspended in 500 µl of the same buffer. 125 µl of anti-VPg polyclonal antibodies was added to the Dynabeads®ProteinA and incubated rotating for 1 h at room temperature. The Dynabeads® were washed twice again and resuspended in 500 µl 0.1 M NaPhosphate buffer (pH8.0). After the 1 h incubation of the replication reaction as described above, 2.5 µl of 0.5 M NaPhosphate buffer and 25 µl of the Dynabeads®ProteinA coupled with anti-VPg antibodies were added. After incubation rotating at 4°C for 1 h, the Dynabeads® were washed four times with phosphate-buffered saline (PBS). The

Dynabeads® were resuspended in 15 µl of Tricine-sample buffer (Bio-Rad, Hercules, CA). The samples were heated at 94°C for 5 min and the supernatant was analyzed on a 20% Tris-Tricine gel at 75 mA for 1 h and then for 72 h at 11 mA at 4°C. After drying the gel, products were visualized by autoradiography using a phosphorimager (Typhoon 9400; GE Healthcare, Piscataway, NJ).

Tricine gel buffer: 3 M Tris, 0.3 % SDS, pH 8.45

Tricine running buffer: 0.1 M Tris, 0.1 M Tricine, 0.1 % SDS

20 % Tricine-gel: 20 ml gel buffer, 30 ml 40 % acrylamide/bis (29:1), 8 g glycerol
adjust volume to 60 ml
add 600 µl 10 % APS, and 60 µl TEMED

Stacking gel: 2 ml gel buffer, 833 µl 40 % acrylamide/bis (29:1), 5.5 ml H_20
add 250 µl 10 % APS and 25 µl TEMED

3.3 Cell culture and viruses

3.31 Cultured cells

3.311 HeLa S3 cells

HeLa S3 cells (ATCC CCL 2.2) were grown either (i) in tissue culture flasks in Dulbecco's modified Eagle medium-nutrient mixture F-12 (Ham) (DMEM/F12) (1:1), supplemented with 2mM L-glutamine, 100 U of penicillin and streptomycin per ml, and 10% newborn calf serum or (NCS) (ii) in suspension, in suspension minimal essential medium (Joklik modified, Cambrex) supplemented with 2 mM L-glutamine, 100 U of penicillin and streptomycin per ml, and 10% newborn calf serum. All medium and supplements (if not mentioned otherwise) were purchased from Cell Culture Facility (UCSF, San Francisco, CA). Cells were incubated at 37°C and 5% CO_2.

3.312 Buffalo green monkey (BGM) cells

BGM cells were grown in minimal essential medium (Invitrogen) supplemented with 10% fetal bovine serum (Invitrogen).

3.32 Transfections

3.321 Poliovirus RNA transfection and luciferase assay

HeLa S3 cells were trypsinized, washed three times with PBS, and adjusted to 5 x 10^6 cells/ml. Then 800 µl aliquots were electroporated in 0.4 cm cuvettes with 20 µg of replicon RNA, using an Electro Cell Manipulator 600 (BTX Inc.) with the following settings: 300 V, 1000 µF, 24 Ω. Subsequently, 16 volumes of medium was added, the cells were divided by half and guanidine hydrochloride (Sigma Chemical Co., St. Louis, MO) was added to one half to a final concentration of 2 mM. 2 x 10^5 cells were plated per well in 12-well plates and incubated at 37°C in a 5% CO_2 incubator until harvested for luciferase assay at indicated time-point. Replicon-transfected cells were scraped off, washed once with PBS, and then lysed in 100 µl cell culture lysis reagent (Promega, Madison, WI). Luciferase activity in 10 µl of lysate was determined in a luminometer using the luciferase assay system (Promega).

3.322 CVB3 RNA transfection and luciferase assay

BGB cells, grown in six-well plates to a confluency of 80%, were transfected as described previously with 4 µg T7 RNA polymerase-generated RNA derived from MluI-linearized replicon plasmid, containing the firefly luciferase gene. Ten hours post-transfection, cells were washed twice with PBS, prior to lysis using 200 µl lysis buffer (Promega). Luciferase activity was measured on a BioOrbit 1251 luminometer using the Luciferase Assay system according to the recommendations of the manufacturer (Promega).

3.33 Virus production of rib(+)Xpa and double-Wt

In vitro RNA transcripts of rib(+)Xpa and double-Wt were electroporated into HeLa S3 cells under the same conditions as described in 3.221, using 20 µg of viral RNA transcripts and 4 x 10^6 cells. After electroporation 5 volumes of medium supplemented with 3% newborn calf serum was added. Cells were then incubated at 37°C and 5% CO_2 over night. After three freeze/thaw cycles viruses were further clarified through centrifugation at 3000 g for 5 min and the virus supernatant was stored at -80°C (P0) virus. The titers of the virus were determined according to standard plaque-assay (see 3.33).

3.34 Plaque-assay

6-well plates were seeded with 10^6 HeLa cells/well and incubated over night at 37°C and 5% CO_2. The next day, the cells were washed once with PBS. Virus supernatant was diluted in a 1:10 dilution series in serum-free DMEM/F12 medium. 250 µl of virus dilution was added / well. The cells were incubated with the virus for 30 min at 37°C and 5% CO_2 to allow virus adsorption. The medium was removed and the cells were washed once with PBS. Each well was overlayed with 3 ml of 1% agarose in 1 x DMEM/F12 medium supplemented with 3% newborn calf serum. Once the agarose had solidified, the plates were incubated for 2 days (if not indicated otherwise) at 37°C and 5% CO_2. Agarose overlays were then removed, and plates were stained with a vital dye (0.1% crystal violet, 20% ethanol) to reveal the viral plaques, which were counted.

3.35 Growth curve with rib(+)Xpa and double-Wt

6-well plates were seeded with 10^6 HeLa S3 cells/well and incubated over night. Cells were washed with PBS and infected with a multiplicity of infection (MOI) of 10 of either rib(+)Xpa or double-Wt viruses (P0 virus) in serum-free medium. After incubation at 37°C for 30 min, cells were washed twice with PBS and fresh medium supplemented with 3% newborn calf serum was added to each well. The plates were incubated at 37°C and 5% CO_2. At indicated time-points viruses were harvested by three freeze/thaw cycles followed by centrifugation. The supernatant contained the virus and was stored at -80°C. The titers of the virus were determined by standard plaque assay (see 3.34).

3.36 Virus production of mutant poliovirus and plaque-purification

In vitro RNA transcripts of mutant polioviruses were transfected into HeLa S3 cells in the same conditions as described in 3.231 using 20 µg of viral RNA transcripts and 4 x 10^6 cells. After electroporation 5 volumes of medium was added. Cells were then incubated at 37°C and 5% CO_2 for 72 hours or until total cytopathic effect was reached. After three freeze/thaw cycles viruses were further clarified through centrifugation at 3000 g for 5 min and the virus supernatant was stored at -80°C (P0) virus. The plaque-phenotype was determined by plaque-assay (see 3.34).

For plaque-purification of viruses, individual plaques were transferred with a pipette tip to 6-well-plates (seeded with 10^6 cells/well the night before) to which 500 µl of fresh

medium/well was added. The 6-well plates were incubated for 72 hours. After three freeze/thaw cycles viruses were further clarified through centrifugation at 3000 g for 5 min. Total RNA from the supernatant was purified by trizol® extraction (Invitrogen) and isopropanol precipitation by the following protocol: to 500 µl of viral suspension 500 µl of trizol reagent was added and incubated for 5 min at room temperature (RT). 100 µl of chloroform was added, and the tube was shaken by hand and incubated for 3 min at RT. After centrifugation for 4 min at 12,000 g at 4°C, the supernatant was transferred to a new tube. The RNA was precipitated by adding 250 µl of isopropanol, and the tube was mixed by inverting several times, and then incubated for 10 min at RT. The RNA was pelleted by centrifugation at 12,000 g for 10 min at 4°C. The isopropanol was removed. The pellet was washed once with 500 µl 75% ethanol. After centrifugation at 12,000 g for 5 min at 4°C, the supernatant was carefully removed. The pellet was air dried for 5 min and resuspended in 15 µl RNase-free water and stored at -80°C.

3.361 RT-PCR of plaque-purified viruses and sequencing

cDNA was synthesized using the Thermoscript^{TM} RT-PCR system for First-Strand cDNA Synthesis (Invitrogen, Carlsbad, CA): in a PCR tube, 10 µl of the resuspended RNA was mixed with dNTPs (final concentration 0.5 mM) and 1 µl dT primer. The tube was incubated for 5 min at 65°C, then placed on ice. 4 µl 5 x RT reaction buffer, 1 µl RNase OUT, 5 mM DTT, and 1 µl of Thermoscript was added to the tube in a total volume of 20 µl, incubated at 50°C for 1 hour and then stored at 4°C.

Using specific primers for the poliovirus genome, the viral genome was amplified in a PCR reaction: 1 x PCR reaction buffer (Invitrogen), 1.5 mM $MgCl_2$, 2 µl RT reaction (from previous step), 0.4 µM forward and reverse primer, 200 µM dNTP, 2.5 U Taq DNA polymerase (Invitrogen) and H_2O to 50 µl. The DNA was amplified with the following program:

- Denaturing for 2 min at 94°
- 33 cycles of : 30 seconds at 94°, annealing for 30 seconds at 55°C, elongation for 1 min per 1000 bp at 72°C
- Elongation for 8 min at 72°C

The amplified DNA fragments were then sequenced (by Elim Biopharmaceuticals) using poliovirus specific primers.

3.362 5'-RACE

The 5'-RACE system for rapid amplification of cDNA ends (Invitrogen) was used to amplify the very 5'-end of the plaque-purified virus RNA. With this system, cDNA is synthesized from the purified viral RNA using a virus-specific reverse primer located within the capsid region. After first strand cDNA synthesis, the original RNA template is removed by RNase treatment with the RNase mix. Unincorporated dNTPs, primer, and proteins are separated from cDNA using a S.N.A.P. column. A homopolimeric tail is then added to the 3'-end of the cDNA using terminal transferase (TdT) and dCTP. PCR amplification is then accomplished using Taq DNA polymerase, a nested, 5'UTR specific viral primer that anneals to a site located within the cDNA molecule, and a novel deoxyinosine-containing anchor primer provided with the system.

cDNA-production: After the trizol extraction and isopropanol precipitation 14.5 µl of RNA and 0.5 µM reverse primer (specific for the capsid region of poliovirus) were mixed and incubated for 10 min at 70°C, and then put on ice. A reaction containing the RNA, the reverse primer, 1 x PCR-buffer, 1 mM $MgCl_2$, 0.4 mM dNTPs and 4 mM DTT in a total volume of 25 µl was incubated for 1 min at 42°C. 1 µl of Superscript II was added, and the reaction was subsequently incubated for 50 min at 42°C, then for 15 min at 70°C, and then for 1 min at 37°. 1 µl of RNase mix was added and the reaction incubated for 30 min at 37°C and then put on ice.

Purification of cDNA: The cDNA was purified using the provided S.N.A.P. columns according to the manufacturer's protocol.

dC-tailing of cDNA: 10 x tailing buffer (to a final concentration of 1 x) and 0.2 mM dCTPs in a volume of 7.5 µl was added to 16.5 µl of purified cDNA. The reaction was incubated for 2 min at 94°C, then transferred on ice. 1 µl of TdT was added and incubated for 37°C, followed by incubation for 10 min at 65°C and then transferred on ice.

PCR of dC-tailed cDNA: Using one specific reverse primer for the poliovirus 5'UTR and one forward primer that binds to the poly(C) tail of the cDNA, the viral genome was amplified in a PCR reaction containing: 1 x PCR reaction buffer (Invitrogen), 1.5 mM $MgCl_2$, 5 µl dC-tailed cDNA (from previous step), 0.2 µM forward and reverse primer, 200 µM dNTP (Invitrogen), 2.5 U Taq DNA polymerase (Invitrogen) and H_2O to 50 µl. The DNA was amplified with the following program:

- Denaturing for 2 min at 94°

- 35 cycles of : 30 seconds at 94°, annealing for 30 seconds at 55°C, elongation for 1 min at 72°C
- Elongation for 8 min at 72°C

If the yield of this PCR was too low, another nested PCR was performed using the previous PCR product as a template. The amplified DNA fragments were gel purified using the QIAquick gel extraction kit (Qiagen), then sequenced on an ABI 3730xl sequencer (by Elim Biopharmaceuticals) using poliovirus specific primers.

3.4 Biochemistry

3.41 Purification of anti-2C and pre-immune serum

Anti-2C polyclonal antibodies were obtained commercially by the inoculation of the 2C C-terminal peptide (CNIGNCMEALFQ) conjugated to KLH into rabbits (HTI Bioproducts, Ramona, CA). 2 ml of anti-2C polyclonal antibodies and 2 ml of pre-immune serum taken before inoculation, were purified on an Äkta FPLC (GE Healthcare, Piscataway, NJ) using a 1 ml HiTrap Protein A column (GE Healthcare). The serum was mixed 1:5 with 20 mM NaPhosphate buffer (pH 7.0) before loading onto the column. The column was washed twice with 20 ml of 20 mM NaPhosphate buffer (pH 7.0). The antibodies were eluted with 0.1 M citric acid (pH 4.0) in 500 µl fractions into collection tubes which each contained 125 µl of 1 M Tris-HCl (pH 9.0). Fractions were tested for their specific recognition of 2C protein in Western Blots (see 3.43)

3.42 Expression and purification of MBP-2C

Expression: 20 ng of pMBP-2C was transformed into 5 µl ElectroMAX™ DH5α-E™ Cells (Invitrogen) in 0.1 cm cuvettes in a total volume of 40 µl using an Electro Cell Manipulator 600 (BTX) with the following settings: 1.4 kV, 129 Ω. 100 µl of a 1:10 dilution of the bacteria was plated on an LB plus ampicillin plate and incubated at 37°C over night to allow for single colony formation. An individual colony was picked and transferred into 40 ml of LB medium containing 100 µg/ml ampicillin and 0.2 % glucose, and incubated shaking at 37°C over night. The next day, the 40 ml culture was transferred into 2 l of LB medium also supplemented with ampicillin and glucose and incubated shaking at 37°C until A_{600} = 0.6 was reached (approximately 3.5 h). The culture was then induced by adding 600 µl of 1 M IPTG (final = 0.3 mM IPTG) and

incubated shaking for 2 h at 37°C. The cells were harvested by centrifugation at 6000 g for 15 min at 4°C. The supernatant was removed and the cells washed once with 20 ml of PBS. The pellet was stored at -80°C.

Purification: 4 ml of Amylose resin (NEB) was washed three times with 4 ml column buffer (10 mM Na-phosphate-buffer, pH 7.2; 0.5 M NaCl; 1 mM DTT; 1 mM EGTA), then resuspended in 45 ml of column buffer. The pellet of 2 l cells was thawed quickly at 37°C and resuspended in 5 ml lysis buffer (10 mM Naphosphate-buffer, pH 7.2; 0.5 M NaCl; 0.25% Tween 20; 1 mM DTT; 10 mM EDTA; 10 mM EGTA). The cells were broken by 5 cycles of 40 seconds each of sonication using a microtip (pulse on/off = 1 second/1 second) at setting 4 on ice. The cell lysate was added to the 45 ml of amylose resin from the previous step, and incubated rotating for 2 h at 4°C. The lysate/resin mix was poured onto an empty column and the flow-through was collected. The column was washed once with 10 ml of column buffer containing 0.25 % tween, and then washed once with 40 ml column buffer. The protein was eluted with 13 ml of column buffer containing 10 mM maltose and 1 ml fractions were collected. 10 µl of each fraction was mixed in equal amounts with Laemmli-loading buffer (Bio-Rad) and analyzed on an SDS-polyacrylamide gel (ReadyGel, Precast SDS-PAGE Gels, 12% Tris-HCL, 10 Well; Bio-Rad). The gel was stained with Commassie blue (100 ml acetic acid, 900 ml ddH_20:Methanol (1:1), 2.5 g Commassie blue G-250), then destained (100 ml acetic acid, 900 ml ddH2O:Methanol (1:1)), and then photographed using a gel-imaging system (FluorChem^{TM}8900, Alpha Innotech, San Leandro, CA). The fractions with the biggest yield were combined and dialyzed in Slide-A-Lyzer Dialysis cassette (Pierce) against column buffer containing 10% glycerol. After dialysis the protein was concentrated using Amicon ultra centrifugal filter device (10,000 MW, Millipore, Billerica, MA) by spinning at 4000 g for 30 min at 4°C. The protein concentration was determined by measuring the A_{280} in the presence of 6 M guanidine hydrochloride and using the following absorbance coefficients: 111 270 $M^{-1}cm^{-1}$.

3.43 Western Blot with anti-2C

Testing purified anti-2C and pre-immune serum: 10 µl of cell extract from MPB-2C induced and non-induced cells after sonication in lysis buffer (see 3.42) was mixed with 10 µl of Laemmli-loading buffer, incubated for 5 min at 94°C (Bio-Rad, Hercules, CA), and separated on an SDS-PAGE (ReadyGel, Precast SDS-PAGE Gels, 10% Tris-HCL, 10 Well; Bio-Rad; Running-buffer: 25 mM Tris, 0.192 M glycine, and 0.1% SDS (pH

8.3)). The gel was transferred in a wet transfer onto nitrocellulose membrane (Bio-Rad) using the Bio-Rad Mini-PROTEAN system (Bio-Rad) for 1 h at 450 mA in transfer buffer. After transfer, the membrane was blocked for 1 h shaking with 5 % non-fat milk in TBST (Tris-Buffered Saline Tween 20, see below). The membrane was blotted with either the purified anti-2C antibodies or pre-immune serum (see 3.41) diluted 1:500 in 5% non-fat milk in TBST by shaking for 1 h. The membrane was washed 5 times for 5 min each with TBST shaking. Then, the membrane was blotted with the secondary antibodies ECL^{TM} anti-rabbit IgG, horseradish peroxidase linked (from donkey, GE Healthcare, Piscataway, NJ) diluted 1:10,000 in 5% non-fat milk in TBST by shaking for 1 h. The membrane was washed 5 times for 5 min each with TBST. After the final wash the bands were visualized using the SuperSignal West Pico Chemiluminescent Substrate (Pierce) and the exposed films were scanned.

Testing fractions after MBP-2C purification: The fractions of purified MBP-2C protein as analyzed on SDS-PAGE and Commassie blue staining in 3.42 were also detected by Western Blot using anti-2C antibodies, in the same way as described in the above section.

Transfer buffer:

75 ml of 10 x transfer buffer (30.3 g Tris base, 144 g glycine, in1 l distilled water, adjust pH with HCl to pH 8.3)
150 ml methanol
fill up with H_2O to 750 ml

TBST:

- Dissolve the following in 800 ml of distilled H_2O: 8.8 g of NaCl, 0.2 g of KCl, 3 g of Tris Base
- Add 500 µl of Tween 20
- Adjust the pH to 7.4
- Add distilled H_2O to 1 l

3.44 Mobility shift assay with MBP-2C

Probe preparation: A DNA fragment containing the T7 promoter, the hammerhead ribozyme sequences and the cDNA of the wild-type positive-strand cloverleaf, was generated in a standard PCR reaction using prib(+)Luc-Wt as a template and the following primers: forward 5'- GCAGAGGCCGAGGCCGCCTCGGCCTCTGAG

CTATT-3' and reverse 5'-GAACTTGGTTTTGTGCGTCTAAGTAAC-3'. A second DNA fragment was generated containing the T7 promoter and the cDNA of the wild-type negative-strand cloverleaf using prib(+)LucWt as a template and the following primers: forward 5'-TTAATTTAATACGACTCACCTATAGGCCTTCTATTGAACTTGGTTTTG-3' and reverse 5'-TTAAAACAGCTCTGGGGTTGTAC-3'. The PCR fragments were purified using the QIAquick PCR purification kit (Qiagen). 12 µl of the PCR product was used in a transcription reaction containing 1 x transcription buffer (80 mM HEPES-KOH, pH 7.5; 24 mM $MgCl_2$; 2 mM spermidine; 40 mM DTT), 5 µl NTP-mix (500 µM UTP, 4 mM ATP, GTP, CTP), 25 µCi [α^{32}P]UTP (800 Ci / mmol; Perkin Elmer), and 0.5 µl T7 RNA polymerase. The reaction was incubated for 2 h at 37°C. 25 µl of formamide-loading buffer (90% formamide, 1 x TBE, 0.5% bromphenolblue) was added to the reaction.

Gel-purification of probes: The complete RNA reaction was separated on an 8% acrylamide / UREA gel (13.25 ml 30% acrylamide/bis (37.5:1)), 1 x TBE, 21 g UREA, add H_2O to 50 ml, then add 500 µl of 10% APS and 50 µl TEMED. The gel was run at 15 W for 40 min. The gel was exposed for 5 seconds to a film, by matching the film and the gel, the bands were cut out and soaked over night at 37 °C in 700 µl NaOAc (0.3 M), 0.1% SDS (pH 7.0). After the overnight elution, the gel pieces were removed, 1 µl of yeast tRNA (10 mg/ml), and 1 volume of phenol/chloroform/Isoamylalcohol (25:24:1, v/v) was added to precipitate the labeled RNA. After centrifugation at 12,000 g for 3 min the upper phase was transferred to a new tube and 600 µl of Isopropanol was added. The RNA was precipitated over night at -20°C. The RNA was pelleted by centrifugation at 12,000 g for 40 min at 4°C, washed once with 70% ethanol, and air-dried for 5 min. CPM was measured of the RNA pellet in a scintillation counter (LS6500, Beckman Coulter, Fullerton, CA). The RNA was resuspended in HMK buffer (200 mM HEPES, pH7.9; 600 mM KCl; 100 mM $MgCl_2$) to a concentration of 20,000 CPM/µl.

Mobility shift of probes:

For binding, 20,000 CPM of probe is mixed in 1 x binding buffer (10 x binding buffer: 50 mM HEPES,pH 8.0; 250 mM KCl; 20 mM $MgCl_2$; 38% glycerol) with 20 mM DTT, 10 µg tRNA and 2 mM ATP. The desired amount of MPB-2C protein is added and/or protein buffer to a total volume of 15 µl. The binding reactions are incubated for 15 min at 30°C and analyzed on a polyacrylamide glycerol gel (20 ml of 30% acrylamide/bis (30:1), 7.5 ml of 10 x TBE, 7.5 ml glycerol, add H_2O to a total volume of 150 ml; then add 1.5 ml

10% APS, and 150 µl TEMED). The gel is run with 0.5 x TBE as running buffer for 4 h at 120 V constant current at 4°C. The gel was dried and autoradiographed for visualization of product using a phosphorimager (Typhoon, 9400, GE Healthcare).

3.45 Structural mapping of tandem cloverleaf probe

Probe preparation: A DNA fragment containing the T7 promoter, the hammerhead ribozyme sequences and the cDNA of the two cloverleaf structures, was generated in standard PCR reaction using pdouble-Luc-Wt as a template and the following primers: forward 5'- GCAGAGGCCGAGGCCGCCTCGGCCTCTGAGCTATT-3' and reverse 5'-GAACTT GGTTTTGTGCGTCTAAGTAAC-3'. The PCR fragments were purified using the QIAquick PCR purification kit (Qiagen). 0.5 µl of the DNA fragments were used in a transcription reaction (as described in 3.25) to transcribe a tandem cloverleaf RNA.

Labeling the probe:

1.5 µl of RNA transcripts (=> 100 pmol of 5'-ends) were dephosphorylated in a reaction containing 1 x dephosphorylation buffer (Roche) and 2 U of alkaline phosphatase (Roche) in a total volume of 150 µl. The mixture was incubated for 30 min at 37°C, then another 2 U of alkaline phosphatase was added and the incubation was continued for 30 min.

50 µl of RNase free water, and 200 µl of phenol/chloroform (v/v = 1:1) was added. The mixture was vortexed for 2 seconds and then centrifuged for 3 min at 12,000 g. The upper phase was transferred into a new tube and the RNA was precipitated by adding 500 µl of ethanol and 20 µl of 3M NaOAc (pH 5.2) and vortexing for 2 seconds. The RNA was pelleted by centrifugation at 12,000 g for 20 min. The supernatant was removed and the pellet washed once with 500 µl of 70% ethanol and then air-dried for 5 min. The pellet was resuspended in 10.5 µl of RNase free water.

2.5 µl of 10 x kinase reaction buffer (NEB), 10 µCi of [γ^{32}P]ATP (3000 Ci/mmol, Perkin Elmer), and 20 U of T4 Polynucleotide kinase (NEB) were added to the dephosphorylated RNA. The reaction was incubated for 1 h at 37°C and quenched by adding 25 µl of formamide-loading buffer (90% formamide, 1 x TBE, 0.5% bromphenolblue). The probe was gel-purified as described in 3.44.

Structural mapping:

RNase A (1 µg/ml; Ambion, Austin, TX) was diluted in 1 x RNase structure buffer (provided with enzyme, Ambion) in the following dilution series: 1:40, 1:80, 1:160, 1:320

RNase T1 (1 U/µl; Ambion) and RNase V1 (0.1 U/µl; Ambion) were diluted in 1 x RNase structure buffer in the following dilution series: 1:2, 1:4, 1:8, 1:16.

A reaction mixture in a total volume of 19 µl, containing 1 µl of labeled RNA probe (50,000 CPM/µl), 1 x RNA structure buffer and 1 µl of yeast t-RNA (10 mg/ml) was heated for 2 min at 94°C and let slowly cool down. 1 µl of enzyme dilution was added to a 19 µl reaction mixture, 1 µl H_2O was added as a negative-control. The reactions were incubated for 10 min at 28°C, and the RNA fragments were extracted by adding 100 µl of phenol/chloroform (1:1, v/v) and 80 µl H_2O. After centrifugation for 3 min at 12,000 g, the upper phase was transferred to a new tube. The RNA was precipitated by adding 250 µl of ethanol, 10 µl of 0.3 M sodium acetate, and 5 µg glycogen and incubation over night at -20°C. The RNA was pelleted by centrifugation at 12,000 g for 20 min, and the pellet was washed once with 70% ethanol. The RNA was resuspended in 3 µl loading buffer II (provided with the RNases, Ambion).

To produce a hydroxyl radical 1 bp ladder (OH-ladder) 1,000,000 CPM of RNA probe was mixed with 10 µg of tRNA and dried under vacuum for 15 min (setting “high”). The pellet was resuspended in 20 µl 1x alkaline hydrolysis buffer (provided with enzymes, Ambion), and heated for 2 min at 94°C. 20 µl of loading buffer II was added, and 5 µl was loaded onto the gel.

The reactions were separated on a 12% sequencing gel (20 ml of 30% acrylamide/bis (19:1), 24 g UREA, 5 ml of 10 x TBE, add H_2O to a total volume of 50 ml; then add 180 µl of 10% APS, and 30 µl TEMED) using 1 x TBE as running buffer. The gel was run at 45 W. The gel was dried and autoradiographed for visualization of product using a phosphorimager (Typhoon, 9400, GE Healthcare).

3.46 Expression and purification of coxsackie B3 viral $3D^{pol}$ and $3CD^{pro}$6His

Proteins were expressed by using the pET26-Ub-based prokaryotic expression system as reported previously (Gohara et al., 1999), which generates N-terminally linked yeast ubiquitin-fusion proteins. Overexpression of protein is performed in the BL21

(DE3)pCG1 strain of *Escherichia coli*. CVB3 $3D^{pol}$ and $3CD^{pro}$-6His were expressed essentially in the same manner as the poliovirus proteins described previously (Gohara et al., 1999) from the polyethyleneimine precipitation. The protein concentration of each collected fraction (0.5 ml) was determined by measuring the A_{280} in the presence of 6 M guanidine hydrochloride and using the following absorbance coefficients: 3D, 69 270 $M^{-1}cm^{-1}$; 3CD, 82 640 $M^{-1}cm^{-1}$. Samples were aliquoted and stored at -80°C.

3.47 *In vitro* VPg-uridylylation of coxsackievirus B3

For short RNA transcripts of wild-type and *cre*(2C) loop mutants, a PCR product was generated, using wild-type or mutant infectious clones as template, with reverse primer 5'-CAGGCGCAAACATACAGGTTCAA-3' and forward primer 5'-GGGGGG*TAA-TACGACTCACTATAG*GGCGAATGAGCAATTACATACAGTTCAA-3' containing a T7 polymerase sequence (italic sequence). For the generation of genomic wild-type and mutant RNA transcripts, infectious clone p53CB3/T7 was linearized by using MluI. Synthesis of VPgpU was measured by using a reaction mixture (20 µl) containing 50 mM HEPES (pH 7.5), 8% (v/v) glycerol, 3.5 mM magnesium acetate, 0.7 µM $3CD^{pro}$, 2 µM $3D^{pol}$, 40 µM synthetic CVB3 VPg, 0.75 µCi (0.277 MBq) [α^{32}P]UTP (3000 Ci $mmol^{-1}$) and 25 µM unlabeled UTP. Amount of template for the reaction was 0.5 µg for *cre*(2C) transcript RNA and 2 µg for genomic transcript RNA. Reaction mixtures were incubated for 1 h at 34°C and the reaction was quenched by adding 5 µl gel-loading buffer. The samples were analyzed by Tris/Tricine SDS-PAGE (Bio-Rad) with 13.5% acrylamide. The gels were dried and autoradiographed for visualization of product. Reaction products were quantified by measuring amount of [^{32}P]UMP incorporated into the product by using a phosphorimager (Storm 860; GE Healthcare) and converting it into cpm by using a radioactive marker.

4. Results

4. Results

4.1 The role of the cloverleaf structure in poliovirus replication

4.11 Cloverleaf mutations and their effect on negative-strand RNA synthesis

The first mutational analysis of the cloverleaf structure was undertaken when a cell-free translation replication system was not yet developed. In cell cultures viral RNA transcripts carrying cloverleaf mutations were analyzed mainly by their plaque phenotype (Andino et al., 1990). Additionally, northern blot analysis of transfected cells revealed that some cloverleaf mutations led to a dramatic decrease in the ratio of positive- to negative-strands from 30:1 to 1:1. This result indicated a role of the cloverleaf structure in positive-strand RNA synthesis. In more recent studies it has been demonstrated that the cloverleaf RNA is a key *cis*-acting element and absolutely required for negative-strand RNA synthesis (Barton et al., 2001; Herold & Andino, 2001).

To start out, we wanted to take advantage of the now available *in vitro* system, with which we can distinguish between negative- and positive-strand synthesis. With the help of this system, we analyzed some of the cloverleaf mutations that were described in the original cloverleaf study for their ability to synthesize plus- and minus-strands. The cloverleaf RNA forms three important stem-loop structures, with *stem a* being the main stem and basis of the structure. *Stem b* and *stem d* have been identified as important domains for the formation of the ternary complex with PCBP (which binds to stem-loop b) and $3CD^{pro}$ (which binds to stem-loop d) (Andino et al., 1990; Andino et al., 1993; Gamarnik & Andino, 1997; Parsley et al., 1997). Disruption of either duplex structure is lethal for the virus (Andino et al., 1990). Therefore, several poliovirus replicons were engineered carrying either a mutation within *stem b* or *stem d* of the cloverleaf. These poliovirus replicons carry a luciferase reporter gene in place of the capsid region which enables us to monitor translation indirectly by measuring luciferase activity (Fig. 4.1A). All replicons transcribed from plasmids, contained a hammerhead ribozyme 5' of the poliovirus sequence that cleaves itself off and releases a virus transcript with precise 5' sequences (Herold & Andino, 2000). An overview of the mutations that were introduced into the cloverleaf is seen in Fig. 4.1B.

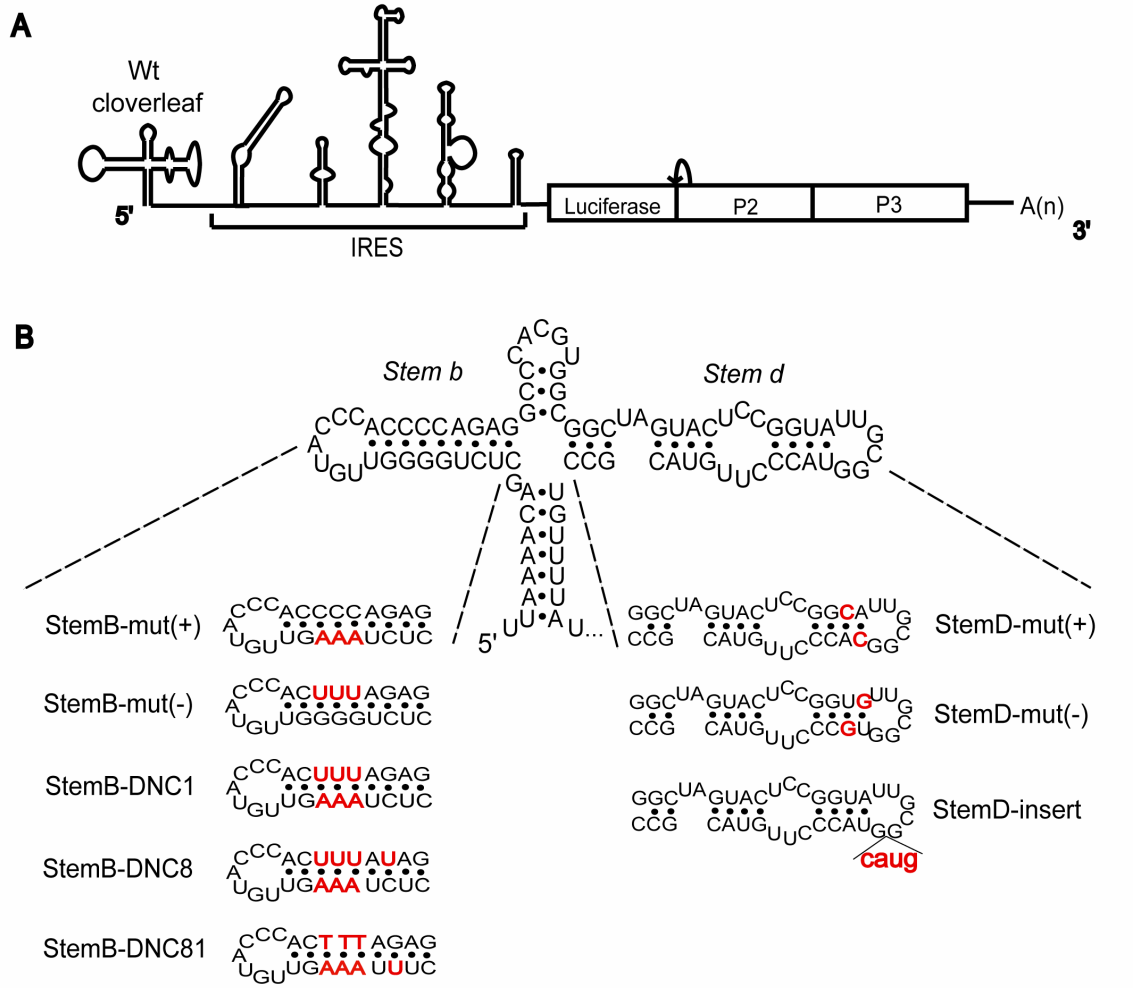

Figure 4.1: Schematic of poliovirus replicons with cloverleaf mutations. (A) Schematic representation of rib(+)Luc-Wt replicon RNA transcript used throughout this study. The capsid region is replaced by luciferase, which is cleaved off by $2A^{pro}$ during translation of the polyprotein. (B) Schematic representation of mutations introduced in either *stem b* or *stem d* of the cloverleaf using rib(+)Luc-Wt replicon as the parental construct. Mutated sequences are highlighted in red.

The cell-free replication system was used to study the replication phenotype of the new engineered constructs (Fig. 4.2A). In this system it is possible to compare the levels of negative- and positive-strand RNA synthesis of different viral RNA transcripts by the detection of replicative form (RF), a double-stranded intermediate which is synthesized during negative-strand RNA synthesis; replicative intermediate (RI), the complex synthesized during positive-strand RNA synthesis; and new synthesized single-stranded RNA (ssRNA). Replication of rib(+)Luc-Wt (see Fig. 4.1A) resulted in the

synthesis of RF, RI and new ssRNA (Fig.4.2A, lane 1), as previously shown (Herold & Andino, 2000). RF and ssRNA are detected as a sharp band. Each RI complex contains one negative-strand, as well as different amounts of unfinished positive-strands; and thus, RI is seen as a smear. GuHCl was added (lane 2) as a negative control for replication since it inhibits replication. rib(-)Luc-Wt (lane 3) contains the same Wt replicon sequences as rib(+)Luc-Wt but contains a point mutation in the hammerhead ribozyme that renders the ribozyme inactive, which results in additional non-viral nucleotides 5'- of the poliovirus sequence (Herold & Andino, 2000). These extra sequences result in inhibition of positive-strand RNA synthesis *in vitro*, and thus, only RF is detectable as seen in lane 3 of Fig. 4.2A. This construct was used as a Wt replicon control to measure the level of negative-strand RNA synthesis when positive-strand RNA synthesis is blocked. Five different mutations were introduced into *stem b* and three into *stem d* of the cloverleaf (Fig. 4.1B). As a result of base-pairing, a similar cloverleaf structure is predicted either at the 5'-end of the positive-strand or at the 3'-end of the negative-strand (Andino et al., 1990). Since initiation of positive-strand synthesis occurs at the 3'-end of the negative-strand where the viral primer, VPgpUpU, binds, it is possible that the cloverleaf structure in the negative-strand functions as a promoter for positive-strand synthesis. To determine whether one or both strands require the structure, we used the particular property of G-U base-pairs to selectively disrupt the structure in either the positive- or negative-strand. Such G-U pairs can replace A-U pairs in one strand, but on the opposite strand the A-C base pairs cannot form and the stem structure will be compromised. Thus, by incorporating G-U/A-C regions into the *stem b* or *stem d* regions of the 5'-cloverleaf, the requirement for structure in the two strands for RNA synthesis can be selectively evaluated. First, we mutated three consecutive base-pairs in *stem b*. In StemB-mut(+), the sequence GGG was replaced by AAA. This mutation should disrupt the stem in the positive-strand but should maintain the structure in the negative-strand. In contrast, the mutation in StemB-mut(-) (CCC to UUU) should disrupt the duplex structure in the negative-strand but should not alter the structure in the positive-strand. The disruption of the plus-strand led to a decrease of minus- and plus-strand synthesis *in vitro* (lane 5); whereas the disruption of the minus-strand resulted in the wild-type levels of RNA synthesis (lane 6). Consistent with these results, when the *stem b* sequences were changed but the base-pairing on both strands were maintained (StemB-DNC1), no effect on RNA synthesis was observed. In StemB-DNC8 and StemB-DNC81, the same sequence

changes as in StemB-DNC1 were introduced in addition to one G-U base-pair, such that it disrupts the structure in the plus-strand in StemB-DNC8 and the minus-strand in StemB-DNC81. This time, the one base-pair disruption on the plus-strand did not have any effect on negative- or positive-strand RNA synthesis (lane 7), whereas the disruption of the minus-strand led to a slight decrease of RF and ssRNA (lane 8). Similar as in *stem b*, we also used the advantage of G-U base-pairing in *stem d* of the cloverleaf. When the structure of the positive-strand of the *stem d* duplex structure was disrupted in StemD-mut(+) a much bigger decrease in RF and ssRNA was observed than with any *stem b* mutation (lane 9). Maintaining the structure on the plus-strand but disrupting it on the minus-strand (StemD-mut(-)), resulted in much higher levels of RNA synthesis as in StemD-mut(+), but still showed some decrease in replication in comparison to the replicon Wt. The biggest effect on both negative- and positive-strand RNA synthesis was observed when four nucleotides were inserted into the loop region of *stem d* (StemD-insert), which essentially resulted in complete inhibition of RNA synthesis. These results demonstrate that mutations in the cloverleaf structure can have a dramatic effect on RNA synthesis.

It has been proposed that the cloverleaf is involved in both negative- and positive-strand RNA synthesis, and the *in vitro* assay shows the results of RNA synthesis accomplished after 2 h of incubation time representing several rounds of replication. This makes it difficult to distinguish between effects on minus-strand synthesis which then subsequently will affect plus-strand synthesis, or the other way round, effects on positive-strand synthesis in the first round of replication will then affect negative-strand synthesis in the subsequent round of replication. Therefore, we decided to clone these same mutations as just described into ribozyme(-) constructs, which contain the same hammerhead mutation as in rib(-)Luc-Wt, and hence, bear non-viral sequences at their 5'-ends when transcribed. These extra sequences will inhibit plus-strand RNA synthesis *in vitro*, and enable us to evaluate the ability of the mutated cloverleaves to synthesize negative-strands in the form of RF. Here, only StemB-DNC1 shows Wt-levels of RF, now compared to rib(-)Luc-Wt (Fig. 4.2A, lane 15 compare to lane 14). StemB-mut(+) shows no RF synthesis (lane 16), whereas the other *stem b* mutations all led to a decrease in RF levels (lane 17-19). No detectable levels of RF were observed for any *stem d* mutations (lane 20-22). The effect on negative-strand RNA synthesis was not due to a decrease in translation, since translation levels for all constructs as measured as luciferase activity were similar to replicon Wt levels (data

not shown). These results clearly confirm the importance of the cloverleaf structure for negative-strand RNA synthesis.

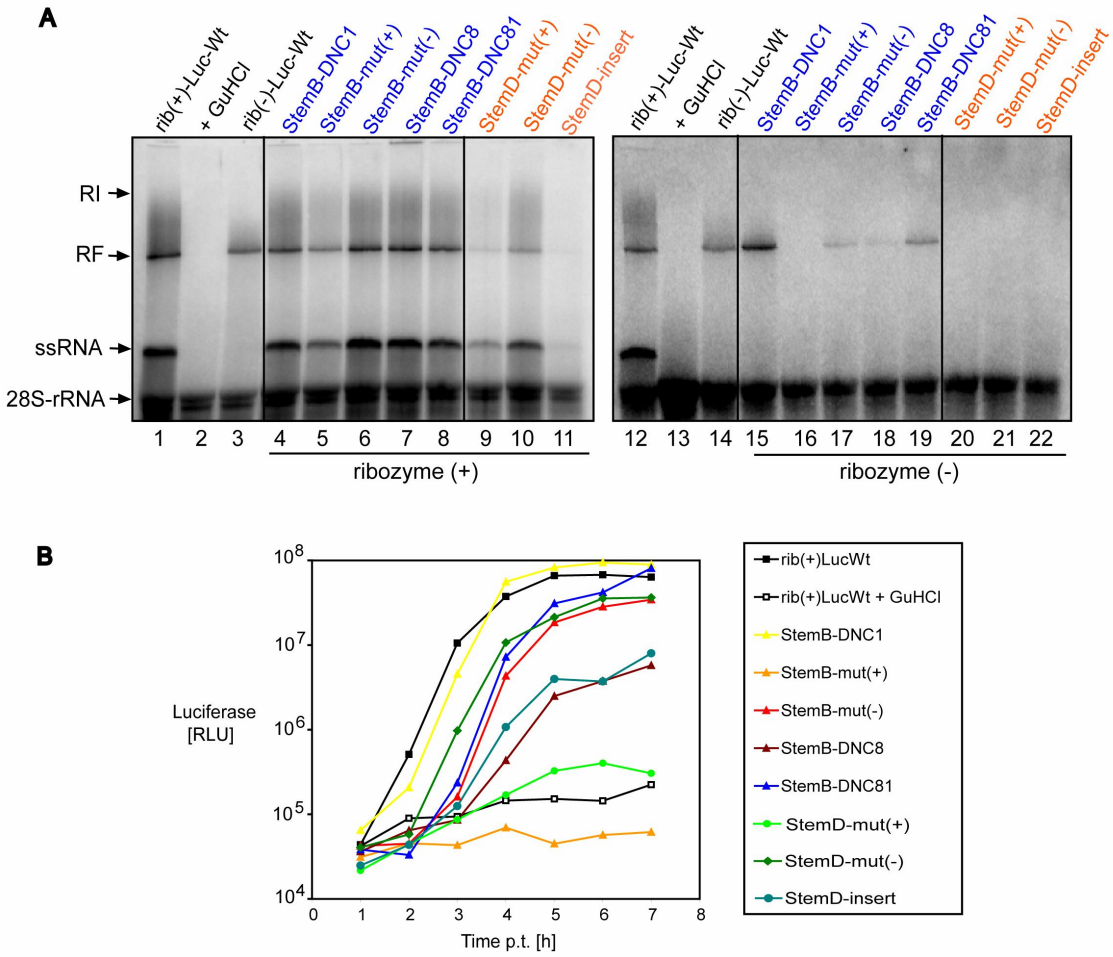

Figure 4.2: Replication of poliovirus replicon RNA transcripts with cloverleaf mutations in a cell-free translation replication system and in tissue culture cells. (A) RNA replication in translation-replication extracts. HeLa S10 extract was programmed with 1 µg of RNA transcripts containing either an active (ribozyme(+)) or an inactive (ribozyme(-)) hammerhead ribozyme at their 5'-end. After 4 h of incubation at 30°C in the presence of 2 mM guanidine hydrochloride, preinitiation complexes were isolated by centrifugation at 15,000 x g. Preinitiation complexes were resuspended in labeling mix containing [α-^{32}P]UTP and incubated for 2 h. Total RNA was prepared and separated on native agarose gels and detected by autoradiography. (B) Luciferase expression in replicon RNA-transfected HeLa cells. After transfection of the RNA transcripts into HeLa cells, the luciferase activity (relative light units [RLU]) corresponding to 2 x 10^4 cells was measured every hour for 7 h. The cells were either kept in the presence (+GuHCl) or absence of 2 mM guanidine hydrochloride.

Next, we wanted to evaluate the results seen in the *in vitro* system by monitoring the replication phenotype of the cloverleaf mutants in complete cells. We transfected all the ribozyme(+) constructs containing the cloverleaf mutations into HeLa cells in the

presence or in the absence of GuHCl and monitored replication by measuring luciferase activity over time (Fig. 4.2B). Monitoring luciferase activity in the presence of GuHCl provides a measurement of the translation level of the input-RNA in the absence of replication, and permits us to ensure that none of the mutations negatively impacts translation directly, since low translation levels would in turn have a negative effect on replication. The replication phenotypes of the mutants can be divided into three groups. In the first group, both constructs, StemB-mut(+) and StemD-mut(+), in which the positive-strand duplex structure is disrupted either in *stem b* or *stem d* of the cloverleaf, show very little or no replication *in vivo*. The second group contains StemB-DNC8, which has one base-pair disruption on the plus-strand of *stem b*, and StemD-insert, which has the increased loop in *stem d*. Both show more than one log-scale decrease in replication levels in comparison to rib(+)Luc-Wt. The third group contains all other mutants. They all replicate with nearly wild-type levels in HeLa cells. These *in vivo* results verify the requirement of the cloverleaf structure formed on the plus-strand for RNA synthesis. In addition, we could confirm a role of the cloverleaf for negative-strand RNA synthesis using the ribozyme(-) constructs. However, no conclusions can be made about the involvement of the cloverleaf in positive-strand RNA synthesis.

4.12 Poliovirus replicons with separate promoters for positive- and negative-strand RNA synthesis

To specifically study the role of the cloverleaf in positive-strand RNA synthesis, we needed to develop a system in which we can separate the promoter function of the RNA element for minus- and plus-strand synthesis. Since it was shown that the cloverleaf can initiate negative-strand RNA synthesis internally, thus does not have to be located at the very 5'-end of the genome (Herold & Andino, 2000). We thus generated tandem cloverleaf replicons with two wild-type cloverleaves next to each other at the 5'-end of the genome. The idea is that the second, internal Wt cloverleaf can initiate negative- but not positive-strand RNA synthesis, which enables us to study the effect of the cloverleaf mutation in the 5' cloverleaf on positive-strand RNA synthesis. Both cloverleaves were linked by poliovirus sequence 96-112 and a SacI-site for easier cloning, resulting in Wt-Wt (Fig. 4.3A). Using the Wt-Wt replicon, we then engineered three more replicons in which we introduced in each one of the three *stem d* mutations (as described in the previous section) into the upstream, 5'-cloverleaf,

resulting in StemD-mut(+)-Wt, StemD-mut(-)-Wt, and StemD-insert respectively (Fig. 4.3B). We started out with these *stem d* mutations since they had the most dramatic effect on negative-strand RNA synthesis. We then compared replication of these new replicons with the replicons with just one cloverleaf, carrying the same cloverleaf mutation (Fig. 4.4A). The Wt-Wt replicon showed both negative- and positive-strand RNA synthesis but at decreased levels in comparison to rib(+)Luc-Wt (compare lane 3 with lane 1). Strikingly, all three tandem cloverleaf replicons with *stem d* mutations showed improved replication levels in comparison to their counterpart with the same mutation but only one cloverleaf. The decreased levels of RF and ssRNA as seen for StemD-mut(-) (lane 4) were completely restored to Wt-levels of rib(+)Luc-Wt (lane 5). Both StemD-mut(+) and StemD-insert showed no detectable levels of RF or ssRNA, but synthesized both when in the tandem cloverleaf constructs, although to a lower level than Wt. The demonstrated defect on the level of negative-strand RNA synthesis for these *stem d* mutations as seen in Fig. 4.2A, could be at least partially restored by providing a second cloverleaf internally.

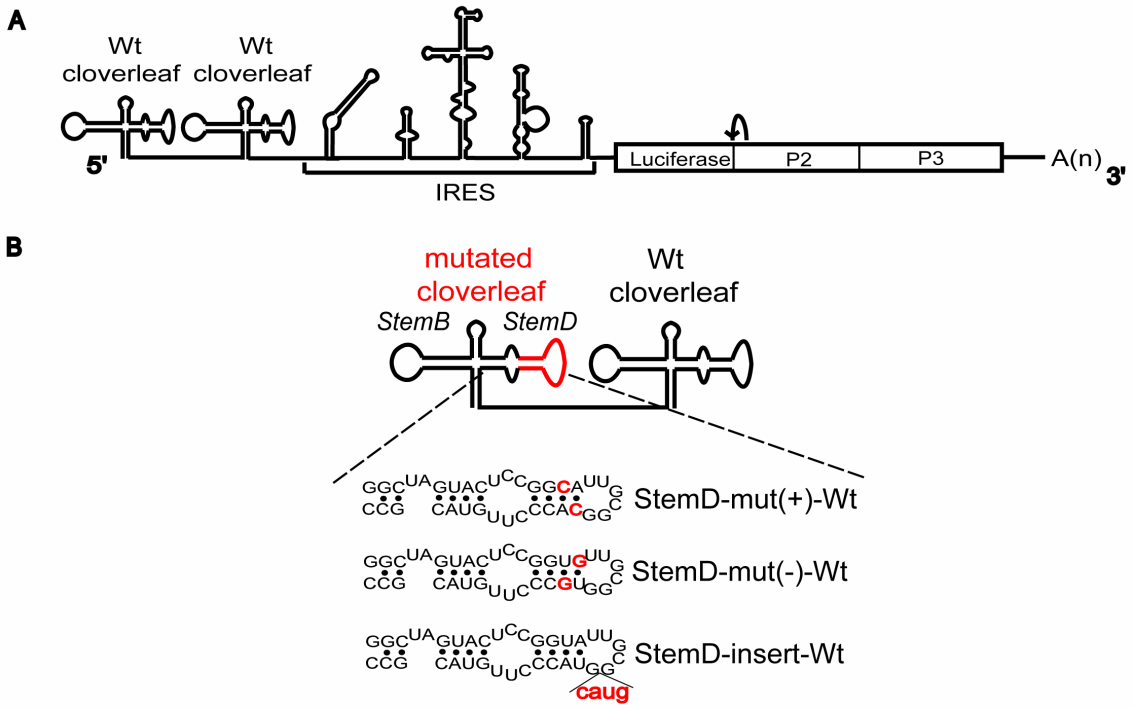

Figure 4.3: Schematic of poliovirus replicons with two cloverleaf structures at their 5'-end. (A) Schematic of Wt-Wt replicon RNA transcript, containing two wild-type cloverleaf structures at the 5'-end of the genome. (B) Schematic representation of mutations introduced in *stem d* of the 5'-end cloverleaf of the Wt-Wt replicon. Mutated sequences are highlighted in red.

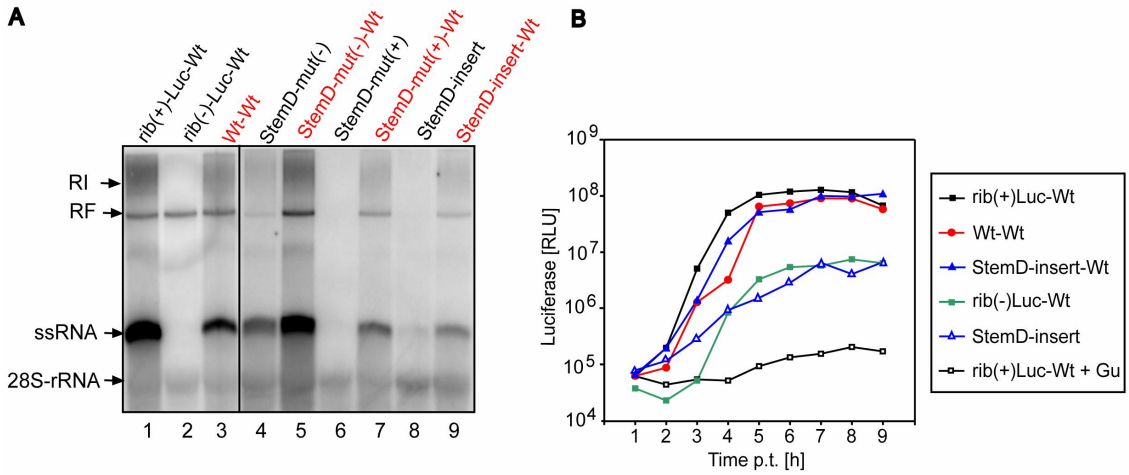

Figure 4.4: Replication of poliovirus replicon RNA transcripts with either one or two cloverleaves at their 5'-end in a cell-free translation replication system and in tissue culture cells. (A) RNA replication in translation-replication extracts. HeLa S10 extract was programmed with 1 µg of RNA transcripts. After 4 h of incubation at 30°C in the presence of 2 mM guanidine hydrochloride, preinitiation complexes were isolated by centrifugation at 15,000 x g. Preinitiation complexes were resuspended in labeling mix containing [α-^{32}P]UTP and incubated for 2 h. Total RNA was prepared and separated on native agarose gels and detected by autoradiography. (B) Luciferase expression in replicon RNA-transfected HeLa cells. After transfection of the RNA transcripts into HeLa cells, the luciferase activity (relative light units [RLU]) corresponding to 2 x 10^4 cells was measured every hour for 9 h. The cells were either kept in the presence (+ Gu) or absence of 2 mM GuHCl.

Next, we wanted to know if a similar effect can be observed *in vivo*. We transfected the Wt-Wt construct as well as the StemD-insert and the StemD-insert-Wt into HeLa cells and monitored luciferase activity over a time course of 8 hours, the typical replication cycle of poliovirus (Fig. 4.4B). Wt-Wt replicated nearly with identical levels as observed for rib(+)Luc-Wt. StemD-insert reached about 50% of Wt-replication levels; whereas in StemD-insert-Wt, this defect in replication was restored to Wt-levels. These findings demonstrate that the internal downstream cloverleaf is able to restore a defect in negative-strand RNA synthesis caused by a mutation in the upstream cloverleaf. The only concern with this tandem cloverleaf construct is, that any additional sequences that are not required for replication and are located 5' of a Wt cloverleaf, will be eventually deleted when transfected into cells. This can be observed with rib(-)Luc-Wt in Fig. 4.4B. The additional sequences 5' of the Wt-sequences in this RNA leads to a two hour delay in replication and the new synthesized RNA has lost the additional sequences as it was demonstrated recently by our lab (Herold & Andino, 2000). StemD-insert-Wt does not show the same kind of delay in replication, which suggests that the upstream cloverleaf has not been deleted. However, for further studies of such

tandem cloverleaf constructs we must avoid this possibility by replacing the internal wild-type cloverleaf with a cloverleaf that can only support negative-strand RNA synthesis, thus requiring the virus to maintain the 5'-cloverleaf for initiation of positive-strand RNA synthesis. In addition, the fact that the Wt-Wt construct did not replicate at the same level as rib(+)Luc-Wt, indicates that the two cloverleaves of identical sequences somehow hinder each other in promoting replication, possibly through interaction of complementary sequences between the two cloverleaves. Nonetheless, the results so far have been encouraging.

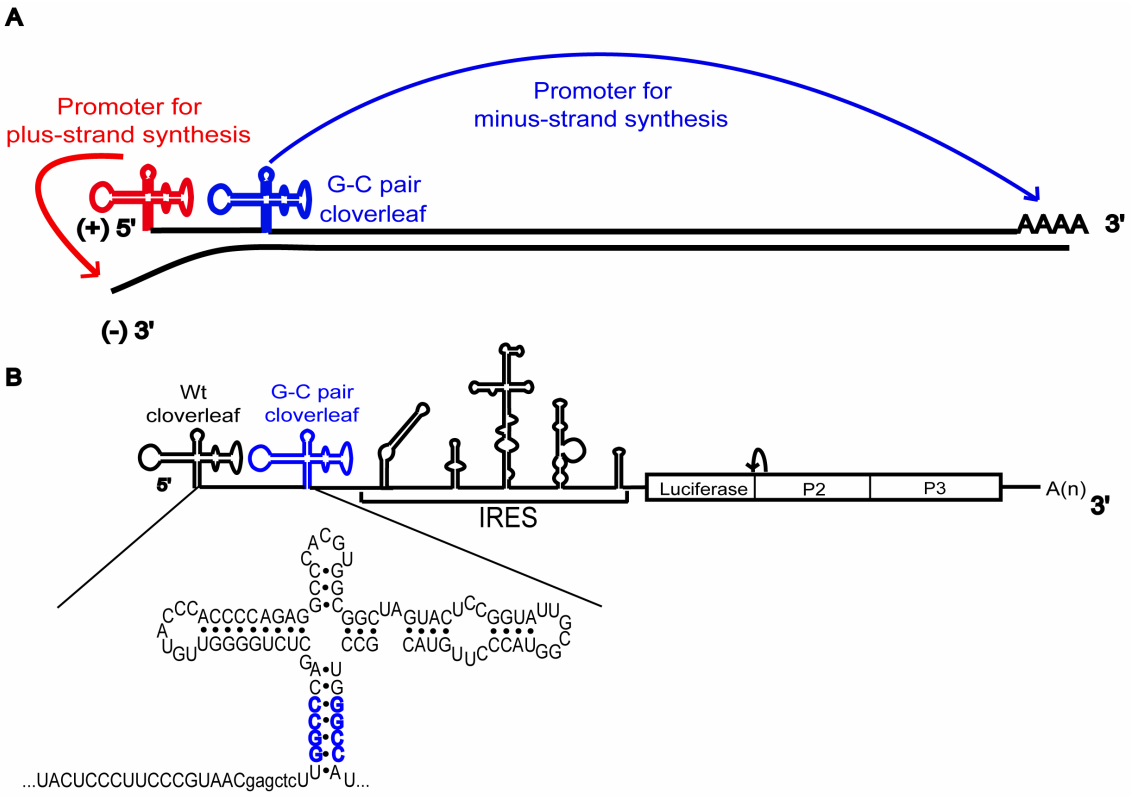

Figure 4.5: Schematic representation of the tandem cloverleaf replicon with separate promoters for initiation of negative- and positive-strand RNA synthesis. (A) Model of the tandem cloverleaf construct. The replicon RNA transcripts carry two cloverleaf structures at their 5'-end. The downstream G-C pair cloverleaf can only initiate negative-strand RNA synthesis, whereas the 5'-terminal cloverleaf functions as a promoter for positive-strand RNA synthesis. In this context the 5'-end cloverleaf can be mutated and analyzed for its ability to support positive-strand RNA synthesis. (B) Schematic representation of the double-luc-Wt RNA transcripts, showing the precise sequence of the downstream cloverleaf that contains four G-C pairs (highlighted in blue) in *stem a* instead of the wild-type A-U pairs. Nucleotides 96 – 112 (upper case letters) of the poliovirus sequence was inserted as linker in between the two cloverleaf structures, as well as a SacI site, which is represented by lower case letters.

Using the previous results as a basis, we then designed an improved version of replicon RNAs with tandem cloverleaf structures, with the goal of separating the promoters for positive- and negative-strand RNA synthesis. Thus, a downstream cloverleaf which only supports minus-strand RNA synthesis allows the genetic analysis of a 5'-terminal cloverleaf dedicated to promote plus-strand RNA synthesis, as demonstrated in Fig. 4.5A. The requirements of the cloverleaf structure for negative-strand RNA synthesis have been well defined. Previous results have shown that only the structure, and not the sequences, of *stem a* of the cloverleaf are required for negative-strand RNA synthesis; but these sequences are important for efficient initiation of plus-strand RNA synthesis (Sharma et al., 2005). It was shown that additional sequences at the 5'-end of the viral genome lead to a defect in positive- but not negative-strand RNA synthesis *in vitro* (Herold & Andino, 2000). Therefore, a replicon with tandem cloverleaf structures was engineered in the following way: In the downstream cloverleaf, the four A-U pairs in *stem a* were replaced with G-C pairs (called G-C pair cloverleaf) resulting in a cloverleaf that can only support negative-strand RNA synthesis. A wild-type cloverleaf was then inserted 5' of the G-C pair cloverleaf, and both cloverleaves were linked by poliovirus nucleotides 96-112 and a SacI-site for easier cloning, resulting in double-luc-Wt (see Fig. 4.5B). The cell-free replication system was used to study the replication phenotype of the new engineered construct (Fig. 4.6A). A construct containing only a G-C pair cloverleaf was used to verify that the downstream cloverleaf in the tandem cloverleaf construct can only support negative-strand RNA synthesis (lane 4). The level of translation (measured as luciferase-activity, data not shown) and the level of negative-strand RNA synthesis were comparable to rib(-)Luc-Wt (lane 3). The double-Luc-Wt RNA, which contains the tandem cloverleaf structures, generated the same amount of negative- and positive-strand RNA synthesis as the rib(+)Luc-Wt RNA with one cloverleaf (compare lane 5 to 7). We then transfected rib(+)Luc-Wt RNA and double-Luc-Wt RNA into HeLa cells in the presence and in the absence of GuHCl to monitor replication by measuring luciferase activity over time (Fig 4.6B). Again, the construct with two cloverleaf structures showed identical replication kinetics to the RNA with one cloverleaf. Double-Luc-Wt RNA translated with the same efficiency as rib(+)Luc-Wt RNA. These results confirm that the double-Luc-Wt RNA is able to support efficient replication *in vitro* and *in vivo*, and therefore, provides a suitable system to study the effect of 5'-cloverleaf mutations on positive-strand RNA synthesis. All further experiments using tandem

cloverleaf constructs will be based on double-luc-Wt containing the G-C pair cloverleaf at the downstream position.

To confirm that both cloverleaves located next to each other in double-Luc-Wt form two individual structures, we employed enzymatic mapping using RNA transcripts of the two Wt-G-C-pair cloverleaf structures as in double-Luc-Wt that were 5'-labeled with [γ^{32}P]ATP as a probe. Fig. 4.7 shows an autoradiograph with the cleavage products of the probe by different RNases. The very left lane contains a hydroxyl radical 1bp ladder produced from the same probe. As the outline on the left side of the autoradiograph demonstrates, the cleavage pattern of the 5'-cloverleaf showed the expected pattern for the predicted structure of the cloverleaf. Since the probe was over 200 nucleotides long, it was not possible to get the same resolution of the cleavage products of the 3' cloverleaf as for the 5' one. However, even compressed, the same cleavage pattern by the different RNases can be seen for the 3'-cloverleaf as seen for the 5' cloverleaf. Based on this result as well as the studies *in vitro* and *in vivo* of double-Luc-Wt, we conclude that both cloverleaf structures are able to individually fold into the proper structure, and thus, both are able to form the required complexes for RNA synthesis.

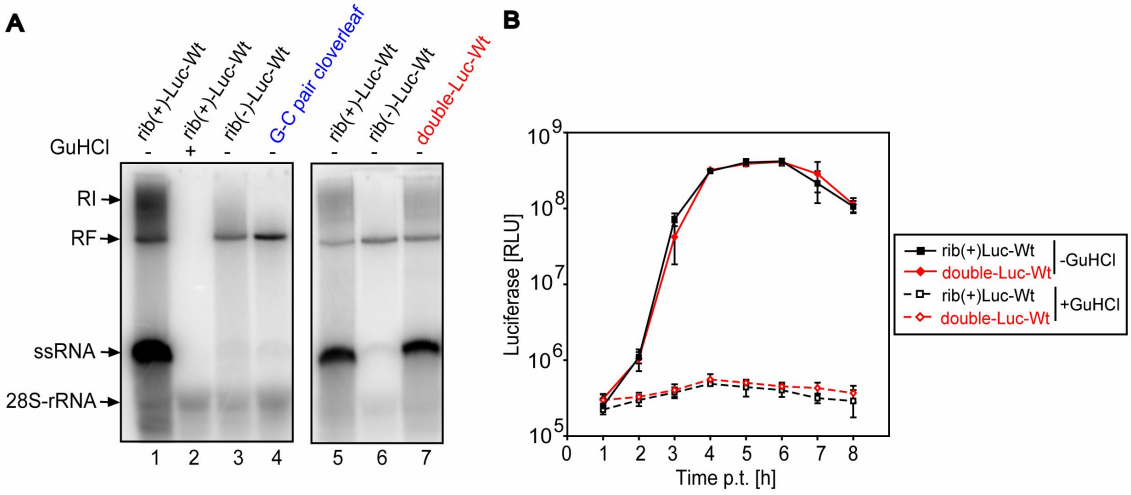

Figure 4.6: Replication of poliovirus tandem cloverleaf replicons in a cell-free translation replication system and in tissue culture cells. (A) RNA replication in translation-replication extracts. HeLa S10 extract was programmed with 1 µg of rib(+)Luc-Wt and double-Luc-Wt RNA transcripts. After 4 h of incubation at 30°C in the presence of 2 mM guanidine hydrochloride, preinitiation complexes were isolated by centrifugation at 15,000 x g. Preinitiation complexes were resuspended in labeling mix containing [α-^{32}P]UTP and incubated for 2 h. Total RNA was prepared and separated on native agarose gels and detected by autoradiography. (B) Luciferase expression in replicon RNA-transfected HeLa cells. After transfection of the RNA transcripts into HeLa cells, the luciferase activity (relative light units [RLU]) corresponding to 2 x 10^4 cells was measured every hour for 8 h. The cells were either kept in the presence (+ GuHCl) or absence (- GuHCl) of 2 mM guanidine hydrochloride. Each time point represents the mean of three independent experiments and SD is indicated.

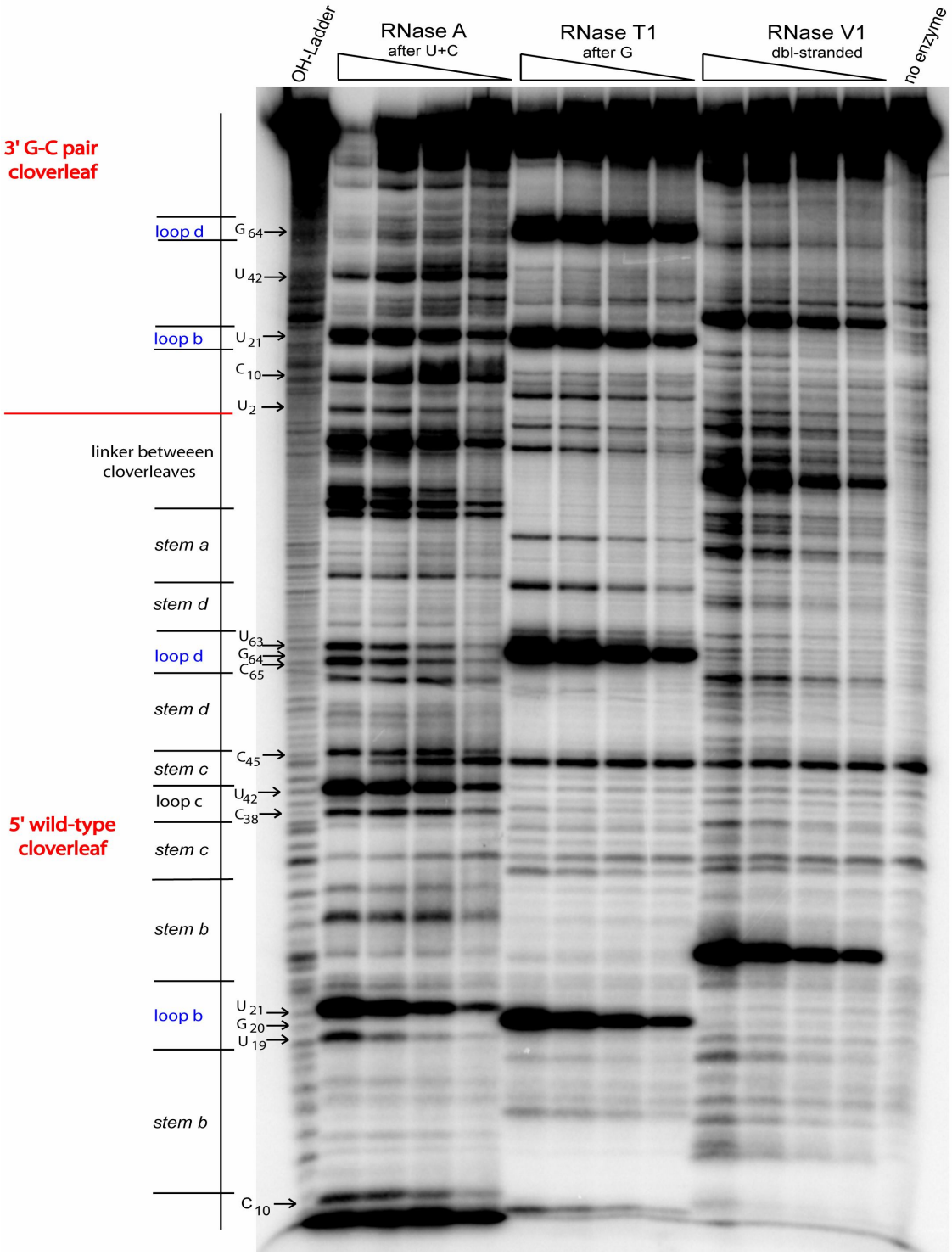

Figure 4.7: Structural mapping of the tandem cloverleaf structures of double-Luc-Wt. The autoradiograph of a representative mapping acrylamide gel is shown. The corresponding area within the cloverleaf structure is indicted on the left hand side of the autoradiograph. Major ribonuclease cleavages are indicted by arrow and the corresponding nucleotide of the cloverleaf RNA starting at the 5'-end. The very left lane (OH-ladder) contains a hydroxyl radical 1bp ladder produced from the same probe. The very right lane contains probe without any enzyme as a negative-control.

4.13 Partial cloverleaf structures at the 5'-end do not support initiation of positive-strand RNA synthesis

It has been shown that the 5'-terminal sequence is required for efficient initiation of positive-strand RNA synthesis (Herold & Andino, 2000; Sharma et al., 2005). As the cloverleaf structure is at the 5'-end of the poliovirus genome, those sequences are part of the *stem a* duplex structure of the cloverleaf. To test what the minimal structural requirements at the 5'-end are to efficiently initiate positive-strand RNA synthesis, we engineered tandem cloverleaf constructs in which different parts of the 5' cloverleaf structure were deleted in a way that the 5'-end sequence was left intact. In all cases the negative-strand RNA synthesis was ensured by the downstream G-C pair cloverleaf (see Fig. 4.8A). The plus9 construct contains only the nine 5'-most-terminal nucleotides, plus the SacI site, instead of a second 5' cloverleaf. In the plus20 RNA, the 5'-end sequence is part of *stem a*, and in the plus27 RNA *stem a* and *stem c* have been left at the 5'-end. Analyzing these constructs in the cell-free replication system revealed that no positive-strand RNA synthesis could be detected for any of them (Fig. 4.8B). Similar levels of negative-strand synthesis was observed for plus9, plus20 and plus27 RNA, which was initiated by the downstream G-C pair cloverleaf. These results suggest that more than just the very 5'-terminal sequence and structure is involved in initiation of positive-strand RNA synthesis.

To further address the question of what 5'-end structure is required for initiation of positive-strand RNA synthesis, double-Luc-StemA-disr RNA was engineered in which the *stem a* duplex structure of the 5'-end cloverleaf was disrupted but leaving the 5'-terminal sequences intact (see Fig. 4.8A). This construct shows a big defect in positive-strand synthesis in the *in vitro* system. The ratio of positive-strand RNA to RF for double-luc-StemA-disr was equal to that for G-C-pair cloverleaf RNA (compare Fig. 4.8B, lane 1 and 6) and was 20 fold lower than in the Wt control (lane 2). Furthermore, when double-Luc-StemA-disr RNA was transfected into HeLa cells no replication could be detected as seen in Fig. 4.8C. The same could be observed for plus9 after transfection (Fig. 4.8C) as well as for plus20 and plus 27 (data not shown). These results establish that not only the 5'-end sequence, but also the 5'-end structure is required for efficient positive-strand RNA synthesis. This shows that an intact *stem a* structure is required, but alone is not sufficient, for synthesis of plus-strands.

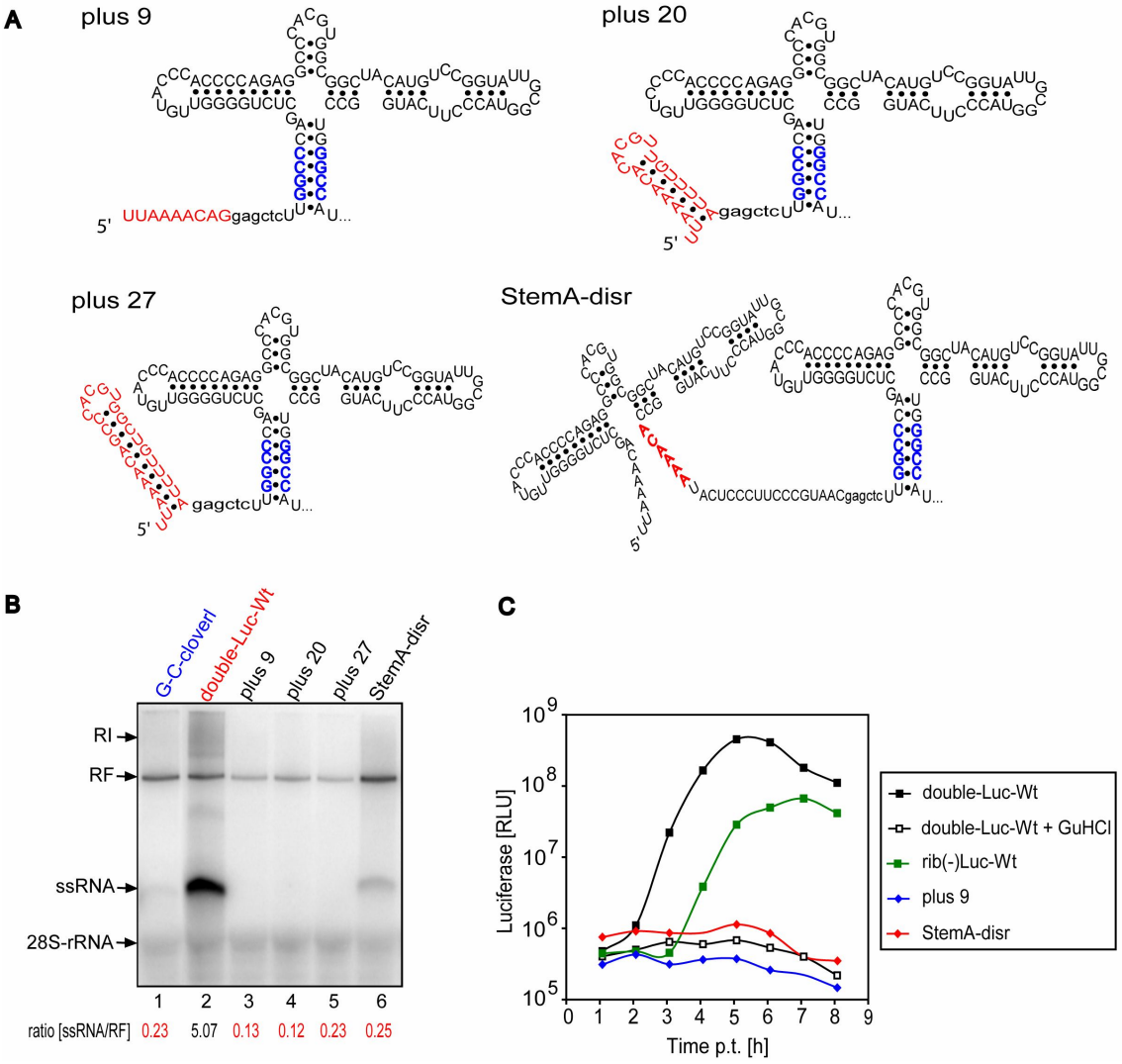

Figure 4.8: Schematic of tandem cloverleaf replicons with partial cloverleaf structures at their 5'-end and their replication phenotype *in vitro* and *in vivo*. (A) Schematic representation of tandem cloverleaf replicon RNA transcripts with partial cloverleaf structures at their 5'-end. In addition to the G-C-pair cloverleaf, plus9 contains the 9 wild-type 5'-terminal nucleotides of poliovirus at its 5'-end. Plus20 contains *stem a* and loop sequences of stem-loop c, and plus27 contains *stem a* and complete *stem c* at its 5'-end. Sequences in lower case represent a SacI site. StemA-disr. contains two cloverleaf structures, downstream the G-C pair cloverleaf and 5' a cloverleaf with mutations in *stem a* that disrupt the duplex structure but maintains the wild-type 5'-terminal sequences. (B) RNA replication *in vitro*. HeLa S10 extract was programmed with 1 µg of RNA transcripts. After 4 h of incubation at 30°C in the presence of 2 mM guanidine hydrochloride, preinitiation complexes were isolated by centrifugation at 15,000 x g. Preinitiation complexes were resuspended in labeling mix containing [α-^{32}P]UTP and incubated for 2 h. Total RNA was prepared and separated on native agarose gels and detected by autoradiography. (C) Luciferase expression in replicon RNA-transfected HeLa cells. After transfection of the RNA transcripts into HeLa cells, the luciferase activity (relative light units [RLU]) corresponding to 2 x 10^4 cells was measured every hour for 8 h. The cells were either kept in the presence (+ GuHCl) or absence of 2 mM guanidine hydrochloride.

4.14 *Stem b* and *stem d* mutations and their effect on positive-strand RNA synthesis

4.141 The cloverleaf structure is required in the positive-strand for positive-strand RNA synthesis.

With the help of G-U base-pairing as already described in section 4.11, we wanted to determine whether the cloverleaf structure was required on the positive- and/or on the negative-strand for positive-strand RNA synthesis. We engineered two tandem cloverleaf constructs by introducing the StemB-mut(+) and the StemB-mut(-) into the 5' cloverleaf of the tandem cloverleaf construct (see Fig. 4.9). Both mutations lead to a great deficiency in positive-strand RNA synthesis in the cell-free replication system; although, with StemB-mut(-) resulting in a 3-fold higher ratio of positive-strands to RF (Fig. 4.10A, lane 3 + 4). Strikingly, the small difference of both constructs in synthesis of positive-strands seen *in vitro*, resulted in a considerable difference in replication when transfected into HeLa cells (Fig. 4.10B). Here, StemB-mut(+) was not able to replicate at all; whereas StemB-mut(-), shows wild-type replication kinetics although reaching approximately 2-fold less in luciferase-activity at 8 hours post-transfection than double-Luc-Wt. These results suggest that the cloverleaf structure in the *stem b* region is absolutely required in the positive-strand for positive-strand RNA synthesis. The slight defect seen in replication of StemB-mut(-) could be due to the weaker G-U base-pairing in the positive-strands than the G-C base-pairs existing in the Wt-sequence or due to slight changes in the structure as a result of the mutations.

To further confirm the importance of the *stem b* structure for positive-strand RNA synthesis, we generated additional mutations within the *stem b* region (for overview see Fig. 4.9). In StemB-swap, the entire *stem b* base-pair sequence was swapped so that sequences on the top part of the stem were exchanged with the sequences on the lower part of the stem. In StemB-shuffle, the consecutive base-pair sequences of *stem b* were shuffled around, resulting in a different order of the original base-pairs but still maintaining the same original structure. Both constructs showed a big defect in positive-strand synthesis in the cell-free replication system (Fig. 4.10A, lane 5 + 6), but were able to replicate with nearly Wt efficiency in HeLa cells (Fig. 4.10B). Again, our results suggest that maintaining the *stem b* structure is important for positive-strand synthesis and that changes to the original sequence affect the level of plus-strand RNA synthesis.

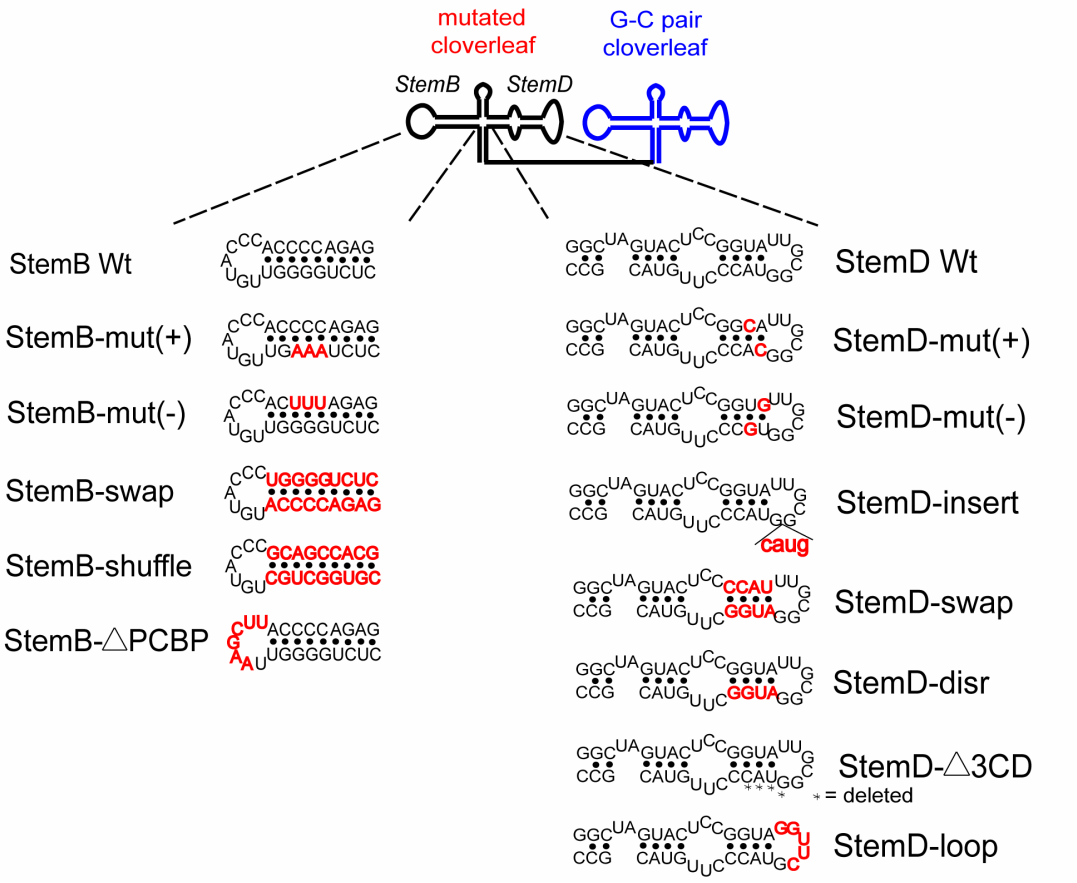

Figure 4.9: Schematic representation of tandem cloverleaf replicons with cloverleaf mutations in *stem b* or *stem d* of the 5'-terminal cloverleaf. The mutated sequence is highlighted in red.

As a next step, we introduced G-U/A-C pairs into the *stem d* region of the 5' cloverleaf of the tandem cloverleaf RNA (see Fig. 4.9). In StemD-mut(+), two A-U pairs were replaced by A-C pairs, which results in disruption of the *stem d* duplex structure on the positive-strand but not the negative-strand. In contrast, two G-U pairs were introduced within the *stem d* region of StemD-mut(-), which should maintain the duplex structure on the positive-strand yet alter the structure on the negative-strand. When tested in the cell-free replication system, StemD-mut(+) showed a reduced level of positive-strands in comparison to double-Luc-Wt (Fig. 4.10C, lane 2 + 4). Strikingly, StemD-mut(-) resulted in an increased level of positive-strand synthesis by over two fold when the ratio of positive-strands to RF was calculated and compared to Wt (Fig. 4.10C, lane 2 + 3). After transfection of these constructs into HeLa cells, wild-type levels of replication was observed for StemD-mut(-), whereas, StemD-mut(+) showed a 10-fold decrease in

replication when compared to double-Luc-Wt (Fig. 4.10D). These results further confirm that compromising the cloverleaf structure in the positive-strand leads to a defect in positive-strand RNA synthesis.

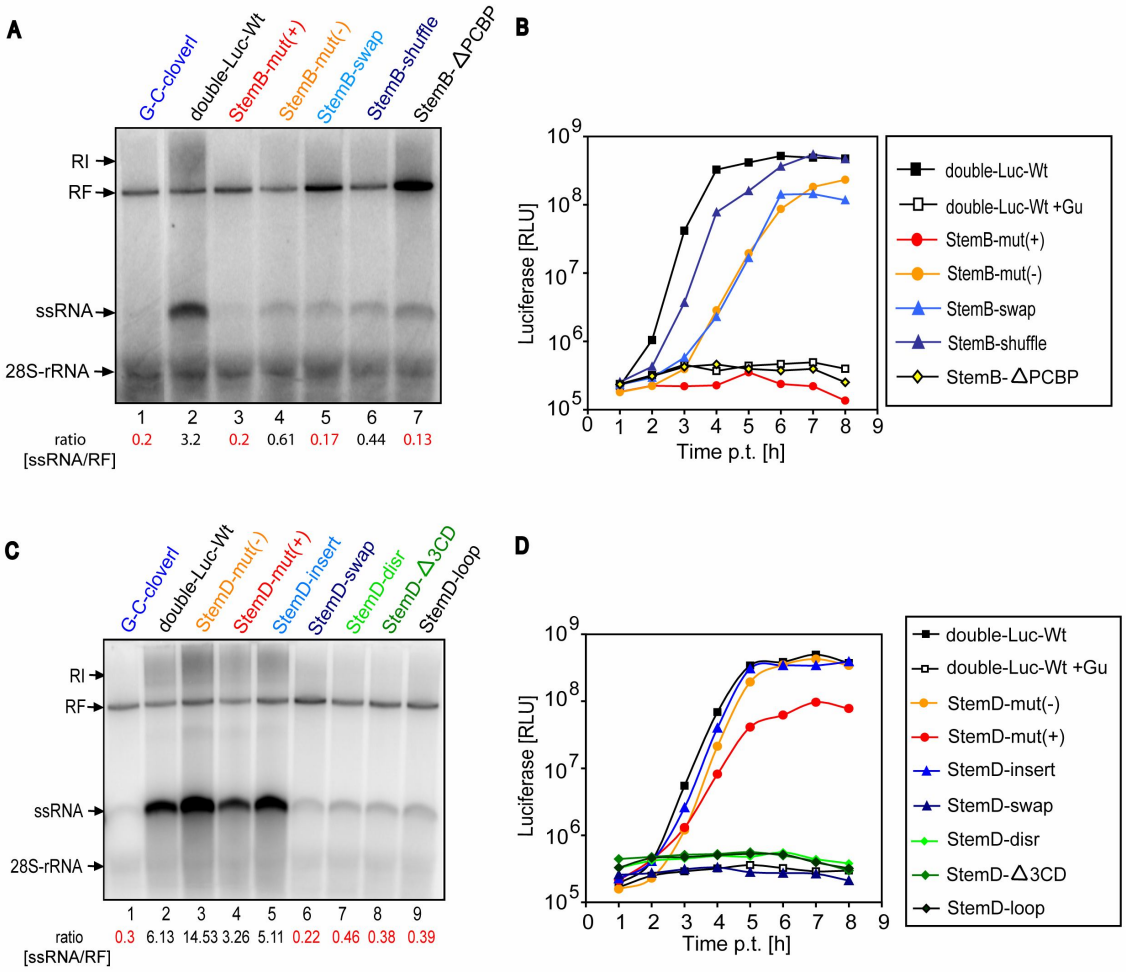

Figure 4.10: Replication of tandem cloverleaf replicon RNA transcripts with *stem b* or *stem d* mutations in the 5'-terminal cloverleaf in a cell-free translation replication system and in tissue culture cells. (A)+(C) RNA replication in translation-replication extracts. HeLa S10 extract was programmed with 1 µg of RNA transcripts. After 4 h of incubation at 30°C in the presence of 2 mM guanidine hydrochloride, preinitiation complexes were isolated by centrifugation at 15,000 x g. Preinitiation complexes were resuspended in labeling mix containing [α-^{32}P]UTP and incubated for 2 h. Total RNA was prepared and separated on native agarose gels and detected by autoradiography. (B)+(D) Luciferase expression in replicon RNA-transfected HeLa cells. After transfection of the RNA transcripts into HeLa cells, the luciferase activity (relative light units [RLU]) corresponding to 2 x 10^4 cells was measured every hour for 8 h. The cells were either kept in the presence (+ Gu) or absence of 2 mM guanidine hydrochloride.

We further investigated the structural requirement of *stem d* for positive-strand RNA synthesis by introducing more mutations within this region (see Fig. 4.9). When the loop region of stem-loop d was increased by insertion of four additional nucleotides,

(StemD-insert) no significant changes in replication in either cell extract (Fig. 4.10C, lane 5) or in HeLa cells (Fig 4.10D) was observed. However, more drastic changes, such as a complete swap of the base-pair sequences (StemD-swap), a complete disruption of the duplex structure (StemD-disr) or a complete sequence change within the loop region (StemD-loop), all resulted in a big defect on the level of positive-strand synthesis in the *in vitro* system (Fig. 4.10C, lane 6, 7, 9). Strikingly, none of these constructs showed any replication in cells (Fig. 4.10D). Therefore, the *stem d* structure appears to be important for the synthesis of positive-strands. These results confirm that the cloverleaf structure as it was originally predicted (Andino et al., 1990) plays an important role in positive-strand RNA synthesis.

4.142 Binding-sites for PCBP2 and 3CD^{pro} in the cloverleaf are required for positive-strand RNA synthesis.

It was shown that the host factor, PCBP2 (Gamarnik & Andino, 1997; Parsley et al., 1997), and the viral polymerase precursor, 3CD^{pro} (Andino et al., 1990; Andino et al., 1993; Silvera et al., 1999), bind to the cloverleaf structure and form a ternary complex at the 5'-end of the viral genome, a requirement for negative-strand RNA synthesis (Barton et al., 2001; Herold & Andino, 2001). Having defined the structural requirements of the cloverleaf RNA for positive-strand synthesis, we examined the requirements of intact binding-sites for PCBP2 and 3CD^{pro} within the cloverleaf for positive-strand RNA synthesis. A poly(C) stretch within the stem-loop b of the cloverleaf has been identified as the binding-site for PCBP2. Using the tandem cloverleaf replicon, we introduced a mutation within the 5' cloverleaf that abolishes binding of PCBP2 to the cloverleaf (S1-mutation in (Parsley et al., 1997)), to generate StemB-ΔPCBP (Fig. 4.9). This RNA showed a severe defect in positive-strand RNA synthesis when tested in the cell-free replication system (Fig. 4.10A, lane 7) and was unable to replicate in cells (Fig. 4.10B). This result demonstrates that an intact binding-site for PCBP2 in the cloverleaf structure is required for positive-strand synthesis. In the next step, we engineered StemD-Δ3CD, which has a deletion within the *stem d* region of the 5' cloverleaf of the tandem cloverleaf RNA (Fig. 4.9). This deletion has been previously described as 5'Δd-mutation (Parsley et al., 1997). This mutation was shown to disrupt 3CD^{pro} binding to the cloverleaf structure. When cell extract was programmed with StemD-Δ3CD, only a very small amount of positive-strand RNA was detected (Fig. 4.10C, lane 8). Furthermore, this construct was unable to replicate *in*

vivo (Fig. 4.10D). These findings establish the requirements for intact binding-sites for PCBP and $3CD^{pro}$ within the cloverleaf structure for efficient positive-strand synthesis.

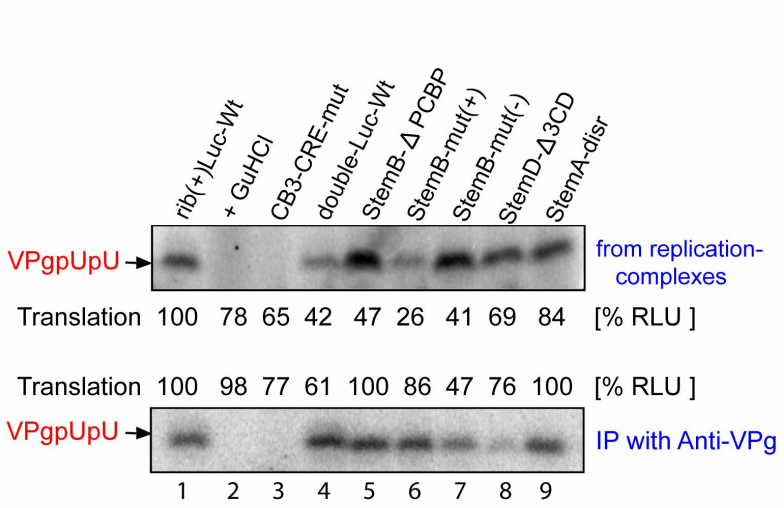

Figure 4.11: VPgpUpU formation in a cell-free translation-replication system. HeLa S10 extract was programmed with 1 µg of RNA transcripts. After 4 h of incubation at 30°C in the presence of 2 mM guanidine hydrochloride, preinitiation complexes were isolated by centrifugation at 15,000 x g. Preinitiation complexes were resuspended in labeling mix containing [α-^{32}P]UTP and incubated for 1 h. Top: Replication complexes were isolated by centrifugation at 15,000 x g, resuspended in Tricine-sample buffer, separated on a Tris-Tricine gel, and detected by autoradiography. Bottom: VPgpUpU was isolated by immunoprecipitation using polyclonal anti-VPg antibodies, separated on a Tris-Tricine gel and detected by autoradiography. Translation levels are represented by luciferase activity (relative light units [RLU]) measured after the 4 h incubation in the presence of GuHCl. The activity measured for rib(+)Luc-Wt was set to 100%. All other translation levels are expressed as % in relation to rib(+)Luc-Wt.

4.143 Constructs with two cloverleaf structures support *cre*(2C) mediated VPg-uridylylation.

A *cis*-acting replication element (*cre*) has been identified within the coding region of the picornavirus genome (McKnight & Lemon, 1998; Lobert et al., 1999; Goodfellow et al., 2000; Gerber et al., 2001a; Mason et al., 2002). For poliovirus, this *cre* is located within the 2C-coding region. This hairpin structure functions as a template for the covalent linkage of two UMP nucleotides to the viral primer, VPg, resulting in VPgpUpU (Paul et al., 2000; Rieder et al., 2000; Gerber et al., 2001a; Paul et al., 2003). There is evidence that *cre*(2C) mediated VPgpUpU functions as a primer for both negative- and positive-strand synthesis (van Ooij et al., 2006). However, it is only absolutely required for positive-strand RNA synthesis (Goodfellow et al., 2003b; Morasco et al., 2003; Murray & Barton, 2003). Since mutations in the cloverleaf negatively affect VPgpUpU formation, this structure has been indicated to have a role in VPg-uridylylation (Lyons et al., 2001). Most mutants tested in our studies show a severe defect in positive-

strand synthesis, therefore we wanted to examine if the tandem cloverleaf replicons with mutations severely disrupting the structure or protein binding-sites within the 5'-cloverleaf still support *cre*(2C) mediated VPg-uridylylation. We programmed HeLa S10 extract with replicon RNA and stopped the reaction after one hour of replication. Two different methods were then used to isolate VPg-pUpU: (i) The replication complexes were isolated and separated on a Tris-Tricine gel to be identified. (ii) After the reaction was stopped, VPgpUpU was isolated by immuno-precipitation (IP) using polyclonal anti-VPg-antibodies and then separated on a gel for detection. rib(+)Luc-Wt was used as a positive-control. GuHCl was added as a negative-control, since it is known to prevent the formation of VPgpUpU. In addition, a *cre*-mutant coxsackievirus B3 RNA that carries a mutation within the *cre*(2C) region that prevents VPgpUpU formation (A_5 to C mutation; as decribed later in section 4.2) was used. Using either method, similar levels of VPgpUpU synthesis were observed for rib(+)Luc-Wt RNA as well as for double-Luc-Wt RNA (Fig. 4.11; lane 1 + 4). VPgpUpU formation was also detected for all tandem cloverleaf replicons carrying mutations in the 5' cloverleaf that either disrupted the *stem b* duplex structure on the positive- or the negative-strand (StemB-mut(+) and StemB-mut(-)); that disrupted the *stem a* structure (StemA-disr); or that disrupted the binding-sites for PCBP or $3CD^{pro}$ (StemB-ΔPCBP and StemD-Δ3CD), as described before (Fig. 4.11, lane 5-9). These results confirm that the defect in positive-strand synthesis, when structure or protein binding-sites are disrupted, is not due to a lack of VPgpUpU formation. Furthermore, the replication complex formed by the downstream cloverleaf to initiate negative-strand synthesis is also able to support the *cre*(2C) mediated formation of VPgpUpU.

4.15 *Stem a* sequences are required for positive-strand RNA synthesis.

The *stem a* duplex structure in the cloverleaf is required for negative-strand RNA synthesis (Sharma et al., 2005). Using double-Luc-StemA-disr RNA, we established that the *stem a* structure is also required for positive-strand RNA synthesis. However, changes in the base-pair sequences of *stem a* only affect negative- but not positive-strand synthesis, as previously demonstrated (Sharma et al., 2005) and shown here with the G-C pair cloverleaf RNA. To further investigate the precise sequence requirements of *stem a* in the cloverleaf for positive-strand synthesis, we engineered tandem cloverleaf replicons with a series of *stem a* mutations within the 5' cloverleaf (for overview see Fig. 4.12A). Since disrupting the duplex structure leads to a decrease

in the level of positive-strand synthesis, base-pair sequences were replaced by different base-pair sequences without disrupting the structure. The 5' terminal two U's were always kept intact since they are the template for the 3' terminal two A's on the negative-strand, which is the location where the primer, VPgpUpU, binds. Following the first two U's, there are four consecutive A's, which all base pair with U on the other side of the stem. Those four A-U pairs were replaced in 10 different combinations. All mutated tandem cloverleaf RNAs were tested for positive-strand synthesis in the cell-free replication system (Fig 4.12B) and transfected into HeLa cells to identify their replication phenotype *in vivo* (Fig. 4.12C). The mutants could be separated into three groups based on their replication phenotype:

Group 1 (highlighted in blue): When the upper two A-U pairs were swapped to U-A pairs, or either the first (starting count on the lowest), third or fourth A-U pair replaced with G-C pairs (StemA-mut2, -mut4, -mut6, -mut7, respectively; Fig. 4.12A), a clear defect in positive-strand synthesis could be observed *in vitro* (Fig. 4.12B, lane 4, 6, 8, 9). However, the levels of positive-strands for those mutants were higher than for any other mutants. In addition, they all showed similar replication kinetics and reached the same level of luciferase-activity in cells as double-Luc-Wt (Fig. 4.12C). This shows that those mutations have no significant effect on replication *in vivo*.

Group 2 (highlighted in green) contained StemA-mut1, StemA-mut5, and StemA-mut9 where either the lower two A-U pairs were swapped into U-A pairs, the second A-U pair replaced by G-C, or the upper two A-U pairs were replaced with G-C pairs, respectively (Fig. 4.12A). Hardly any positive-strands could be detected for mutants in this group when tested in the cell-free replication system (Fig. 4.12B, lane 3, 7, 11). After transfection into cells, they all showed significantly decreased replication levels in comparison to double-Luc-Wt (Fig. 4.12C). These results establish that the decrease in replication seen in cells for those mutants is due to their defect in positive-strand synthesis as seen *in vitro*.

Group 3 (highlighted in red) contained the mutants with the most severe changes in base-pairing. In StemA-mut3 all four A-U pairs were swapped into U-A pairs, in StemA-mut8 the lower two A-U pairs were replaced by G-C pairs, and in StemA-mut10 all four A-U pairs were replaced by two G-C pairs and two C-G pairs (Fig. 4.12A). None of these mutants was able to synthesize detectable levels of positive-strands in cell extract (Fig. 4.12B, lane 5, 10, 12). Furthermore, no replication could be observed for either of them in cells (Fig. 4.12C).

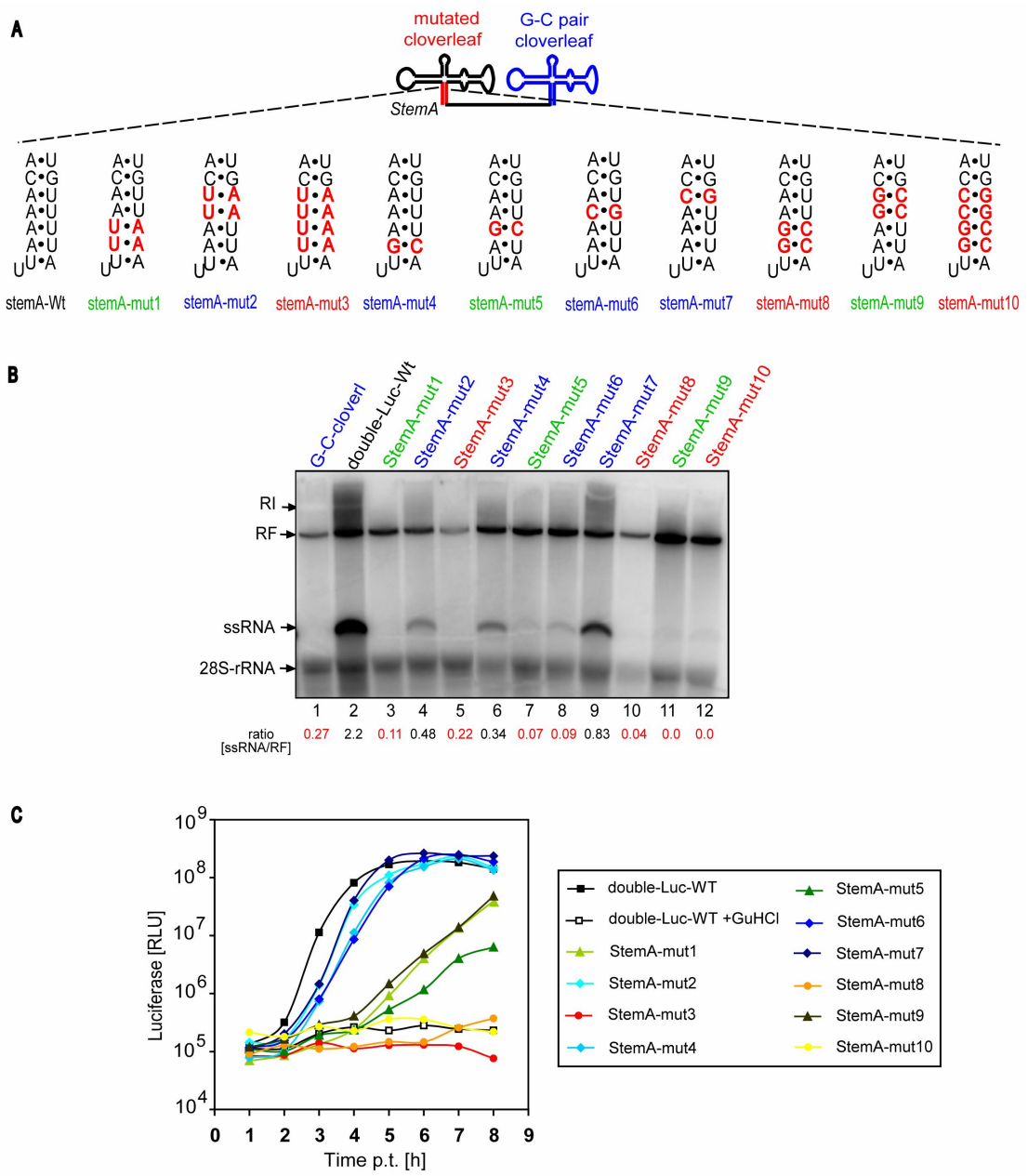

Figure 4.12: Schematic of tandem cloverleaf replicons with *stem a* mutations in their 5'-terminal cloverleaf and their replication phenotype *in vitro* and *in vivo*. (A) Schematic representation of tandem cloverleaf replicon RNA transcripts with *stem a* mutations in their 5'-terminal cloverleaf. Mutated sequences are highlighted in red. (B) RNA replication *in vitro*. HeLa S10 extract was programmed with 1 µg of RNA transcripts. After 4 h of incubation at 30°C in the presence of 2 mM guanidine hydrochloride, preinitiation complexes were isolated by centrifugation at 15,000 x g. Preinitiation complexes were resuspended in labeling mix containing [α-^{32}P]UTP and incubated for 2 h. Total RNA was prepared and separated on native agarose gels and detected by autoradiography. (C) Luciferase expression in replicon RNA-transfected HeLa cells. After transfection of the RNA transcripts into HeLa cells, the luciferase activity (relative light units [RLU]) corresponding to 2 x 10^4 cells was measured every hour for 8 h. The cells were either kept in the presence (+ GuHCl) or absence of 2 mM guanidine hydrochloride.

These results establish the importance of the sequences of all four A-U pairs in *stem a* for positive-strand RNA synthesis, since changes in the upper and lower part results in a defect in positive-strand RNA synthesis. However, more dramatic changes from A-U to G-C pairs can easier be tolerated in the upper two base-pairs than in the lower two, showing that the lower two A-U base-pairs are the most important ones for the synthesis of positive-strands.

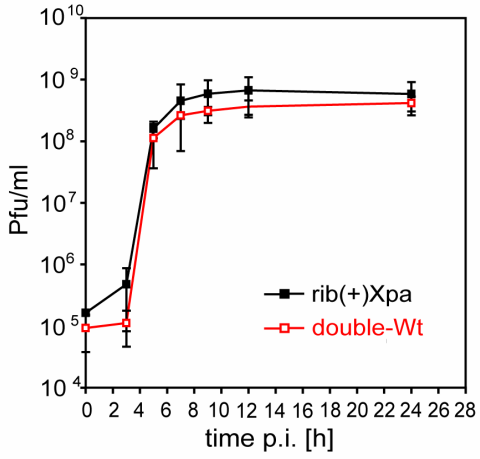

Figure 4.13: One-step growth curve of rib(+)Xpa and double-Wt viruses. HeLa cells were infected at a MOI of 10 Pfu/cell with either rib(+)Xpa or double-Wt viruses. At different time-points post infection (p.i.) supernatants were harvested and their virus titers were determined by standard plaque-assays. Each time-point represents the mean of triplicate samples and SD is indicated.

4.16 The importance of *stem a* sequences in the full-length virus

Our study of *stem a* mutations within the cloverleaf revealed the importance of the *stem a* sequences for positive-strand synthesis. We wanted to further investigate the significance of these sequences in the context of the full-length virus. To do so, we engineered virus RNA transcripts carrying the same tandem cloverleaf structures as in double-Luc-Wt, resulting in double-Wt RNA. This new RNA was transfected into HeLa cells and viruses were harvested and titered in standard plaque assays. First, we compared virus growth between double-Wt virus and rib(+)Xpa virus, the previously described wild-type poliovirus Mahoney strain 1 (Herold & Andino, 2000). A one-step growth curve of these two viruses revealed that their growth kinetics are identical (Fig. 4.13). An RT-PCR on virus sampled at 12 and 24 hours post-infection confirmed that the two cloverleaf structures in double-Wt were maintained (data not shown). The plaque-phenotypes for both were also similar in that the diameters for the biggest

plaques they both produced were the same (Fig. 4.14A). However, double-Wt produced a higher quantity of smaller plaques than rib(+)Xpa. These results establish that even full-length viruses with tandem cloverleaf structures provide a suitable system to study the promoter activity of the cloverleaf for positive-strand RNA synthesis.

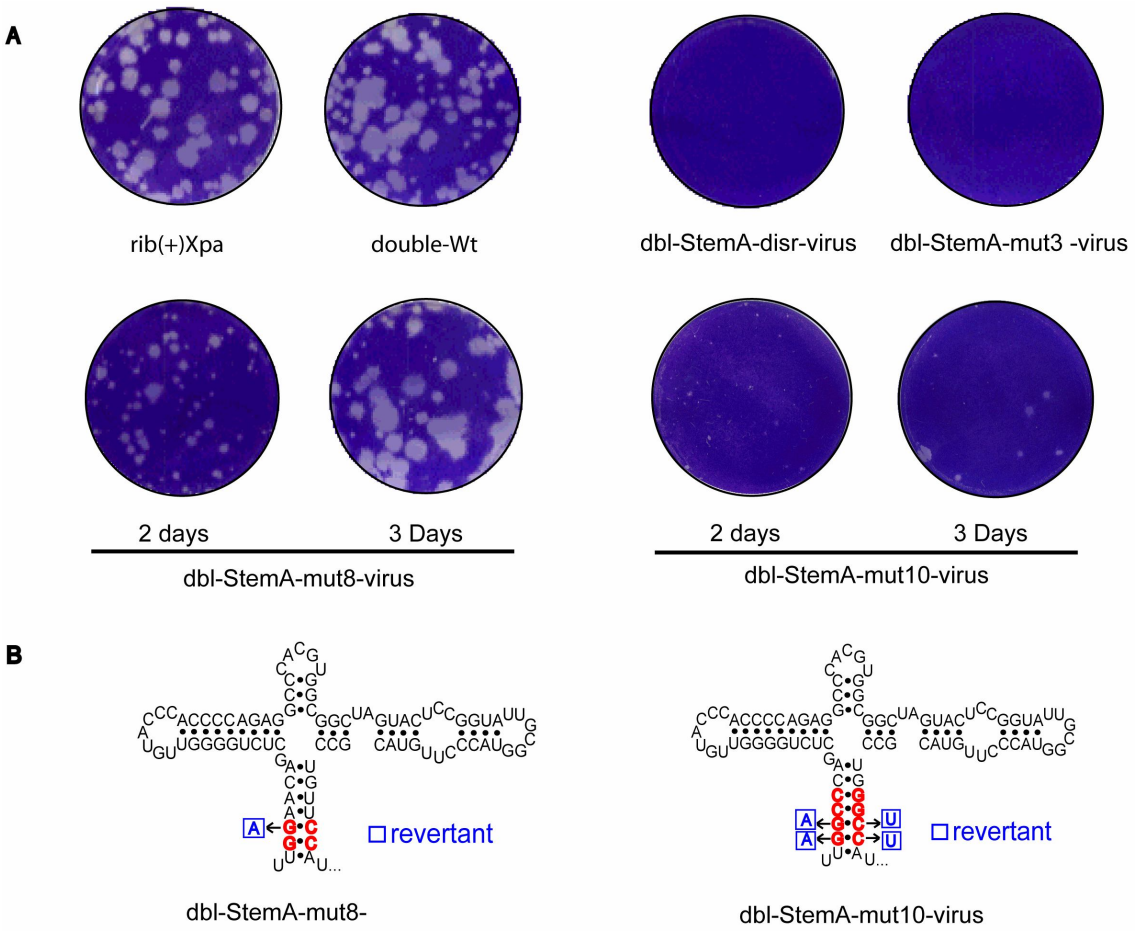

Figure 4.14: Plaque morphology of tandem cloverleaf viruses with *stem a* mutations in the 5'-terminal cloverleaf and sequences of revertant viruses. (A) Plaque morphology of tandem cloverleaf viruses with *stem a* mutations are shown in comparison to rib(+)Xpa (Poliovirus type 1 Mahoney) and double-Wt. Monolayers of HeLa cells were infected with the virus produced after transfection of viral *in vitro* RNA transcripts into HeLa cells. The cells were overlaid with DMEM/F12 medium, 1% agar and incubated at 37°C for 2 days if not indicated otherwise. Plaques were visualized by staining the monolayers with 0.02% crystal violet. Representative wells for the virus produced in the transfections containing rib(+)Xpa and each of the indicated tandem cloverleaf virus RNA are shown. (B) Sequences of 5'-terminal ends of input virus transcript RNA (mutations are highlighted in red) and recovered progeny virion RNA (revertant sequences are indicated in blue). The sequences for wild-type poliovirion RNA and for the virion RNAs from virus produced after transfection into HeLa cells were determined using a 5'-RACE procedure as described in Materials & Methods.

RNA-dependent-RNA polymerases such as in poliovirus have no proof-reading mechanism and, therefore, display a very high error rate when synthesizing new RNA. Under pressure, for example when the viral genome carries lethal mutations, revertant viruses can emerge. These viruses contain mutations that either compensate for the original lethal mutations or the lethal mutations have reverted back to the wild-type sequence to make the virus viable. For this reason, we chose four different mutations within *stem a*, StemA-disr, StemA-mut3, StemA-mut8, and StemA-mut10 (see Fig. 4.12A), that all lead to a complete inhibition of replication in cells and introduced them into the 5' cloverleaf of the tandem cloverleaf virus RNA. We transfected the *in vitro* transcribed virus RNA into HeLa cells and incubated them for three days or until total cytopathic effect was reached. Viruses were harvested and tested for their ability to form plaques in a standard plaque-assay. No plaques were detected for either StemA-disr-virus, with a complete disruption of *stem a*, or StemA-mut3 virus, that had all four A-U pairs swapped to U-A pairs within *stem a* (Fig. 4.14A). However, plaques were detected for StemA-mut8-virus and StemA-mut10-virus. StemA-mut8-virus, in which the lower two A-U pairs of *stem a* were replaced by G-C pairs, showed mostly smaller plaques after two days incubation than double-Wt; and after three days incubation, the plaques reached the same size than double-Wt reached after two days (Fig. 4.14A). StemA-mut10, in which the lower two A-U base pairs of *stem a* were replaced with G-C pairs, showed hardly visible plaques after two days incubation, which slightly increased in size after three days incubation. Even longer incubation did not result in bigger plaque-sizes than what was observed after three days (data not shown). The complete genomes of several plaque-purified StemA-mut8-viruses and StemA-mut10-viruses were sequenced. No mutations were found for either virus within the coding region or anywhere other than the very 5'-end. Using 5'-RACE, the mutated *stem a* area was sequenced and mutations identified. In StemA-mut8, in which two base pairs were mutated, the same point mutation was identified in all nine plaque-purified viruses that were sequenced. A reversion of the G of the second G-C base pair to A was observed, which represents the wild-type sequence, resulting in one mismatch within the *stem a* duplex structure (Fig. 4.14B). For StemA-mut10-virus, the other mutant that generated plaques, the population of the original passage 0 virus was used for sequencing of the 5'-end. Strikingly, it was found that the lower two G-C base-pairs reverted back to wild-type A-U pairs, a result that requires four individual point mutations to occur (Fig.

4.14B). These results strongly support the idea that the sequences of *stem a* are essential determinants for positive-strand RNA synthesis of poliovirus.

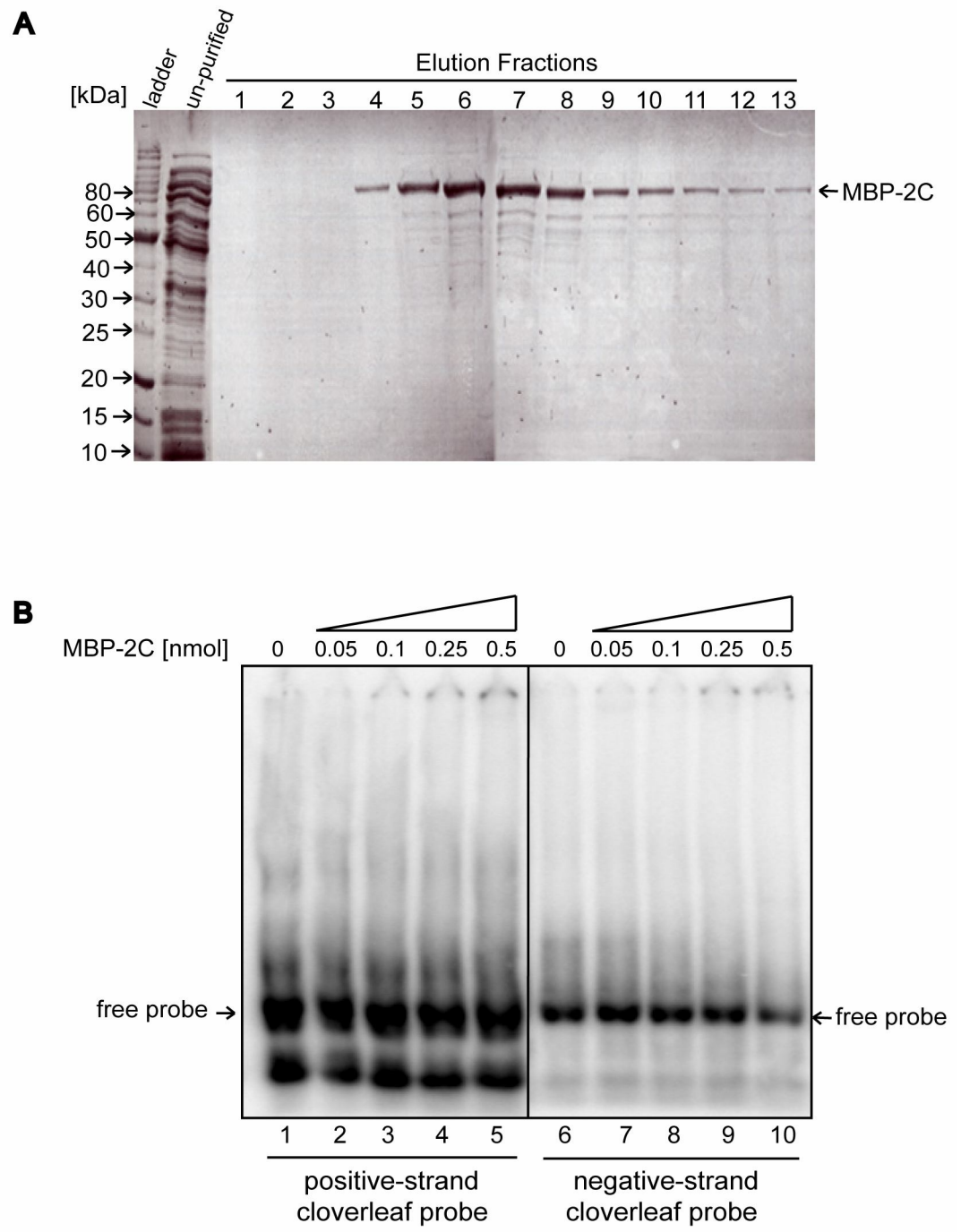

Figure 4.15: MBP-2C expression and purification, and mobility shift assay with cloverleaf probes. (A) SDS-PAGE gel with fractions eluted during purification of MBP-2C from an amylose column. MBP-2C was expressed in *E.coli*. Crude *E. coli* extract was purified by binding of MBP to amylose resin, which was subsequently, after washing, eluted in the presence of 10 mM maltose. Samples were mixed with protein-sample buffer, separated on SDS-polyacrylamide gel and stained with Coomassie blue. (B) Autoradiograph of Mobility shift assay with either a [α-^{32}P]UTP-labeled positive- or negative-strand cloverleaf probe using increasing amounts of MBP-2C protein.

4.17 The role of 2C^{ATPase} in positive-strand RNA synthesis

4.171 Binding affinities of MBP-2C to the cloverleaf

The viral protein 2C^{ATPase} is implicated in a variety of functions during viral replication, ranging from virus uncoating (Li & Baltimore, 1990) and host cell rearrangement to RNA synthesis (Cho et al., 1994) and encapsidation (Vance et al., 1997). The 2C^{ATPase} protein has ATPase and GTPase activity as well as two NTP-binding domains (Rodriguez & Carrasco, 1993, 1995). GuHCl, which inhibits initiation but not elongation of negative-strand synthesis (Barton & Flanegan, 1997), targets the 2C^{ATPase} protein (Pincus & Wimmer, 1986), although the mechanism by which it does so is not clear. Banerjee et al. reported that both 2C^{ATPase} and its precursor 2BC have binding-affinity to the 3'-end of the negative-strand of poliovirus, implicating a role of 2C^{ATPase} in positive-strand RNA synthesis (Banerjee et al., 1997; Banerjee et al., 2001). This interaction was shown to require the sequence of UGUUU in *stem a* of the minus-strand cloverleaf in the form of a double-stranded structure. However, the 2C^{ATPase} polypeptide analyzed in these studies was a renatured product isolated originally from an insoluble fraction after expression in *E. coli*. The studies demonstrating the ATPase and GTPase activity of 2C^{ATPase}, on the other hand, used a fusion protein of 2C^{ATPase} with the Maltose-binding-protein (MBP) (Rodriguez & Carrasco, 1993, 1995). In this case, the expression of 2C^{ATPase} as MBP-2C in *E. coli* produces a soluble fusion protein that does not need denaturing and renaturing for purification steps. We wanted to see if such a MBP-2C fusion protein also possesses a specific binding-affinity to the minus-strand cloverleaf. To this end, poliovirus 2C^{ATPase} was expressed in *E. coli* as a fusion polypeptide containing MBP at the amino-terminus. Expression and purification of MBP-2C was monitored on a Coomassie-stained SDS-PAGE gel (Fig.4.15A) and MBP-2C was purified on an amylose resin. Figure 4.15A shows the crude extract before purification (lane 1) and 13 fractions eluted during purification from the amylose column. The fractions with the strongest bands (fractions 5 - 8) were combined and further concentrated. The protein was then used for mobility shift assays using a [^{32}P]UMP-labeled probe of either the positive- or negative-strand cloverleaf. Neither probe showed any specific RNA binding affinities with the MBP-2C protein as seen in Figure 4.15B. This result indicates that the MBP-2C protein expressed in our study does not possess the same binding affinities as the 2C^{ATPase} protein isolated from insoluble fractions by Banerjee et al. (1997, 2001).

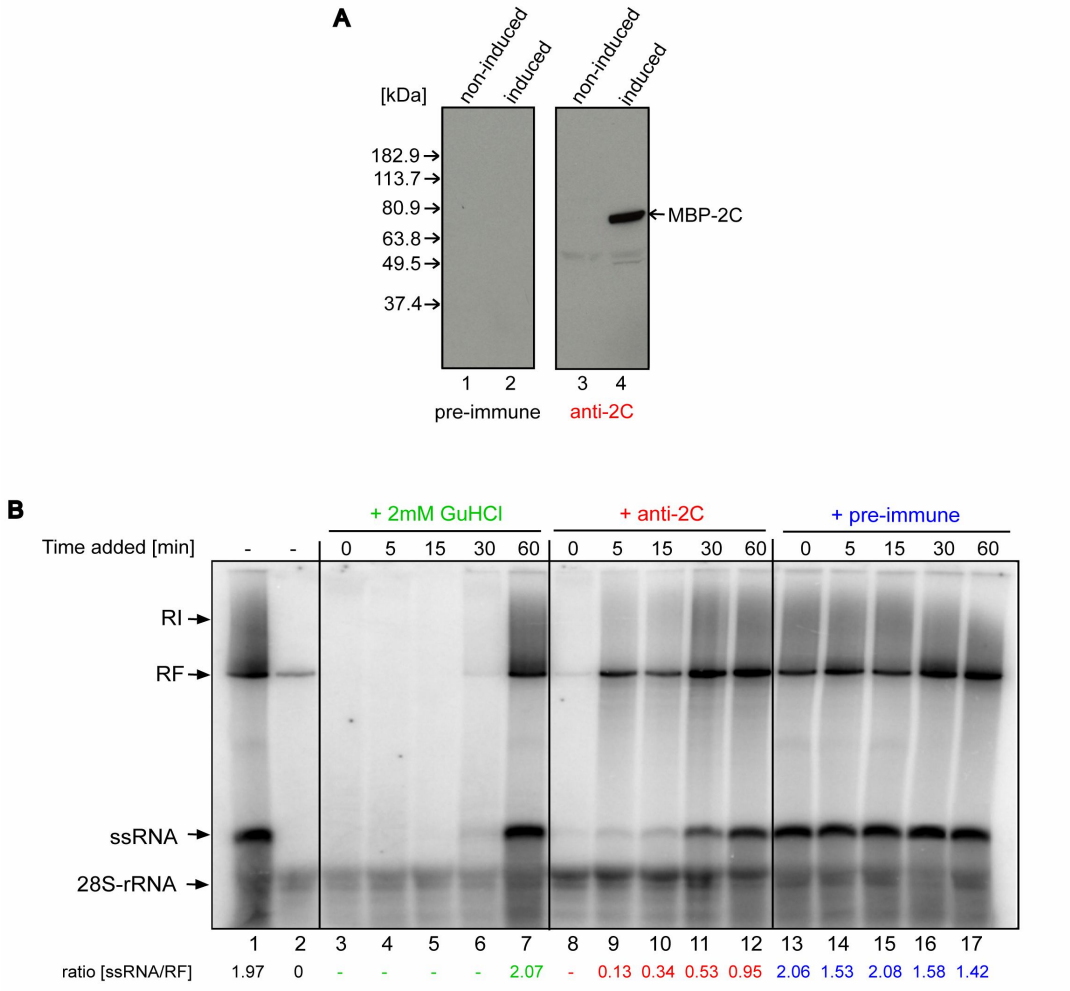

Figure 4.16: Replication of rib(+)Luc-Wt RNA transcripts in translation-replication extracts in the presence of guanidine hydrochloride or anti-2C antibodies. (A) Western Blot demonstrating the specific recognition of MBP-2C, before or after induction with 0.3 M IPTG, by purified polyclonal anti-2C antibodies and pre-immune serum. (B) HeLa S10 extract was programmed with 1 µg of rib(+)Luc-Wt RNA transcripts. After 4 h of incubation at 30°C in the presence of 2 mM guanidine hydrochloride (GuHCl), preinitiation complexes were isolated by centrifugation at 15,000 x g. Preinitiation complexes were resuspended in labeling mix containing [α-^{32}P]UTP and incubated for 90 min. At indicated time-points either 2 mM GuHCl, polyclonal anti-2C antibodies, or pre-immune serum was added to the reaction. Total RNA was prepared and separated on a native agarose gel and detected by autoradiography.

4.172 A role for 2C^{ATPase} in positive-strand RNA synthesis

Using the cell-free replication system, we wanted to specifically answer the question if 2C^{ATPase} has any role in positive-strand RNA synthesis. We programmed HeLa cell extract with rib(+)Luc-Wt RNA and added either GuHCl, polyclonal anti-2C antibodies or pre-immune serum (as a control) at different time points during a 90 min replication period. The polyclonal anti-2C antibodies and the pre-immune serum used in this

experiment were purified on an FPLC using a protein A column. The specificity of the antibodies after purification are demonstrated in a Western Blot using crude extract from *E.coli* before and after induction of MBP-2C expression as seen in Figure 4.16A. The pre-immune serum did not recognize any protein before or after induction (compare lane 1 and 2), whereas anti-2C antibodies recognized a single band of the expected size of approximately 80 kDa, only after induction of MBP-2C (compare lane 3 and 4). As expected, when adding GuHCl up to 30 min into the replication period, negative- and positive-strand RNA synthesis was inhibited (Fig. 4.16, lane 3-6). When the drug was added after 60 min, no inhibition of either strand synthesis was detected (Fig. 4.16, lane 7). The ratio of ssRNA to RF in this sample was the same as when no drug was added (Fig. 4.16, lane 1). When anti-2C antibodies were added at time-point 0 min, severe inhibition of both negative- and positive-strand RNA synthesis was observed (Fig. 4.16, lane 8). However, when anti-2C antibodies were added at 5 min or at any later time-point, a specific inhibition of positive-strand synthesis could be observed. When anti-2C antibodies were added at 5 min, the ratio of ssRNA to RF was decreased 12-fold in comparison to when pre-immune serum was added at this time (Fig. 4.16, compare lane 9 to 14). This decrease in ratio declined when anti-2C antibodies were added at a later time-point but was still 6-fold at 15 min and 3-fold at 30 min, and 1.5-fold when the antibodies were added at 60 min, in comparison to the samples with pre-immune serum (Fig. 4.16, compare lanes 10-12 with 15-17). These results show that the viral 2C protein has an important role in initiation of both negative-strand (as seen when GuHCl was added to the *in vitro* assay) and positive-strand RNA synthesis (as demonstrated when anti-2C antibodies were added).

4.2 The role of *cre*(2C) in RNA synthesis of coxsackievirus B3

4.21 Identification of the CVB3 *cre*(2C)

The genome of coxsackievirus B3 (CVB3) resembles that of poliovirus in organization of the UTRs and the coding region (Fig. 4.17a). Based on homology with poliovirus, it was suggested that a *cre* RNA is also located in the 2C coding region of coxsackievirus B3 (Goodfellow et al., 2000; Paul et al., 2000; Rieder et al., 2000; Witwer et al., 2001). Experimental evidence, however, is lacking. The corresponding region was predicted by MFOLD (Zuker, 1999) to form a hairpin structure with a terminal loop region of 14 nt (Fig. 4.17b). In order to investigate whether this RNA structure is indeed required for CVB3 replication, silent mutations designed to disrupt the stem of *cre* were introduced into a CVB3 replicon in which the capsid region was replaced by a luciferase gene (distortion mutant, CRE(2C)-DM, Fig. 4.17c). Transfection of this replicon into susceptible BGM cells yielded less luciferase activity (< 1%) than transfection of a wild-type replicon (Fig. 4.18a). The same translational levels were achieved by the replicon wild-type RNA in the presence of guanidine hydrochloride, emphasizing the strong defect in RNA replication (Fig. 4.18a).

In poliovirus and rhinovirus, the *cre* RNAs within the coding-region are the primary templates required for VPg-uridylylation (Paul et al., 2000; Gerber et al., 2001a; Yang et al., 2002; Goodfellow et al., 2003a). This prompted us to establish whether the CVB3 *cre*(2C) is also the primary site for VPgpUpU synthesis. Full-length genomic RNA transcripts, containing either wild-type *cre*(2C) or the DM mutant, were used as templates together with purified CVB3 $3D^{pol}$, $3CD^{pro}$, VPg and Mg^{2+} in an *in vitro* uridylylation assay. Using full-length genomic RNA transcripts, wild-type RNA was able to support VPg-uridylylation in the presence of both $3D^{pol}$ and $3CD^{pro}$, whereas no detectable amount of uridylylated VPg was observed upon distortion of the *cre*(2C) structure (Fig. 4.18b). These results suggest that the CVB3 *cre*(2C) is indeed the primary template for VPg-uridylylation.

4.22 Effect of disrupting the CVB3 *cre*(2C) stem-loop structure on negative-strand RNA synthesis

A cell-free translation replication system (as demonstrated in detail in part 4.1 of this thesis) has been used to study the effect of mutations on replication in *poliovirus*, including the effect of gross distortions of the *cre* structure on negative-strand RNA

synthesis (Goodfellow et al., 2003b; Morasco et al., 2003; Murray & Barton, 2003). However, this system has never been used to study replication of coxsackievirus. To ascertain whether CVB3 transcript RNA is able to function as a template for RNA replication in the cell-free system, CVB3 replicon RNA containing different 5'-ends was used (Fig. 4.18c). RNA containing the 5' hammerhead ribozyme (HR) sequence (Herold & Andino, 2000), which produces RNA with authentic 5' termini after transcription, efficiently produced both negative-stranded (RF) and positive-stranded RNA (ssRNA). Absence of this HR sequence produced CVB3 transcripts that contained two non-viral guanosine residues at their 5'-terminus, which only produced RF intermediates (Herold & Andino, 2000) and therefore efficiently blocked the accumulation of RI and ssRNA during the 2h incubation period (Fig. 4.18c). No bands were observed when CBV3 HR transcripts were incubated in the presence of guanidine hydrochloride, indicating that the cell-free system only displays viral RNA production (Fig. 4.18c).

It was previously shown that disruption of the *cre* structure in poliovirus does not interfere with the accumulation of negative-strands (Goodfellow et al., 2003b). In order to quantify the amount of minus-strands produced by coxsackievirus RNA in HeLa S10 cell extracts, we used RNA transcripts containing two non-viral guanosine residues at their 5'-terminus. Wild-type RNA produced a band corresponding to the RF of RNA replication. Accumulation of this band was abolished upon addition of guanidine hydrochloride, an observation demonstrating that this band is indeed of viral origin (compare WT with WT+GuHCl, Fig. 4.18d). In HeLa S10 cell extracts, CRE(2C)-DM RNA also accumulated RF, indicating that negative-strand RNA synthesis in this mutant is not inhibited (lane DM, Fig. 4.18d). Quantification indicated that CRE(2C)-DM RNA produces comparable amounts of RF to those of wild-type (Fig. 4.18d). In contrast to wild-type transcript containing a cis-acting HR-sequence, HeLa S10 cell extract programmed with CRE(2C)-DM RNA containing an HR sequence produced only the RF intermediates, but no ssRNA accumulation was observed (Fig. 4.18e). These results suggest that, under the conditions of the experiments, *cre*(2C)-mediated VPgpUpU is required for the initiation of positive-strand, but not negative-strand, RNA synthesis.

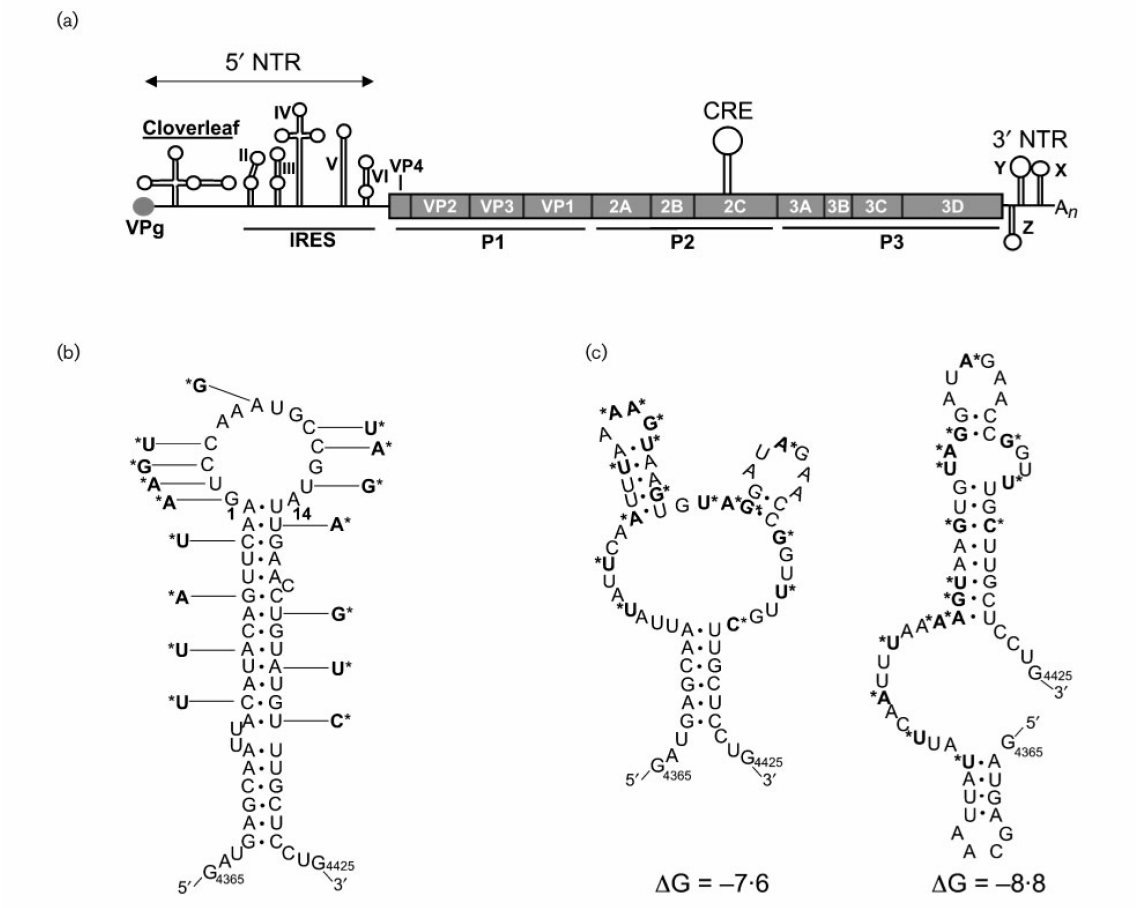

Figure 4.17. Coxsackievirus CRE(2C) and RNA replicons. (a) Schematic representation of the coxsackievirus genome. VPg (3B) is linked covalently to the 5'-end of coxsackieviral RNA. The RNA contains a 5'NTR consisting of two functional domains, the cloverleaf and the IRES, followed by a single open reading frame encoding a single polyprotein and a 3'NTR with a poly(A). The polyprotein contains a structural (P1) and two non-structural (P2, P3) domains, which are processed to the different proteins as indicated in the shaded box. The location of the CBV3 CRE(2C) element within the coxsackievirus genome is also depicted. (b) A representation of the secondary structure of the CBV3 wild-type CRE(2C) from nt 4365 to 4425 in the 2C protein-coding region as predicted by MFOLD. The CRE(2C) folds into a hairpin structure containing a loop of 14 nt and an imperfect stem. The silent mutations introduced to disrupt the CRE(2C) structure are indicated in bold type. (c) Two structural predictions, as proposed by MFOLD, of the disrupted CRE(2C) mutant (DM). The introduced silent mutations are indicated in bold type.

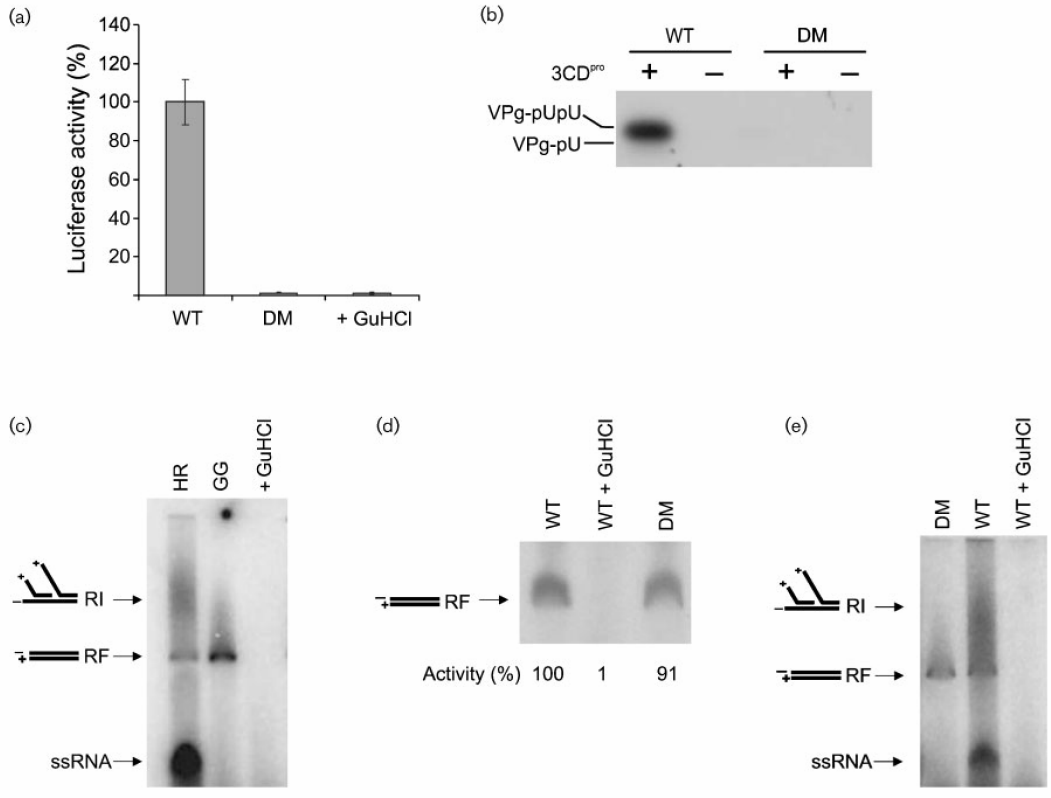

Figure 4.18. Identification of the CVB3 CRE(2C). (a) Replicons in which the capsid-coding region is replaced by a luciferase gene, incubated in the absence or presence (+GuHCl) of guanidine hydrochloride or containing the CRE(2C) distortion mutant, CRE(2C)-DM, were transfected into BGM cells. Ten hours post-transfection, cell lysates were harvested and assayed for luciferase activity. Each column represents the mean of five independent experiments and SD is indicated. (b) Uridylylation of VPg *in vitro* by using genomic CVB3 RNA transcripts containing wild-type (WT) or CRE(2C)-DM as template. Where indicated, $3CD^{pro}$ was omitted from the reaction mixtures. The *in vitro* uridylylation products were separated on a Tris/Tricine SDS-PAGE gel and visualized by using autoradiography. (c) *In vitro* replication assay using wild-type CVB3 RNA containing a 5' hammerhead ribozyme sequence incubated in the absence (HR) or in the presence (+GuHCl) of guanidine hydrochloride and a ribozyme-negative construct, that after RNA transcription using T7 RNA polymerase, gives rise to transcript RNA containing two non-viral guanosine residues at the 5' terminus (GG). (d) *In vitro* replication assay using RNA derived from ribozyme-negative constructs containing wild-type or CRE(2C)-DM. The mutants are indicated above the autoradiography and RF accumulation was quantified by measuring [^{32}P]UMP incorporation by using a phorphorimager. All values were normalized to wild-type RNA. (e) *In vitro* replication assay using wild-type (WT) or CRE(2C)-DM HR transcript RNA. As a control, wild-type CVB3 RNA incubated in the presence of guanidine hydrochloride is shown (WT+GuHCl).

4.23 Effect of *cre*(2C) point mutations on replication efficiency

A functional analysis was undertaken to determine whether the consensus sequence for the apical loop postulated by Yang et al. (2002) (R_1NNNAAR_2NNNNNNR_3 motif; R, A/G; N, any nucleotide) for the loop of rhinovirus and enterovirus *cre*'s, is also applicable to the CVB3 *cre*(2C). Subsequently, every nucleotide involved in this consensus sequence was substituted for almost all other nucleotide possibilities and, additionally, the coxsackie B-specific A_5AAUG_9 loop sequence was substituted for the consensus AAACA sequence (consensus mutant CM) to ascertain the relevance of the CVB3-specific U_8G_9 residues (Fig. 4.19b) (Rieder et al., 2000). Since the *cre* is located within the coding region, point-mutational analysis of the *cre*(2C) at its original location faces complications due to amino acid changes in the 2C region. However, the *cre* function has been described to be position-independent (Goodfellow et al., 2000; Yin et al., 2003), which enabled us to engineer an HR-CRE(Art) construct containing the *cre*(2C) distortion mutant at the original 2C position and a second, artificial *cre* at the junction of the P2 region and the luciferase gene, which replaces the capsid-coding region (Fig. 4.19a). Also, a *cis*-acting hammerhead ribozyme sequence was introduced in order to generate RNA transcripts with authentic 5'-ends (Herold & Andino, 2000). This construct enabled a mutational analysis of the CVB3 *cre*(2C) for its function in RNA replication, without altering the amino acid sequence of the CVB3 2C protein. *In vitro* transcribed RNA was transfected into BGM cells, and at 10 h post-infection luciferase activity was measured as described previously (van Kuppeveld et al., 1995). Substituting the coxsackievirus-specific AAAUG sequence for the consensus AAACA motif showed wild-type-like luciferase activity (lane CM, Fig. 4.19b). Alterations affecting the adenosine triplet showed that A_7 can only be replaced by another purine, whilst for A_5 and A_6, no substitutions were permitted (Fig. 4.19b). Substituting A_5 for a uridine residue, which results in the introduction of a stop codon (UAA), is included as a negative control for further studies described below. In this assay, however, no conclusions can be drawn for this mutation with respect to virus replication. Purine residues at the extreme ends of the *cre*(2C) loop sequence were proposed by Yang et al. (2002) to be required for rhinovirus and enterovirus replication. Substitutions regarding G_1 were in accordance with this consensus, as only a transition to an adenosine conferred the ability to replicate. Interestingly, residue A_{14} can be substituted by both a guanosine and a uridine, although the uridine substitution displayed reduced replication efficiency compared with the guanosine substitution. This

difference in replication efficiency, when comparing $A_{14}U$ with the $A_{14}G$ transition, might be explained by alternative folding of the loop as a result of non-canonical base-pair formation (MFOLD prediction), as opposed to changes in the primary *cre* sequence (data not shown).

In summary, the structure of the CVB3 *cre*(2C) loop resembles previously examined picornavirus *cre* elements and is in accordance with the consensus sequence proposed by Yang et al. (2002), with the exception of nucleotide A_{14}, which can be substituted by a guanosine or a uridine residue.

4.24 Effect of *cre*(2C) point mutations on VPg-uridylylation efficiency

The capacity of CVB3 *cre*(2C) mutants to support VPg uridylylation was tested by using short mutant *cre*(2C) transcripts RNAs, representing only the *cre*(2C). Uridylylation efficiencies were quantified as described in Materials and Methods. Consistent with the results obtained by using genomic RNA transcripts, a short transcripts containing only the *cre*(2C) distortion mutant (Fig. 4.17c) was unable to support uridylylation above detectable levels (lane DM, Fig. 4.19c). Substituting the $AAAUG_9$ sequence for the $AAACA_9$ consensus motif showed only a slight decrease in uridylylation efficiency compared with wild-type (lane CM, Fig. 4.19c). In general, mutants that were able to support RNA replication (Fig. 4.19b) also showed efficient VPg-uridylylation (G_1A, A_7G, U_8C/A, $A_{14}G/U$ and CM, Fig. 4.19c). Interestingly, lower levels of uridylylation did not always correlate with reduced levels of RNA replication, as shown for mutants U_8C and U_8A (compare Fig. 4.19b with Fig. 4.19c). The reason for this might be that the uridylylated products are made in large excess over what is used for RNA synthesis (Murray & Barton, 2003). No VPgpUpU synthesis above background levels, however, could be detected for G_1C, A_7C/U or $A_{14}C$ substitutions or for any of the A_5 or A_6 mutants (Fig. 4.19c), which were also defective for RNA replication (Fig. 4.19b). Therefore, it can be concluded that uridylylation of VPg is essential for viral RNA replication.

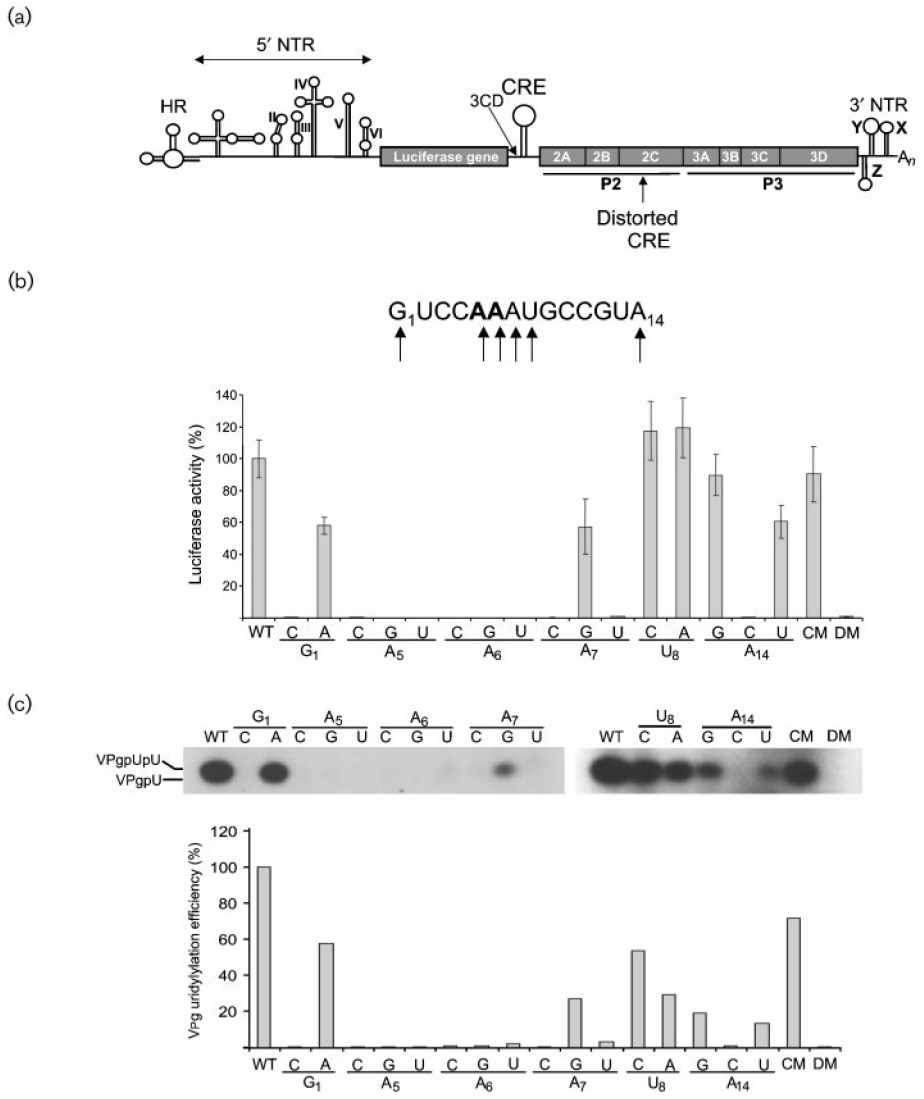

Figure 4.19. RNA replication and uridylylation efficiency of CVB3 CRE(2C) point mutants. HR-CRE(Art) was generated to assess replication capabilities of CRE(2C) mutants. The P1 region was substituted for the firefly luciferase gene. Wild-type or mutant CREs were introduced between the luciferase gene and the 2A junction by using a cloning cassette. Simultaneously, an additional $3CD^{pro}$ cleavage site was introduced to ensure release and activity of the luciferase polypeptide from the polyprotein. The CRE(2C) at its original 2C position was disrupted by using silent mutations as depicted in Fig. 4.17(c). Additionally, a hammerhead ribozyme (HR) sequence was inserted downstream of the promoter sequence to generate RNA transcripts containing authentic 5' ends. (b) Luciferase activity of the HR-CRE(Art) RNA transcripts described above, transfected into BGM cells. Each column represents the mean of five independent experiments and SD is indicated. A luciferase replicon that solely contained the cre(2C)-DM was used as a negative control (DM); mutant CM represents the substitution of the CVB3 AAAUG sequence for the picornaviral consensus sequence AAACA. The sequence above the graph represents the loop region of CRE(2C) and the arrows indicate the nucleotides that have been substituted. The adenosine characters in bold type could not be substituted for any other nucleotide. (c) Determination of uridylylation efficiency, using short RNA transcripts of wild-type and mutant CRE(2C) as templates. The amounts of [α-^{32}]UMP incorporated into the VPgpU and VPgpU(pU) products were quantified by using a phosphorimager. An autoradiograph of the reactions is shown above.

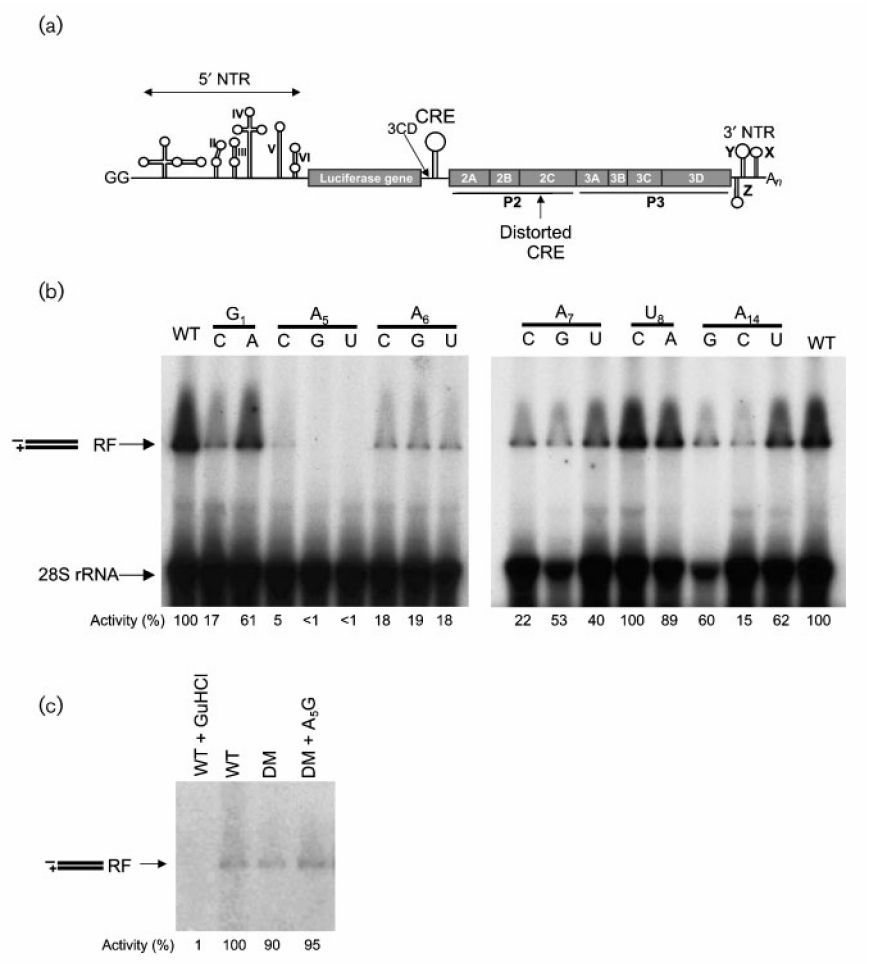

Figure 4.20. Effect of CRE(2C) mutations on RNA-strand synthesis. (a) GG-CRE(Art) transcripts RNA synthesized with T7 RNA polymerase from plasmids lacking a 5'-terminal hammerhead ribozyme. These transcripts carry a non-viral pppGG dinucleotide at their 5' terminus. (b) Pre-initiation complexes were incubated with transcript RNA derived from ribozyme-deletion constructs containing a translocated CRE(2C) (see Fig. 4.20(a)). The tested mutants are indicated above the autoradiograph and both the 28S rRNA band and the RF accumulation were quantified by measuring [^{32}P]UMP incorporation using a phosphorimager. All values were corrected for RNA loading as described in Materials and Methods and normalized to wild-type RNA. (c) *In vitro* replication assay using GG-CRE(Art) transcript RNA containing either a wild-type, the CRE(2C)-DM or CRE(2C)-DM-A5G mutant in the mutation cassette. The mutants are indicated above the autoradiograph and RF accumulation was quantified by measuring [^{32}P]UMP incorporation using a phosphorimager. All values were normalized to wild-type RNA.

4.25 Effect of *cre*(2C) point mutations on negative-strand RNA synthesis

To ascertain the effect of *cre*(2C) point mutations on RF synthesis, we used a construct from which RNA transcripts containing two non-viral guanosine residues at their 5'end, termed GG-CRE(Art), are derived (Fig. 4.20a), allowing us to specifically evaluate and quantify the effect of *cre*(2C) mutations on RF synthesis. A very good correlation was observed between the [^{32}P]UMP labeling of the 28S rRNA band and the ethidium bromide staining of the gel, which allowed us to quantify RF accumulation irrespective of loading by determining the ratio between the 28S rRNA band (Herold & Andino, 2000) and synthesized viral RF.

As a completely distorted *cre*(2C) structure produced RF levels similar to wild-type, and therefore was not or could not be used as a negative control (Fig. 4.18d) (Morasco et al., 2003; Murray & Barton, 2003), it was rather unexpected that the majority of the *cre*(2C) substitutions regarding the enterovirus consensus sequence did not accumulate wild-type-like RF levels. Mutants positive for both luciferase activity (Fig. 4.19b) and VPg uridylylation (Fig. 4.19c) accumulated, albeit with different efficiencies, the highest levels of RF synthesis (G_1A, A_7G, U_8C/A, and $A_{14}G/U$, Fig. 4.20b). Only the U_8 mutants, a residue not belonging to the consensus sequence, showed wild-type RF production (U_8C/A, Fig. 4.20b). In general, a good correlation was observed between the luciferase activity and the efficiency of RF synthesis using these mutants (compare Fig. 4.19b with Fig. 4.20b). VPgpUpU-defective point mutations accumulated RF synthesis only to approximately 20% of that of wild-type CVB3 RNA (G_1C, A_5C, $A_6G/C/U$, A_7C and $A_{14}C$, Fig. 4.20b), whereas the VPgpUpU-defective A_5G mutant was unable to support RF synthesis above detectable levels (Fig. 4.20b). The fact that point mutations reduced in VPgpUpU formation were affected in RF accumulation already suggests that *cre*(2C)-derived VPgpUpU is also utilized to initiate negative-strand RNA synthesis. Because inhibiting RF synthesis by introducing a stop codon (A5U, Fig. 4.20b) displayed results similar to those for the A_5G transition, it was concluded that this latter mutant was defective for negative-strand RNA synthesis. This, again in contrast to previous reports, implies the necessity for the *cre*(2C) not only in positive-strand, but also in negative-strand RNA synthesis. Additionally, GG-CRE(Art) transcript RNA, containing a completely distorted *cre*(2C) with an additional A_5G mutation, still produced wild-type RF levels, concluding that the dominant-negative effect of the A_5G transition is only functional in the context of a wild-type *cre*(2C) structure (Fig. 4.20c).

In summary, all *cre*(2C) point mutations affecting the enteroviral *cre* consensus sequence, so excluding U_8A/C, showed a marked decrease in their capacity to support negative-strand RNA synthesis. Therefore, it can be concluded that these results ascribe an important role to the coxsackievirus *cre*(2C) in the initiation of both positive- and negative-strand RNA synthesis. However, this requires a new model that can explain the apparently contradictory results about he role of *cre*(2C) in negative-strand RNA synthesis.

5. Discussion

5. Discussion

5.1 The multi-functional role of the cloverleaf in poliovirus replication

A functional ribonucleoprotein complex forms around the cloverleaf structure at the 5'-end of the poliovirus genome. The RNA structure is a *cis*-acting replication element that participates in the assembly of the complex that catalyzes the initiation of both negative- and positive-strand RNA synthesis. The interaction of this complex with the 3'-end of the viral genome leads to initiation of negative-strand RNA synthesis. In this case, the cloverleaf structure at the 5'-end acts as a promoter for negative-strand RNA synthesis which is initiated at the opposite end of the genome. Our study demonstrates that the cloverleaf structure in the positive-strand is also required for positive-strand RNA synthesis. Here, the same RNA element at the 5'-end of the genome functions as a promoter for positive-strand RNA synthesis, which is initiated at the 3'-end of the opposite (negative) strand. We provide evidence that the same ternary complex formed around the cloverleaf structure displays a bi-functional role in two subsequent and differently regulated steps in viral replication.

5.11 The role of the cloverleaf in negative-strand RNA synthesis

Using the ribozyme(-) constructs with cloverleaf mutations clearly shows their effect on negative-strand RNA synthesis. For both *stem b* and *stem d* disrupting the positive-strand duplex structure completely abolished the formation of RF. Except for the mutation in StemB-DNC1, in which proper base-pairing is maintained on both strands; all other mutations affected the synthesis of negative-strands to different degrees. Mutations on *stem d* resulted in a much bigger defect in negative-strand RNA synthesis than most mutations in *stem b*. One possibility is that all the mutations in *stem d* that we analyzed might affect binding of $3CD^{pro}$ to this part of the cloverleaf structure, since the exact binding-site of the $3CD^{pro}$ protein is not known. The binding-site of PCBP2 to the cloverleaf, on the other hand, is narrowed down to a poly(C) stretch within the loop of stem-loop b and protein-binding might only be strongly affected by mutations completely disrupting the duplex structure of *stem b* (such as StemB-mut(+)). The effect of cloverleaf mutations on negative-strand RNA synthesis is well in accordance with previous studies that showed that either a complete deletion of the cloverleaf

(Lyons et al., 2001) or the same mutation as in StemD-insert (Barton et al., 2001) abolishes negative-strand RNA synthesis. However, the *in vitro* assay with the ribozyme(+) constructs containing cloverleaf mutations effectively illustrates the problem in analyzing a multi-functional role of a *cis*-acting replication factor in subsequent steps of replication. The defect in negative-strand RNA synthesis, clearly revealed by the study with the ribozyme(-) constructs, is more difficult to identify with the ribozyme(+) replicons. The replicons undergo several rounds of replication within a 2 hour incubation period, and since one minus-strand can be used to synthesize several plus-strands, which then undergo new minus- and plus-strand synthesis, this will eventually result in negative- and positive-strand RNA synthesis as seen for StemB-mut(+). If the same mutation affects minus- and plus-strand RNA synthesis in a similar way, then all replication products such as RF and ssRNA will be synthesized on a lower level than wild-type, but it would be impossible to make any conclusions as to which step in replication is affected. In the original study of the cloverleaf, the StemD-insert mutant (referred to as DNC11 in (Andino et al., 1990)) not only showed a reduction in the ratio of plus- to minus-strand synthesis, but also a dramatic decrease in the synthesis of negative-strands in comparison to wild-type. This result indicates a role of the cloverleaf in both negative- and positive-strand RNA synthesis.

The replication phenotypes of the cloverleaf mutations after transfection into HeLa cells correlate for the most part with the data obtained *in vitro*. They confirm the importance of the cloverleaf structure in the positive-strand for efficient replication. They are also in good agreement with the changes in plaque-phenotypes of these mutants as analyzed in Andino et al. (1990).

In summary, our data demonstrate that the cloverleaf structure in the positive-strand is an important *cis*-acting replication element which is required for negative-strand RNA synthesis.

5.12 A novel system to analyze the role of the cloverleaf in positive-strand RNA synthesis

The findings that the cloverleaf structure functions as a promoter for both positive- and negative-strand RNA synthesis is in agreement with the original implications of such a role for the cloverleaf. As mentioned in the previous section, several point mutations within the cloverleaf RNA reduce both positive- and negative-strand RNA synthesis,

with positive-strand synthesis being more affected, resulting in a 5- to 10-fold decrease in the ratio of plus- to minus-strands (Andino et al., 1990). These results implied that mutations within the cloverleaf abrogated positive-strand RNA synthesis and/or stability (Andino et al., 1990). We developed a novel approach to analyze this dual role of the same RNA element in viral replication by engineering poliovirus replicons carrying tandem cloverleaf structures at their 5'-end. Using the cell-free replication system we showed that the downstream G-C pair cloverleaf in the tandem cloverleaf construct could not only provide negative-strand RNA synthesis, but also VPgpUpU formation, both of which are preconditions for positive-strand RNA synthesis to occur (Goodfellow et al., 2003b; Morasco et al., 2003; Murray & Barton, 2003). This set-up enabled us to examine the direct impact of mutations in the 5'-end structure and sequence on positive-strand RNA synthesis.

One concern we had about placing two cloverleaf structures right next to each other was the risk of interaction between the two identical sequences. There are many interactions between cloverleaf sequences, which result from the stem structures found in the RNA. Having two cloverleaf sequences next to each other could result in interactions between regions of one cloverleaf with the other. Such interactions could interfere with the original role of the cloverleaf in forming a ternary complex with proteins and hence, with the role of the cloverleaf in promoting RNA synthesis. This was reflected in the first tandem cloverleaf construct that was engineered and contained two wild-type cloverleaves at its 5'-end. Its replication phenotype in cells was nearly identical to a wild-type replicon with one cloverleaf; however, it showed some defect in synthesis of both RF and ssRNA in the cell-free replication system. This defect was not observed when the tandem replicon contained a StemD-mut(-) mutation in its 5'-terminal cloverleaf. This result supports the idea that two cloverleaves next to each other with less identical sequences might decrease the possibility of interactions between the two RNA structures. In addition, in replicons that carry a wild-type cloverleaf at its downstream position and a mutated cloverleaf upstream, the mutated cloverleaf will most likely be deleted after transfection into cells, releasing a replicon with all wild-type sequences. This phenomenon can be observed for rib(-)Luc-Wt that contains additional non-viral sequences at its 5'-end that get deleted after transfection into cells (Herold & Andino, 2000), which leads to a two hour delay in viral replication as seen in Figure 4.4B. Based on these findings, we were able to engineer a new tandem cloverleaf replicon that contains a G-C pair cloverleaf at its downstream

position. In this construct, the identical sequences between the two cloverleaves are reduced and the 5'-terminal cloverleaf cannot be deleted since it can only support negative-strand RNA synthesis, as we demonstrated. The new tandem cloverleaf construct double-Luc-Wt was able to replicate identically to rib(+)Luc-Wt *in vitro* and *in vivo*. Structural mapping further confirmed that the two cloverleaf structures in double-Luc-Wt indeed form two separate but identical structures.

5.13 The structural and functional requirements of the cloverleaf for positive-strand RNA synthesis

5.131 The 5'-end sequence and structure

Recent studies identified the importance of the accurate 5'-end sequences for efficient positive-strand RNA synthesis (Herold & Andino, 2000; Sharma et al., 2005). Our lab showed that additional non-viral sequences at the 5'-end of the viral genome leads to a defect in positive-strand RNA synthesis in the cell-free replication system, as well as to a delay in replication in cells (Herold & Andino, 2000). Such additional sequences are eventually deleted after transfection into cells. These results indicate the importance of the 3'-terminal sequences of the negative-strands and suggest that the viral primer for positive-strand RNA synthesis, VPgpUpU, recognizes the 3'-terminal AA only when they are available as terminal sequences. For this reason, we left the two 5'-terminal UU in all tandem cloverleaf constructs intact to not interfere with positive-strand RNA synthesis. Another study identified the 5'-terminal 9 nucleotides of the positive-strand to be important for efficient initiation of positive-strand RNA synthesis, again indicating that these sequences are important on the level of the negative-strand (Sharma et al., 2005). In this study, the authors proposed that there is no structural requirement at the 5'-end of the plus-strand or the 3'-end of the negative-strand to initiate positive-strand RNA synthesis (Sharma et al., 2005). However, the results with the plus9, plus20, and plus27 replicons clearly imply that a promoter element on the very 5'-end of the positive- or the 3'-end of the negative-strand is required to initiate positive-strand RNA synthesis. Even when the terminal 9 nucleotides as part of a wild-type *stem a* duplex structure (plus20) is present, there was no initiation of plus-strand RNA synthesis. The most surprising result was the inability of the plus9 replicon to replicate at all *in vivo* and to synthesize positive-strands *in vitro*. Here, the cloverleaf structure on the positive-strand is only 15 nt away from the 5'-terminus, in addition to the wild-type 9

terminal nucleotides being present on the 3'-end of the negative-strand, and still no positive-strand synthesis could be observed. These findings demonstrate that the terminal structure itself (at the 5'-end of the plus-strand or/and at the 3'-end of the minus-strand) is as important as the precise sequences for initiation of positive-strand RNA synthesis. It also highlights that the cloverleaf structure can only function as a promoter for positive-strand RNA synthesis when it is located at the very end of the genome. This is contrary to the cloverleaf function as a promoter for negative-strand RNA synthesis, for which the cloverleaf can be located hundreds of nucleotides away from the 5'-end of the genome as demonstrated by the G-C pair cloverleaf in the tandem cloverleaf replicon.

5.132 The cloverleaf on the positive-strand

The results with the tandem cloverleaf constructs with *stem b* and *stem d* mutations demonstrate the requirements of the cloverleaf structure in the positive-strand for the synthesis of plus-strands. However, comparing the results in the cell-free replication system and *in vivo* revealed some differences between these two systems. Small differences on the level of positive-strand RNA synthesis such as between StemB-mut(-) and StemB-mut(+) resulted in a big difference in their replication phenotype in cells. This was in agreement with several other *stem b* mutants that were able to synthesize only a small amount of positive-strands *in vitro* but replicated with nearly wild-type level in cells. However, the overall ratio of plus-strand to minus-strand synthesis *in vitro* correlated with the replication level *in vivo*: a higher ratio *in vitro* resulted in better replication *in vivo* and the other way around. Keeping in mind that the cell-free replication system is a more artificial system and replication in cells mimics more closely the events of real host – virus interaction, we always used the *in vivo* data to evaluate the significance of a defect in positive-strand RNA synthesis seen in the *in vitro* system. Based on this guideline, we conclude that the *stem b* sequences are not crucial; but an intact *stem b* duplex structure on the positive-strand is required for efficient positive-strand RNA synthesis. The ratios of positive-strands to RF *in vitro* for the *stem d* mutants also correlate to the replication level of these mutants *in vivo*. However, a lower level of positive-strand RNA synthesis was observed *in vitro* for all *stem d* mutants which were not able to replicate in cells. The same was sometimes observed for the G-C pair cloverleaf construct alone as well as rib(-)Luc-Wt (data not shown). *In vitro*, it might be possible that the primer VPgpUpU binds to the 3'-terminal

AA in a less regulated manner and initiates rather inefficiently positive-strand RNA synthesis. This phenomenon might not occur in cells, and therefore, no replication would be observed. This difference might be due to the location in which replication occurs in both systems. After viral infection of cells, a complete rearrangement of cell organelles can be observed and membranous vesicles are formed to which the replication complexes are attached (Bienz et al., 1983; Bienz et al., 1992; Troxler et al., 1992; Egger et al., 1996). In cell extract as used in our study, the cell organelles are disrupted by homogenizing and the replication complexes are most likely attached to membrane particles rather than defined membranous vesicles. This may enable the synthesis of some positive-strands in a less regulated manner. The StemD-mut(+) mutation did not have such a dramatic effect on positive-strand RNA synthesis and replication in cells as the StemB-mut(+) had. The reason might be that the *stem b* mutant contained three base-pair changes whereas the *stem d* mutant only contained two. The effect of two changes in *stem d* might not disrupt the structure as much as the changes in the *stem b* mutant. However, when four base-pairs were disrupted in *stem d*, as in StemD-disr, no replication was observed in cells. We conclude that the entire cloverleaf structure, including an intact *stem b* and *d*, is required for positive-strand RNA synthesis. Interestingly, for StemD-mut(-) the ratio of plus-strands to minus-strands in the cell-free replication system was increased by over two-fold in comparison to wild-type.

The defects observed *in vitro* in positive-strand RNA synthesis and in cells in replication were not due to problems with RNA stability since no decrease in translation was observed in any of the systems. It is possible that a disrupted *stem d* duplex structure in the cloverleaf on the negative-strand helped the negative-strand to unfold properly for the polymerase to move along and synthesize a new plus-strand. The level of luciferase activity as an indirect measure for translation was approximately the same for all the mutants in comparison to wild-type (data not shown) at the end of the translation period in the cell-free replication system. After transfection into cells we monitored luciferase activity also in the presence of GuHCl for all mutants, which provides the translation levels of just the input RNA (data not shown). If RNA stability was affected we would expect a decrease in translation of the RNA. Though, all mutants reached similar levels of translation as the wild-type RNA. Thus, we exclude RNA stability issues as an explanation for the decrease in positive-strand RNA synthesis.

5.133 PCBP2 and 3CD^{pro} binding sites

The cloverleaf RNA forms a ternary complex together with the cellular PCBP2 and the viral 3CD^{pro} (Andino et al., 1990; Andino et al., 1993; Parsley et al., 1997). As shown in a previous study, this complex can interact with the 3'-end of the viral genome through a RNA-protein-protein-RNA bridge and initiates negative-strand RNA synthesis (Herold & Andino, 2001). Our results show that functioning PCBP2- and 3CD^{pro}-binding sites in the cloverleaf structure are required for efficient positive-strand RNA synthesis *in vitro* and *in vivo*. We conclude that the same ternary complex used for initiation for negative-strand RNA synthesis also plays a role in positive-strand RNA synthesis. However, the mechanism used by this complex to support plus-strand synthesis has to be different from the one used in the synthesis of minus-strands, since positive-strand RNA synthesis is initiated at the 3'-end of the negative-strand. PCBP2 interacts with PABP, which binds to the poly(A) tail for negative-strand synthesis. However, this would not be helpful for initiation of positive-strand RNA synthesis. One can imagine that after unwinding of the RF intermediate, PCBP2 binds to the cloverleaf on the plus-strand to stabilize the complex formation and to keep the plus-strand separated from the minus-strand, which helps with binding of the primer and the polymerase to the minus-strand. 3CD^{pro} might partly play the same role, helping to stabilize the complex formation, but might have additional roles. 3CD^{pro} could provide the viral polymerase 3D^{pol} for initiation of positive-strand RNA synthesis by cleavage of 3CD^{pro}. This way, the ternary complex around the cloverleaf could guide the polymerase to the exact location to synthesize plus-strands. The requirement of 3CD^{pro} in positive-strand RNA synthesis could also be a way to eventually down regulate replication and support encapsidation of viral RNA into new virions. The level of 3CD^{pro} as a protein precursor goes down over time during replication since it gets cleaved into 3C^{pro} and 3D^{pol}. With less 3CD^{pro} available, encapsidation might be favored. Since clear encapsidation signals in poliovirus are missing (reviewed in 1.44), it seems that several steps in the life cycle might contribute to this event. The down regulation of 3CD^{pro} might be one of the factors that eventually contribute to the encapsidation event.

5.134 The significance of *stem a*

Our results using the StemA-disr construct show that the duplex structure *of stem a* in the cloverleaf is required for positive-strand RNA synthesis. In the original analysis of the cloverleaf, a disrupted *stem a* (referred to as DNC91) has proven to be lethal for

the virus (Andino et al., 1990). A previous study identified the importance of an intact *stem a* structure for negative-strand RNA synthesis (Sharma et al., 2005). The disruption of two base-pairs on *stem a* showed no effect on positive-strand RNA synthesis (Sharma et al., 2005). However, we provide evidence that disruption of four base-pairs in *stem a* leads to a severe defect in positive-strand RNA synthesis and completely abrogates replication in cells. We conclude that *stem a* is required for both negative- and positive-strand RNA synthesis. Furthermore, we demonstrate that the entire *stem a* sequence is involved in plus-strand synthesis. Our findings are consistent with the results of a previous study in which the same mutations (StemA-mut1, -mut2, and –mut3) were studied *in vitro* and led to a similar decrease in positive-strand RNA synthesis (Sharma et al., 2005). The importance of the *stem a* sequences for positive-strand RNA synthesis was further demonstrated by our studies using full-length virus. The reversion found in the StemA-mut8-virus highlights the importance of position A_4 in poliovirus. It appears that a one base-pair disruption can be tolerated in this context. Strikingly, the four point mutations found in the viruses isolated from StemA-mut10 restored two of the wild-type base-pairs in *stem a*. Based on our results we cannot identify if the *stem a* duplex structure is required on the positive- or on the negative-strand to support the cloverleaf formation for positive-strand RNA synthesis. However, a recent study identified that hnRNP C1/C2 proteins (heterogeneous nuclear ribonucleoprotein C1/C2) have binding-affinities to the 3'-end of the negative-strand of poliovirus (Sokolowski & Schwartz, 2001; Brunner et al., 2005). Depleting HeLa cell extract of these proteins resulted in a decrease in RNA synthesis, a defect that can be restored when recombinant hnRNP C1 was added. The hnRNP C proteins bind to $(U)_n$ motifs that contain 3 consecutive Us (Sokolowski & Schwartz, 2001). Accordingly, the 3'-terminal sequence of the poliovirus negative-strand, 3'-AAUUUUGU-5', could be a candidate sequence for binding hnRNP C. This could give a possible explanation why we found one point mutation (from G_4 back to A_4) in the StemA-mut8 virus, which restores a previous 3'-$C_4U_5U_6$ stretch in the negative-strand to a 3'-$U_4U_5U_6$ stretch, thus providing a target sequence for hnRNP C to bind. This however, does not explain the requirement of the *stem a* duplex structure for initiation of positive-strand RNA synthesis. One could think, that an intact *stem a* structure might help the cloverleaf to form properly on the positive-strand, and thus, for the proteins to bind the structure and form the required ternary complex. The requirement of the intact sequences at the very end might be an additional requirement to the duplex structure of *stem a* and these

requirements might display two different roles in positive-strand RNA synthesis.

5.14 The role of 2C^{ATPase} in RNA synthesis

Much has been speculated about possible roles of viral proteins in positive-strand RNA synthesis. Viral non-structural proteins and their precursors have several overlapping functions at different steps throughout the viral life cycle. This makes it difficult to dissect those different roles by genetic analysis since one mutation often affects several functions. The viral 2C^{ATPase} protein has been proposed to be involved in negative- and positive-strand RNA synthesis (Banerjee et al., 1997; Barton & Flanegan, 1997; Banerjee et al., 2001). Our results suggest that there might be at least two different functions for 2C^{ATPase} during RNA replication. A guanidine-hydrochloride sensitive function was indicated to be required for initiation but not elongation of negative-strand RNA synthesis (Barton & Flanegan, 1997). Our results using guanidine are in agreement with those findings. In our study GuHCl either inhibited negative-strand RNA synthesis, and consequently, also positive-strand RNA synthesis, or neither when added at a later time point. After addition of anti-2C antibodies we observed a different inhibition pattern. When added at time 0 of replication, we observed inhibition of negative-strand synthesis but when added at 5 minutes or later, we only saw inhibition of positive-strand synthesis. The question is, whether the 2C^{ATPase} function inhibited by the antibodies at time-point 0 is the same as the guanidine-sensitive function, since in both cases negative-strand RNA synthesis is affected. We can think of two possible explanations. One, a different function of 2C^{ATPase} required for negative-strand RNA synthesis is inhibited by anti-2C antibodies than by GuHCl. 2C^{ATPase} can have multiple roles during negative-strand RNA synthesis. The one targeted by the antibodies might only be required at the very first moment of replication initiation. 5 minutes after initiation this function is no longer required. Or two, for antibodies to inhibit the function of a protein they have to interact with this protein. The 2C^{ATPase} protein might not be easy accessible for the antibodies once replication is initiated in the replication complexes, whereas guanidine is still able to reach its protein target and inhibit the 2C^{ATPase} function in negative-strand RNA synthesis. In this case, it is possible that they both inhibit the same function in negative-strand RNA synthesis.

Based on binding-affinity of 2C^{ATPase} and its precursor 2BC to the 3'-end of the negative-strand, a role for 2C^{ATPase} in positive-strand RNA synthesis has been proposed (Banerjee et al., 1997; Banerjee et al., 2001). This interaction was shown to

require the sequence UGUUU in *stem a* of the minus-strand cloverleaf in the form of a double-stranded structure. Such a requirement for interaction of $2C^{ATPase}$ to *stem a* of the minus-strand cloverleaf could explain the requirement of an intact *stem a* for positive-strand RNA synthesis. However, the $2C^{ATPase}$ polypeptide analyzed in these studies was a renatured product isolated originally from inclusion bodies after expression in *E. coli*. The studies demonstrating the ATPase and GTPase activity of $2C^{ATPase}$ used a fusion protein of $2C^{ATPase}$ with the Maltose-binding-protein (Rodriguez & Carrasco, 1993, 1995). The expression of 2C as MBP-2C in *E. coli* produces a soluble fusion protein that does not need denaturing and renaturing for purification steps. With such a fusion protein we were not able to demonstrate specific binding-affinities of $2C^{ATPase}$ to either the positive- or negative-strand cloverleaf RNA. This is in agreement with Pfister & Wimmer (unpublished results in Paul, 2002) who also failed to observe specific interaction of MBP-2C to the minus-strand cloverleaf. Furthermore, they could not detect any ATPase activity in a $2C^{ATPase}$ protein that was renatured after purification from an insoluble fraction in *E.coli*. This suggests that the binding properties of $2C^{ATPase}$ as observed by Banerjee et al. (1997, 2001) might not reflect the binding properties of the $2C^{ATPase}$ protein when expressed during viral infection. However, in our study we provide the first functional evidence that $2C^{ATPase}$ has an important role in positive-strand RNA synthesis. Because of its nucleoside triphosphate binding domain it has been speculated that $2C^{ATPase}$ may function as a helicase with possible involvement in the strand separation during replication (Dmitrieva et al., 1991; Teterina et al., 1992). For such an activity, $2C^{ATPase}$ would not require any specific interaction with either cloverleaf structure since it would act on the level of the double-stranded intermediate (RF). However, such a function for $2C^{ATPase}$ during positive-strand RNA synthesis still needs to be shown.

5.15 A model for initiation of positive-strand RNA synthesis in poliovirus replication

Based on data presented in this study, we propose the following model for initiation of positive-strand RNA synthesis in poliovirus (see Figure 5.1): Negative-strand RNA synthesis results in a double-stranded intermediate, the RF. The end of it, which contains the 5'-end of the plus-strand and the 3'-end of the negative-strand, is recognized by a helicase, possibly the $2C^{ATPase}$ protein (Fig. 5.1A). Upon unwinding of

the strands, the cloverleaf structure forms on the positive-strand. PCBP2 and $3CD^{pro}$ bind to the cloverleaf structure and form a ternary complex (Fig. 5.1B). This will stabilize the complex and also help to keep the 3'-end single-stranded and available for the primer to bind. The primer, VPgpUpU, is recruited (maybe with help of the ternary complex) and binds to the 3'-terminal AA of the minus-strand. Binding of the primer will bring in the polymerase $3D^{pol}$. It is possible that the ternary complex on the plus-strand once again helps recruiting the polymerase for this step, or might provide it directly through cleavage of $3CD^{pro}$. Once positive-strand RNA synthesis is initiated and the polymerase moves along the minus-strand template to synthesize a new plus-strand, this new plus-strand will replace the old positive-strand which eventually will be completely detached from the minus-strand. The new 5'-end of the positive-strand and the 3'-end of the negative-strand will be double-stranded again until it gets unwound, possibly by the $2C^{ATPase}$ protein (Fig. 5.1C). Unwinding the end will result in forming the ternary complex around the cloverleaf of the positive-strand and initiate in return positive-strand RNA synthesis on the negative-strand (Fig. 5.1D). The newly synthesized positive-strand will replace the old one when the polymerase moves along the minus-strand. This way, the latest synthesized positive-strand will always provide the promoter for the initiation of a new plus-strand. New initiation of plus-strand synthesis can occur when still several polymerases are moving along the minus-strand template, each replacing the positive-strand synthesized right before them. This mechanism will not only result in the observed asymmetry in replication, in which more positive- than negative-strands are generated, but also in the replicative intermediate (RI) observed during positive-strand RNA synthesis that is partially single- and partially double-stranded (Wimmer et al., 1993; Agol et al., 1999). It will also ensure that initiation of positive-strand RNA synthesis stays highly regulated within the replication complexes.

The question is, whether this model applies only to poliovirus, or to all enterovirus and rhinovirus, of which most of them have a cloverleaf structure at the 5'-end of their genome. This mechanism might be even a common strategy for positive-strand RNA viruses to initiate positive-strand RNA synthesis. Most positive-strand RNA viruses have large 5' UTRs which contain often several *cis*-acting replication elements. It is possible that some of those RNA elements have dual functions in replication and promote both negative- and positive-strand RNA synthesis. Some viruses might actually have separate promoters for negative-strand RNA synthesis but both in the

5'UTR and both might functioning on the positive-strand. For example, bovine enteroviruses have two cloverleaf-like structures at the 5'-end of their genome. Deletion of either one of them results in non-viable viruses (Zell et al., 1999). However, after exchange of the region spanning both cloverleaves with the CVB3 cloverleaf, a viable chimera was generated (Zell et al., 1999). Therefore, the two cloverleaf structures in bovine enteroviruses can display the same role as the one cloverleaf in CVB3, suggesting that one cloverleaf might function as a promoter for negative- and the other as a promoter for positive-strand RNA synthesis.

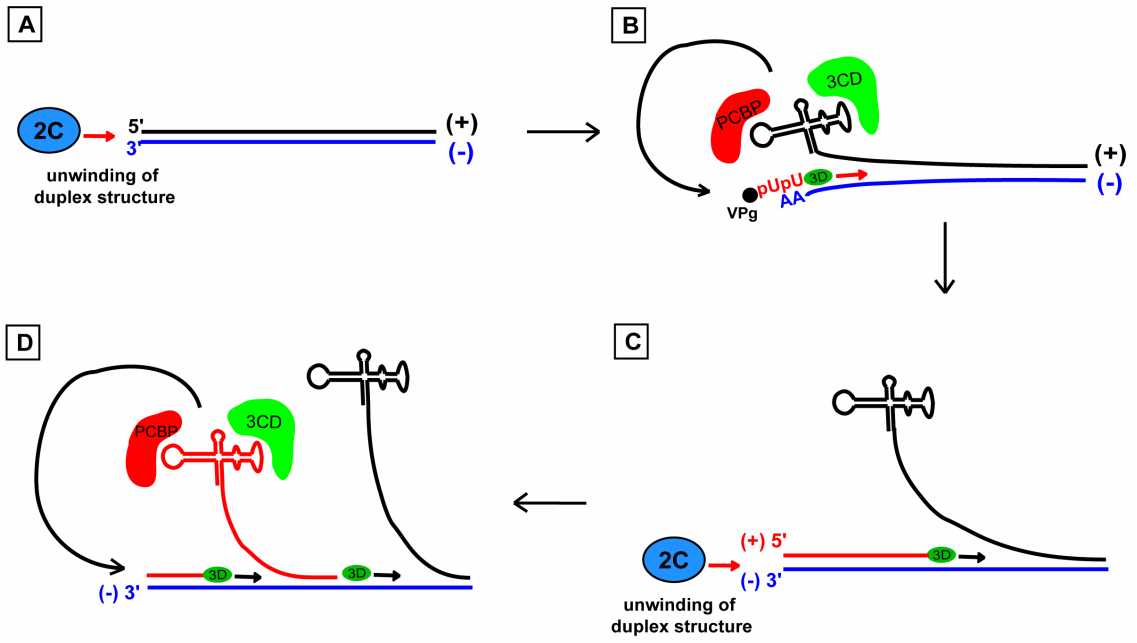

Figure 5.1: A model for initiation of positive-strand RNA synthesis during poliovirus replication. (A) The double-stranded intermediate (RF), after negative-strand RNA synthesis is completed, is unwound by a helicase, possibly 2C. (B) Upon unwinding, the cloverleaf structure in the positive-strand folds into its secondary structure and recruits PCBP and $3CD^{pro}$ to form a ternary complex. This complex promotes initiation of positive-strand RNA synthesis at the 3'-end of the negative-strand. The primer VPgpUpU binds to the terminal sequences of the negative-strand and the polymerase moves along the minus-strand template to synthesize a new plus-strand, this way replacing the old plus-strand in front of it. (C) The new plus-strand displays a double-stranded intermediate at its 5'-end with the minus-strand that needs to be unwound. This could be done by the same helicase as in step 1, possibly 2C. (D) Once the ends are unwound, the ternary complex around the cloverleaf on the positive-strand forms and promotes in return initiation of plus-strand RNA synthesis on the negative-strand. When the polymerase moves along the minus-strand template, it replaces the old plus-strand in front of it.

5.2 The multi-functional role of *cre*(2C) in Coxsackievirus B3 RNA replication

5.21 The coxsackievirus B3 *cre*(2C)

Our study describes the presence of a *cre* within the CVB3 2C coding region, named *cre*(2C), that functions as a template for VPg-uridylylation *in vitro*. We have shown that the *cre*(2C) is required for the initiation of both negative- and positive-strand RNA synthesis. The *cre*(2C) is predicted to fold into an imperfect stem with a large loop region of 14 nt, containing a coxsackie B cluster-specific 5'-AAAUG-3' sequence. Substituting this sequence for the consensus sequence found in all *cre*s described thus far, 5'-AAACA-3' (Paul et al., 2000; Yang et al., 2002) , did not affect VPg-uridylylation efficiency of RNA replication significantly. Characterization of the CVB3 *cre*(2C) loop showed that the proposed entero- and rhinoviral consensus sequence (R_1NNNAAR_2NNNNNNR_3), extrapolated from sequence-alignment studies and extensive mutational analysis of the rhinovirus 14 *cre*(VP1) loop region (Yang et al., 2002; Yin et al., 2003), is also applicable to the CVB3 *cre*(2C) loop sequence; mutations that interfered with this consensus sequence affected CVB3 VPg-uridylylation and RNA replication to a similar extent.

5.22 A role of *cre*(2C) in both negative- and positive-strand RNA synthesis

Consistent with previous reports, a mutant in which the *cre*(2C) structure was completely disrupted still supported efficient negative-strand RNA synthesis in a cell-free replication system (Goodfellow et al., 2003b; Morasco et al., 2003; Murray & Barton, 2003). This suggested that, under the conditions of the experiment, *cre*-mediated VPg-uridylylation is required for positive-strand, but dispensable for negative-strand, RNA synthesis. However, we also found a direct correlation between *cre*(2C) point mutants producing lower, but detectable, amounts of VPgpU(pU) and reduced RF levels, affected to a similar extent. These latter results suggest that *cre*(2C)-derived VPgpU(pU) is also involved in the initiation of negative-strand RNA synthesis. In correlation, *cre*(2C) point mutants unable to support VPg-uridylylation to a detectable level also showed a severe defect in RF accumulation. In addition, the A5G transition that affects the first templating adenosine residue was found to completely abolish RF synthesis completely.

5.23 Is *cre*(2C) mediated VPgpUpU required for negative-strand RNA synthesis?

How can we explain such apparently contradictory results? A recent study reported, by using poliovirus *cre*(2C) mutants, that a dominant-negative effect is observed on wild-type poliovirus replication using *cre*(2C) point mutants, but not when the *cre*(2C) has been disrupted completely (Crowder & Kirkegaard, 2005). This suggests that RNA containing a complete *cre*(2C) distortion mutant, as opposed to point mutants, utilizes an alternative mode of RNA replication that is so distinct form wild-type poliovirus replication that it does not interfere. As RF synthesis, in the absence of detectable levels of VPgpU(pU), was observed in the cell-free replication system using RNA containing a completely distorted *cre*(2C) structure, it was suggested previously that this alternative mode of replication might involve the 3'-poly(A) tail. This homopolymeric stretch might serve as the alternative template for the covalent linkage of uracil residues to VPg (Goodfellow et al., 2003b; Morasco et al., 2003; Murray & Barton, 2003), which was based on the findings that negative-strand RNA synthesis is VPg-dependent (Nomoto et al., 1977a; Nomoto et al., 1977b) and that poly(A) templates supported VPg-uridylylation *in vitro* (Paul et al., 1998).

A wild-type *cre*(2C) structure sequesters replication proteins (Yin et al., 2003) and the formation of such protein-RNA interactions is most probably affected upon distortion of the *cre*(2C) structure. Absence of this RNP complex in a genome containing a completely distorted *cre*(2C) structure might favor the 3'-poly(A) tail as the alternative template for the covalent linkage of UMP to VPg *in vitro*. The ability to detect free VPgpU(pU) within purified replication complexes might imply that VPg is elongated immediately into complementary negative RNA strands (Murray & Barton, 2003). A number of *cre* mutants unable to accumulate detectable levels of uridylylated VPg still retained the ability to induce RF synthesis (e.g. G_1C, $A_6C/G/U$, A_7U/C and $A_{14}C$). Therefore, it can be speculated that these mutants also utilize the proposed alternative, 3'-poly(A) tail-dependent mechanism, to induce negative-strand RNA synthesis. However, whereas the *cre*(2C) distortion mutant showed wild-type levels of RF synthesis at the measured time-point, RF accumulation was reduced severely in *cre*(2C) mutations affecting the enterovirus consensus sequence. Also, in contrast to the *cre*(2C) distortion mutant, the G_1C, $A_6C/G/U$ and A_7U/C substitutions all maintained a wild-type *cre*(2C) conformation, which we propose enabled them to sequester the

proteins required for VPg-uridylylation. As shown previously for poliovirus, A_6 substitutions still produced VPg(pU), albeit with reduced efficiency, which might support this speculation (Paul et al., 2003). Although the $A_{14}C$ mutation is predicted by MFOLD to adopt an alternative conformation due to a GC base pair formation between the G_1 and C_{14} residue, this mutant was found in poliovirus not to be reduced in protein binding (Yin et al., 2003) and might therefore still be able to produce VPgpU(pU). Additionally, Nayak et al. showed that A6 and A7 mutations displayed higher uridylylation activities in the context of full-length RNA compared with short hairpin RNAs, concluding that the template used in the uridylylation reaction determines both the specificity and efficiency of the assay (Nayak et al., 2005). In summary, we speculate that the *cre*-dependent uridylylation mechanism prior to negative-strand RNA synthesis is strongly favored when the *cre* structure is intact.

By using purified components (*cre*(2C), VPg, $3D^{pol}$ and $3CD^{pro}$), poliovirus VPg-nucleotidylylation has been found not to be stringently dependent upon an AAACA motif in the *cre* loop if one of the NTPs other than UTP was present. For example, VPgpG is formed by CAACA and GTP, as the first nucleotide, in this case a C residue, functions as a template (Gerber et al., 2001a; Paul et al., 2003). Similarly, an A_5C transversion or an A_5G transition in the CVB3 A_5AAUG motif yielded VPgpG and VPgpC, respectively, in the CVB3 *cre*(2C) nucleotidylylation reaction (unpublished results). Nucleotidylylation is aborted at the stage of VPgpG or VPgpC because of the 'slideback' mechanism to A_6 (Gerber et al., 2001a; Paul et al., 2003). If dual *cre*(2C) CVB3 transcripts carry a 59-terminal pppG group (Fig. 4.20a), only the A_5C transversion mutant produced some RF, albeit in greatly reduced yield (Fig. 4.20b). The rationale for employing the pppGG transcript was to reduce positive-strand RNA synthesis in the cell-free replication system, thereby shifting the complex to synthesize, if possible, predominantly negative-strand RNA (Herold & Andino, 2000). Virological characterization of both the CVB3 A_5C and A_5G mutants using a single *cre*(2C) construct showed that the A_5G mutation was quasi-infectious and reverted to a wild-type *cre* sequence, whereas, in contrast to previous reports (Morasco et al., 2003; Yin et al., 2003) the A_5C mutant proved to be a lethal mutation, probably caused by a dysfunctional 2C protein (unpublished results). On the basis of these data, we suggest that initiation of negative-strand RNA synthesis in CVB3 requires the A_5 residue, but that, at least in assays performed using cell-free extract, this requirement is leaky (see below).

The stringency of sequence requirement does not appear to apply to the AA_6AUG residue, as all mutations in A_6 still produce RF, albeit also at reduced yield (Fig. 4.20b). This corresponds to data from poliovirus, which have revealed that mutations in the corresponding adenosine residue (AAACA) yielded quasi-infectious phenotypes (Paul et al., 2003). These phenotypes were also found for the analogous point mutants in CVB3 *cre*(2C) (unpublished data). Perhaps VPgpU formed on ANACA *cre*(2C) mutants of the poliovirus or ANAUG *cre*(2C) mutants of CVB3 can still function as primer for negative-strand RNA synthesis on the 39 poly(A) template.

RNA replication of human enterovirus genomes proceeds on membranes in RNP complexes of which the structures have not yet been entirely deciphered. Available evidence suggests that the 59-terminal cloverleaf and the 39-terminal poly(A) tail induce the formation of a circular RNP complex via protein–protein interaction (Barton et al., 2001; Herold & Andino, 2001). Moreover, it has been suggested that the cloverleaf structure is also involved in VPg uridylylation (Lyons et al., 2001). Thus, all three elements, the cloverleaf, the *cre* and the 39 poly(A) tail, may interact for initiation of genome replication to occur. Elimination of the *cre* by destroying its stem–loop structure may allow the system to bypass the *cre* requirement for negative-strand RNA synthesis and, by a default mechanism, make use of the genetically encoded 39 poly(A) tail as template for uridylylation in a cell-free *in vitro* system (Paul et al., 1998; Goodfellow et al., 2003b; Morasco et al., 2003; Murray & Barton, 2003). As viral negative-strand RNA was found to be absent in cells transfected with the complete *cre*(2C) disruption mutant (Goodfellow et al., 2000), it is sensible to conclude that utilization of the 39 poly(A) tail for uridylylation can only be seen in the *in vitro* translation/replication system. In stark contrast, if the replication proteins are presented with a *cre* element which A_5 has been mutated to a G residue, the aberrant nucleotidylylation product VPgpC might operate as a dominant-negative element. The nucleotidylylation complex, however, is not “frozen” on the mutated *cre*(2C) itself, as the addition of a second wild-type *cre* restored the ability to initiate RNA replication (Yin et al., 2003). An alternative mechanism could be envisaged in which the replicase complex containing VPgpC is positioned on the 39 poly(A) tail and thereby might block the initiation of negative-strand RNA synthesis. We speculate that the A_5C transition mutant, accumulating a VPgpG nucleotidylylation product, may form a less-stable RNP complex on the 39 poly(A) tail, allowing a severely reduced yield of complementary

RNA strands via the alternative 39 poly(A) tail-dependent mechanism, although further investigation is required to elucidate the exact mechanism.

5.3 General conclusions

What are the advantages for the virus in having several multi-functional *cis*-acting replication elements? Picornaviruses have very small genomes and to cover all required functions for the various steps in the viral life cycle, the genomes must be used very efficiently. This might require for the virus to have overlapping functions of the same element. However, in the need to organize its genome very resourcefully, the result of this might actually provide the virus with an advantage that ensures efficient RNA synthesis.

Replication of positive-strand RNA viruses occurs in replication complexes attached to membranous vesicles. The advantage of a promoter for positive-strand RNA synthesis to be located in the positive-strand is that all required *trans*-acting factors for replication are recruited early to the replication complex. In poliovirus, the cloverleaf structure will recruit all necessary components for the ternary complex formation to the replication complex before negative-strand RNA synthesis is initiated. By using the same ternary complex also as a promoter for positive-strand RNA synthesis, the virus ensures that the required *trans*-acting factors for positive-strand RNA synthesis are already in the right location. The same is true for the viral $2C^{ATPase}$ protein. Since it has a role in both negative- and positive-strand RNA synthesis, replication can only be initiated when $2C^{ATPase}$ is present in the replication complex, therefore, it will be available for both steps. Finally, our results that *cre*(2C)-derived VPgpUpU is used as a primer for both negative- and positive-strand RNA synthesis in coxsackievirus B3 is in total agreement with this idea. As demonstrated in the VPg-uridylylation experiment with the tandem cloverleaf constructs, VPgpUpU is accumulated in the replication complexes during RNA synthesis, thus, available for both steps in replication. This strategy will ensure efficient positive-strand RNA synthesis, and subsequently efficient virus progeny.

6. References

6. References

Agol VI. 1991. The 5'-untranslated region of picornaviral genomes. *Advances in virus research 40*:103-180.

Agol VI, Paul AV, Wimmer E. 1999. Paradoxes of the replication of picornaviral genomes. *Virus research 62*:129-147.

Ahlquist P, French R, Janda M, Loesch-Fries LS. 1984. Multicomponent RNA plant virus infection derived from cloned viral cDNA. *Proceedings of the National Academy of Sciences of the United States of America 81*:7066-7070.

Aldabe R, Barco A, Carrasco L. 1996. Membrane permeabilization by poliovirus proteins 2B and 2BC. *The Journal of biological chemistry 271*:23134-23137.

Aldabe R, Feduchi E, Novoa I, Carrasco L. 1995. Expression of poliovirus 2Apro in mammalian cells: effects on translation. *FEBS letters 377*:1-5.

Alexander HE, Koch G, Mountain IM, Sprunt K, Van Damme O. 1958. Infectivity of ribonucleic acid of poliovirus on HeLa cell mono-layers. *Virology 5*:172-173.

Alvarez DE, Lodeiro MF, Luduena SJ, Pietrasanta LI, Gamarnik AV. 2005. Long-range RNA-RNA interactions circularize the dengue virus genome. *Journal of virology 79*:6631-6643.

Ambros V, Baltimore D. 1978. Protein is linked to the 5' end of poliovirus RNA by a phosphodiester linkage to tyrosine. *The Journal of biological chemistry 253*:5263-5266.

Ambros V, Baltimore D. 1980. Purification and properties of a HeLa cell enzyme able to remove the 5'-terminal protein from poliovirus RNA. *The Journal of biological chemistry 255*:6739-6744.

Ambros V, Pettersson RF, Baltimore D. 1978. An enzymatic activity in uninfected cells that cleaves the linkage between poliovirion RNA and the 5' terminal protein. *Cell 15*:1439-1446.

Andino R, Rieckhof GE, Achacoso PL, Baltimore D. 1993. Poliovirus RNA synthesis utilizes an RNP complex formed around the 5'-end of viral RNA. *The EMBO journal 12*:3587-3598.

Andino R, Rieckhof GE, Baltimore D. 1990. A functional ribonucleoprotein complex forms around the 5' end of poliovirus RNA. *Cell 63*:369-380.

Andino R, Silvera D, Suggett SD, Achacoso PL, Miller CJ, Baltimore D, Feinberg MB. 1994. Engineering poliovirus as a vaccine vector for the expression of diverse antigens. *Science 265*:1448-1451.

Ansardi DC, Porter DC, Anderson MJ, Morrow CD. 1996. Poliovirus assembly and encapsidation of genomic RNA. *Advances in virus research 46*:1-68.

Arnold E, Luo M, Vriend G, Rossmann MG, Palmenberg AC, Parks GD, Nicklin MJ, Wimmer E. 1987. Implications of the picornavirus capsid structure for polyprotein processing. *Proceedings of the National Academy of Sciences of the United States of America 84*:21-25.

Baltimore D, Eggers HJ, Franklin RM, Tamm I. 1963. Poliovirus-induced RNA polymerase and the effects of virus-specific inhibitors on its production. *Proceedings of the National Academy of Sciences of the United States of America 49*:843-849.

Banerjee R, Echeverri A, Dasgupta A. 1997. Poliovirus-encoded 2C polypeptide specifically binds to the 3'-terminal sequences of viral negative-strand RNA. *Journal of virology 71*:9570-9578.

Banerjee R, Tsai W, Kim W, Dasgupta A. 2001. Interaction of poliovirus-encoded 2C/2BC polypeptides with the 3' terminus negative-strand cloverleaf requires an intact stem-loop b. *Virology 280*:41-51.

Barclay W, Li Q, Hutchinson G, Moon D, Richardson A, Percy N, Almond JW, Evans DJ. 1998. Encapsidation studies of poliovirus subgenomic replicons. *The Journal of general virology 79 (Pt 7)*:1725-1734.

Baron MH, Baltimore D. 1982. In vitro copying of viral positive strand RNA by poliovirus replicase. Characterization of the reaction and its products. *The Journal of biological chemistry 257*:12359-12366.

Barton DJ, Black EP, Flanegan JB. 1995. Complete replication of poliovirus in vitro: preinitiation RNA replication complexes require soluble cellular factors for the synthesis of VPg-linked RNA. *Journal of virology 69*:5516-5527.

Barton DJ, Flanegan JB. 1997. Synchronous replication of poliovirus RNA: initiation of negative-strand RNA synthesis requires the guanidine-inhibited activity of protein 2C. *Journal of virology 71*:8482-8489.

Barton DJ, Morasco BJ, Flanegan JB. 1999. Translating ribosomes inhibit poliovirus negative-strand RNA synthesis. *Journal of virology 73*:10104-10112.

Barton DJ, O'Donnell BJ, Flanegan JB. 2001. 5' cloverleaf in poliovirus RNA is a cis-acting replication element required for negative-strand synthesis. *The EMBO journal 20*:1439-1448.

Basavappa R, Syed R, Flore O, Icenogle JP, Filman DJ, Hogle JM. 1994. Role and mechanism of the maturation cleavage of VP0 in poliovirus assembly: structure of the empty capsid assembly intermediate at 2.9 A resolution. *Protein Sci 3*:1651-1669.

Belnap DM, Filman DJ, Trus BL, Cheng N, Booy FP, Conway JF, Curry S, Hiremath CN, Tsang SK, Steven AC, Hogle JM. 2000a. Molecular tectonic model of virus structural transitions: the putative cell entry states of poliovirus. *Journal of virology 74*:1342-1354.

Belnap DM, McDermott BM, Jr., Filman DJ, Cheng N, Trus BL, Zuccola HJ, Racaniello VR, Hogle JM, Steven AC. 2000b. Three-dimensional structure of poliovirus receptor bound to poliovirus. *Proceedings of the National Academy of Sciences of the United States of America 97*:73-78.

Belov GA, Altan-Bonnet N, Kovtunovych G, Jackson CL, Lippincott-Schwartz J, Ehrenfeld E. 2007. Hijacking components of the cellular secretory pathway for replication of poliovirus RNA. *Journal of virology 81*:558-567.

Belov GA, Fogg MH, Ehrenfeld E. 2005. Poliovirus proteins induce membrane association of GTPase ADP-ribosylation factor. *Journal of virology 79*:7207-7216.

Bergelson JM, Cunningham JA, Droguett G, Kurt-Jones EA, Krithivas A, Hong JS, Horwitz MS, Crowell RL, Finberg RW. 1997. Isolation of a common receptor for Coxsackie B viruses and adenoviruses 2 and 5. *Science 275*:1320-1323.

Bienz K, Egger D, Pasamontes L. 1987. Association of polioviral proteins of the P2 genomic region with the viral replication complex and virus-induced membrane synthesis as visualized by electron microscopic immunocytochemistry and autoradiography. *Virology 160*:220-226.

Bienz K, Egger D, Pfister T. 1994. Characteristics of the poliovirus replication complex. *Archives of virology 9*:147-157.

Bienz K, Egger D, Pfister T, Troxler M. 1992. Structural and functional characterization of the poliovirus replication complex. *Journal of virology 66*:2740-2747.

Bienz K, Egger D, Rasser Y, Bossart W. 1983. Intracellular distribution of poliovirus proteins and the induction of virus-specific cytoplasmic structures. *Virology 131*:39-48.

Blair WS, Li X, Semler BL. 1993. A cellular cofactor facilitates efficient 3CD cleavage of the poliovirus P1 precursor. *Journal of virology 67*:2336-2343.

Blyn LB, Swiderek KM, Richards O, Stahl DC, Semler BL, Ehrenfeld E. 1996. Poly(rC) binding protein 2 binds to stem-loop IV of the poliovirus RNA 5' noncoding region: identification by automated liquid chromatography-tandem mass spectrometry. *Proceedings of the National Academy of Sciences of the United States of America 93*:11115-11120.

Bodian D. 1955. Emerging concept of poliomyelitis infection. *Science 122*:105-108.

Bodian D. 1958. Some physiologic aspects of poliovirus infections. *The Harvey Lectures 1956-1957, series 52*: Academic Press, New York, N.Y. pp 23-56.

Brunner JE, Nguyen JH, Roehl HH, Ho TV, Swiderek KM, Semler BL. 2005. Functional interaction of heterogeneous nuclear ribonucleoprotein C with poliovirus RNA synthesis initiation complexes. *Journal of virology 79*:3254-3266.

Bubeck D, Filman DJ, Hogle JM. 2005. Cryo-electron microscopy reconstruction of a poliovirus-receptor-membrane complex. *Nature structural & molecular biology 12*:615-618.

Carrasco L. 1981. Modification of membrane permeability induced by animal viruses early in infection. *Virology 113*:623-629.

Carrasco L. 1995. Modification of membrane permeability by animal viruses. *Advances in virus research 45*:61-112.

Carrasco L, Otero MJ, Castrillo JL. 1989. Modification of membrane permeability by animal viruses. *Pharmacology & therapeutics 40*:171-212.

Carrasco L, R. Guinea, A. Iruzun, A. Barco. 2002. Effects of Viral Replication on Cellular Membrane Metabolism and Function. In: B.L. Semler EW, ed. *Molecular Biology of Picornaviruses*. Washington, DC.: ASM Press. pp 337-354.

Chapman NM, Ragland A, Leser JS, Hofling K, Willian S, Semler BL, Tracy S. 2000. A group B coxsackievirus/poliovirus 5' nontranslated region chimera can act as an attenuated vaccine strain in mice. *Journal of virology 74*:4047-4056.

Cho MW, Teterina N, Egger D, Bienz K, Ehrenfeld E. 1994. Membrane rearrangement and vesicle induction by recombinant poliovirus 2C and 2BC in human cells. *Virology 202*:129-145.

Clark ME, Dasgupta A. 1990. A transcriptionally active form of TFIIIC is modified in poliovirus-infected HeLa cells. *Molecular and cellular biology 10*:5106-5113.

Clark ME, Hammerle T, Wimmer E, Dasgupta A. 1991. Poliovirus proteinase 3C converts an active form of transcription factor IIIC to an inactive form: a mechanism for inhibition of host cell polymerase III transcription by poliovirus. *The EMBO journal 10*:2941-2947.

Clark ME, Lieberman PM, Berk AJ, Dasgupta A. 1993. Direct cleavage of human TATA-binding protein by poliovirus protease 3C in vivo and in vitro. *Molecular and cellular biology 13*:1232-1237.

Colter JS, Bird HH, Moyer AW, Brown RA. 1957. Infectivity of ribonucleic acid isolated from virus-infected tissues. *Virology 4*:522-532.

Compton SR, Nelsen B, Kirkegaard K. 1990. Temperature-sensitive poliovirus mutant fails to cleave VP0 and accumulates provirions. *Journal of virology 64*:4067-4075.

Corver J, Lenches E, Smith K, Robison RA, Sando T, Strauss EG, Strauss JH. 2003. Fine mapping of a cis-acting sequence element in yellow fever virus RNA that is required for RNA replication and cyclization. *Journal of virology 77*:2265-2270.

Crawford NM, Baltimore D. 1983. Genome-linked protein VPg of poliovirus is present as free VPg and VPg-pUpU in poliovirus-infected cells. *Proceedings of the National Academy of Sciences of the United States of America 80*:7452-7455.

Crowder S, Kirkegaard K. 2005. Trans-dominant inhibition of RNA viral replication can slow growth of drug-resistant viruses. *Nature genetics 37*:701-709.

Dales S, Eggers HJ, Tamm I, Palade GE. 1965. Electron Microscopic Study of the Formation of Poliovirus. *Virology 26*:379-389.

Das S, Dasgupta A. 1993. Identification of the cleavage site and determinants required for poliovirus 3CPro-catalyzed cleavage of human TATA-binding transcription factor TBP. *Journal of virology 67*:3326-3331.

Davies MV, Pelletier J, Meerovitch K, Sonenberg N, Kaufman RJ. 1991. The effect of poliovirus proteinase 2Apro expression on cellular metabolism. Inhibition of DNA replication, RNA polymerase II transcription, and translation. *The Journal of biological chemistry 266*:14714-14720.

De Gregorio E, Preiss T, Hentze MW. 1999. Translation driven by an eIF4G core domain in vivo. *The EMBO journal 18*:4865-4874.

De Sena J, Mandel B. 1977. Studies on the in vitro uncoating of poliovirus. II. Characteristics of the membrane-modified particle. *Virology 78*:554-566.

DeTulleo L, Kirchhausen T. 1998. The clathrin endocytic pathway in viral infection. *The EMBO journal 17*:4585-4593.

Diez J, Ishikawa M, Kaido M, Ahlquist P. 2000. Identification and characterization of a host protein required for efficient template selection in viral RNA replication. *Proceedings of the National Academy of Sciences of the United States of America 97*:3913-3918.

Dmitrieva TM, Norkina KB, Agol VI. 1991. Encephalomyocarditis virus RNA polymerase preparations, with and without RNA helicase activity. *Journal of virology 65*:2714-2717.

Doedens JR, Giddings TH, Jr., Kirkegaard K. 1997. Inhibition of endoplasmic reticulum-to-Golgi traffic by poliovirus protein 3A: genetic and ultrastructural analysis. *Journal of virology 71*:9054-9064.

Doedens JR, Kirkegaard K. 1995. Inhibition of cellular protein secretion by poliovirus proteins 2B and 3A. *The EMBO journal 14*:894-907.

Dorner AJ, Semler BL, Jackson RJ, Hanecak R, Duprey E, Wimmer E. 1984. In vitro translation of poliovirus RNA: utilization of internal initiation sites in reticulocyte lysate. *Journal of virology 50*:507-514.

Egger D, Pasamontes L, Bolten R, Boyko V, Bienz K. 1996. Reversible dissociation of the poliovirus replication complex: functions and interactions of its components in viral RNA synthesis. *Journal of virology 70*:8675-8683.

Egger D, Teterina N, Ehrenfeld E, Bienz K. 2000. Formation of the poliovirus replication complex requires coupled viral translation, vesicle production, and viral RNA synthesis. *Journal of virology 74*:6570-6580.

Ehrenfeld E. 1997. Initiation of translation by picornavirus RNAs. In: Hershey J, MB. Mathews, N. Sonenberg, ed. *Translational Control.* Plainview, N.Y.: Spring Harbor Laboratory Press. pp 549-573.

Fenwick ML, Cooper PD. 1962. Early interactions between poliovirus and ERK cells: some observations on the nature and significance of the rejected particles. *Virology 18*:212-223.

Flanegan JB, Baltimore D. 1977. Poliovirus-specific primer-dependent RNA polymerase able to copy poly(A). *Proceedings of the National Academy of Sciences of the United States of America 74*:3677-3680.

Flanegan JB, Petterson RF, Ambros V, Hewlett NJ, Baltimore D. 1977. Covalent linkage of a protein to a defined nucleotide sequence at the 5'-terminus of virion and replicative intermediate RNAs of poliovirus. *Proceedings of the National Academy of Sciences of the United States of America 74*:961-965.

Franklin RM, Baltimore D. 1962. Patterns of macromolecular synthesis in normal and virus-infected mammalian cells. *Cold Spring Harbor symposia on quantitative biology 27*:175-198.

Fricks CE, Hogle JM. 1990. Cell-induced conformational change in poliovirus: externalization of the amino terminus of VP1 is responsible for liposome binding. *Journal of virology 64*:1934-1945.

Gamarnik AV, Andino R. 1996. Replication of poliovirus in Xenopus oocytes requires two human factors. *The EMBO journal 15*:5988-5998.

Gamarnik AV, Andino R. 1997. Two functional complexes formed by KH domain containing proteins with the 5' noncoding region of poliovirus RNA. *RNA (New York, NY 3*:882-892.

Gamarnik AV, Andino R. 1998. Switch from translation to RNA replication in a positive-stranded RNA virus. *Genes & development 12*:2293-2304.

Gamarnik AV, Andino R. 2000. Interactions of viral protein 3CD and poly(rC) binding protein with the 5' untranslated region of the poliovirus genome. *Journal of virology 74*:2219-2226.

Gerber K, Wimmer E, Paul AV. 2001a. Biochemical and genetic studies of the initiation of human rhinovirus 2 RNA replication: identification of a cis-replicating element in the coding sequence of 2A(pro). *Journal of virology 75*:10979-10990.

Gerber K, Wimmer E, Paul AV. 2001b. Biochemical and genetic studies of the initiation of human rhinovirus 2 RNA replication: purification and enzymatic analysis of the RNA-dependent RNA polymerase 3D(pol). *Journal of virology 75*:10969-10978.

Giachetti C, Hwang SS, Semler BL. 1992. cis-acting lesions targeted to the hydrophobic domain of a poliovirus membrane protein involved in RNA replication. *Journal of virology 66*:6045-6057.

Gohara DW, Ha CS, Kumar S, Ghosh B, Arnold JJ, Wisniewski TJ, Cameron CE. 1999. Production of "authentic" poliovirus RNA-dependent RNA polymerase (3D(pol)) by ubiquitin-protease-mediated cleavage in Escherichia coli. *Protein expression and purification 17*:128-138.

Goodfellow I, Chaudhry Y, Richardson A, Meredith J, Almond JW, Barclay W, Evans DJ. 2000. Identification of a cis-acting replication element within the poliovirus coding region. *Journal of virology 74*:4590-4600.

Goodfellow IG, Kerrigan D, Evans DJ. 2003a. Structure and function analysis of the poliovirus cis-acting replication element (CRE). *RNA (New York, NY 9*:124-137.

Goodfellow IG, Polacek C, Andino R, Evans DJ. 2003b. The poliovirus 2C cis-acting replication element-mediated uridylylation of VPg is not required for synthesis of negative-sense genomes. *The Journal of general virology 84*:2359-2363.

Gradi A, Svitkin YV, Imataka H, Sonenberg N. 1998. Proteolysis of human eukaryotic translation initiation factor eIF4GII, but not eIF4GI, coincides with the shutoff of host protein synthesis after poliovirus infection. *Proceedings of the National Academy of Sciences of the United States of America 95*:11089-11094.

Grist NR, Bell EJ, Assaad F. 1978. Enteroviruses in human disease. *Progress in medical virology Fortschritte der medizinischen Virusforschung 24*:114-157.

Gromeier M, Bossert B, Arita M, Nomoto A, Wimmer E. 1999. Dual stem loops within the poliovirus internal ribosomal entry site control neurovirulence. *Journal of virology 73*:958-964.

Hanecak R, Semler BL, Anderson CW, Wimmer E. 1982. Proteolytic processing of poliovirus polypeptides: antibodies to polypeptide P3-7c inhibit cleavage at glutamine-glycine pairs. *Proceedings of the National Academy of Sciences of the United States of America 79*:3973-3977.

Hanecak R, Semler BL, Ariga H, Anderson CW, Wimmer E. 1984. Expression of a cloned gene segment of poliovirus in E. coli: evidence for autocatalytic production of the viral proteinase. *Cell 37*:1063-1073.

Harris KS, Reddigari SR, Nicklin MJ, Hammerle T, Wimmer E. 1992. Purification and characterization of poliovirus polypeptide 3CD, a proteinase and a precursor for RNA polymerase. *Journal of virology 66*:7481-7489.

Harris KS, Xiang W, Alexander L, Lane WS, Paul AV, Wimmer E. 1994. Interaction of poliovirus polypeptide 3CDpro with the 5' and 3' termini of the poliovirus genome. Identification of viral and cellular cofactors needed for efficient binding. *The Journal of biological chemistry 269*:27004-27014.

Heinz BA, Vance LM. 1995. The antiviral compound enviroxime targets the 3A coding region of rhinovirus and poliovirus. *Journal of virology 69*:4189-4197.

Herold J, Andino R. 2000. Poliovirus requires a precise 5' end for efficient positive-strand RNA synthesis. *Journal of virology 74*:6394-6400.

Herold J, Andino R. 2001. Poliovirus RNA replication requires genome circularization through a protein-protein bridge. *Molecular cell 7*:581-591.

Hogle JM, Chow M, Filman DJ. 1985. Three-dimensional structure of poliovirus at 2.9 A resolution. *Science 229*:1358-1365.

Hogle JM, Racaniello VR. 2002. Poliovirus Receptors and Cell Entry. In: Semler BL, Wimmer E, eds. *Molecular Biology of Picornaviruses*. Washington, DC: ASM Press. pp 71-83.

Holland JJ, McLaren L. 1959. The mammalian cell-virus relationship. II. Adsorption, reception, and eclipse of poliovirus by HeLa cells. *The Journal of experimental medicine 109*:487-504.

Honda T, Saitoh H, Masuko M, Katagiri-Abe T, Tominaga K, Kozakai I, Kobayashi K, Kumanishi T, Watanabe YG, Odani S, Kuwano R. 2000. The coxsackievirus-adenovirus receptor protein as a cell adhesion molecule in the developing mouse brain. *Brain research 77*:19-28.

Hope DA, Diamond SE, Kirkegaard K. 1997. Genetic dissection of interaction between poliovirus 3D polymerase and viral protein 3AB. *Journal of virology 71*:9490-9498.

Hunt SL, Jackson RJ. 1999. Polypyrimidine-tract binding protein (PTB) is necessary, but not sufficient, for efficient internal initiation of translation of human rhinovirus-2 RNA. *RNA (New York, NY 5*:344-359.

Hyypiä T, Kallajoki M, Maaronen M, Stanway G, Kandolf R, Auvinen P, Kalimo H. 1993. Pathogenetic differences between coxsackie A and B virus infections in newborn mice. *Virus research 27*:71-78.

Jackson RJ. 2002. Proteins involved in the Function of Picornavirus Internal Ribosomal Entry Site. In: Semler BL, Wimmmer E, eds. *Molecular Virology of Picornaviruses*. Washington, DC. pp 171-183.

Jacobson MF, Baltimore D. 1968. Polypeptide cleavages in the formation of poliovirus proteins. *Proceedings of the National Academy of Sciences of the United States of America 61*:77-84.

Jang SK, Kräusslich HG, Nicklin MJ, Duke GM, Palmenberg AC, Wimmer E. 1988. A segment of the 5' nontranslated region of encephalomyocarditis virus RNA directs internal entry of ribosomes during in vitro translation. *Journal of virology 62*:2636-2643.

Joachims M, Etchison D. 1992. Poliovirus infection results in structural alteration of a microtubule-associated protein. *Journal of virology 66*:5797-5804.

Joachims M, Harris KS, Etchison D. 1995. Poliovirus protease 3C mediates cleavage of microtubule-associated protein 4. *Virology 211*:451-461.

Joachims M, Van Breugel PC, Lloyd RE. 1999. Cleavage of poly(A)-binding protein by enterovirus proteases concurrent with inhibition of translation in vitro. *Journal of virology 73*:718-727.

Johansen LK, Morrow CD. 2000. The RNA encompassing the internal ribosome entry site in the poliovirus 5' nontranslated region enhances the encapsidation of genomic RNA. *Virology 273*:391-399.

Johnson KL, Sarnow P. 1991. Three poliovirus 2B mutants exhibit noncomplementable defects in viral RNA amplification and display dosage-dependent dominance over wild-type poliovirus. *Journal of virology 65*:4341-4349.

Joklik WK, Darnell JE, Jr. 1961. The adsorption and early fate of purified poliovirus in HeLa cells. *Virology 13*:439-447.

Kaariainen L, Ranki M. 1984. Inhibition of cell functions by RNA-virus infections. *Annual review of microbiology 38*:91-109.

Kaminski A, Hunt SL, Gibbs CL, Jackson RJ. 1994. Internal initiation of mRNA translation in eukaryotes. *Genetic engineering 16*:115-155.

Ketterlinus R, Wiegers K. 1994. Mapping of antigenic domains in poliovirus VP1 involved in structural rearrangements during virus morphogenesis and antigenic alterations of the virion. *Virology 204*:27-37.

Khromykh AA, Meka H, Guyatt KJ, Westaway EG. 2001. Essential role of cyclization sequences in flavivirus RNA replication. *Journal of virology 75*:6719-6728.

King A, QF. Brown, P. Christian, T. Hovi, T. Hyypiä, NJ. Knowles, SM. Lemon, PD. Minor, AC. Palmenberg, T. Skern, G. Stanway. 2000. Picornaviridae. In: Van Regenmortel MHV, C.M. Fauquet, D.H.L. Bishop, C.H. Calisher, E.B. Carsten, M.K. Estes, S.M. Lemon, J. Maniloff, M.A. Mayo, D.J. McGeoch, C.R. Pringle, R.B. Wickner, ed. *Virus Taxonomy. Seventh Report of the International Committee on the Taxonomy of Viruses.* New York, N.Y.: Academic Press. pp 657-573.

Kitamura N, Semler BL, Rothberg PG, Larsen GR, Adler CJ, Dorner AJ, Emini EA, Hanecak R, Lee JJ, van der Werf S, Anderson CW, Wimmer E. 1981. Primary structure, gene organization and polypeptide expression of poliovirus RNA. *Nature 291*:547-553.

Klump WM, Bergmann I, Muller BC, Ameis D, Kandolf R. 1990. Complete nucleotide sequence of infectious Coxsackievirus B3 cDNA: two initial 5' uridine residues

are regained during plus-strand RNA synthesis. *Journal of virology 64*:1573-1583.

Koike S, Horie H, Ise I, Okitsu A, Yoshida M, Iizuka N, Takeuchi K, Takegami T, Nomoto A. 1990. The poliovirus receptor protein is produced both as membrane-bound and secreted forms. *The EMBO journal 9*:3217-3224.

Koike S, Ise I, Nomoto A. 1991a. Functional domains of the poliovirus receptor. *Proceedings of the National Academy of Sciences of the United States of America 88*:4104-4108.

Koike S, Taya C, Kurata T, Abe S, Ise I, Yonekawa H, Nomoto A. 1991b. Transgenic mice susceptible to poliovirus. *Proceedings of the National Academy of Sciences of the United States of America 88*:951-955.

Kräusslich HG, Holscher C, Reuer Q, Harber J, Wimmer E. 1990. Myristoylation of the poliovirus polyprotein is required for proteolytic processing of the capsid and for viral infectivity. *Journal of virology 64*:2433-2436.

Kräusslich HG, Nicklin MJ, Toyoda H, Etchison D, Wimmer E. 1987. Poliovirus proteinase 2A induces cleavage of eucaryotic initiation factor 4F polypeptide p220. *Journal of virology 61*:2711-2718.

Kräusslich HG, Wimmer E. 1988. Viral proteinases. *Annual review of biochemistry 57*:701-754.

Kuge S, Saito I, Nomoto A. 1986. Primary structure of poliovirus defective-interfering particle genomes and possible generation mechanisms of the particles. *Journal of molecular biology 192*:473-487.

Kuyumcu-Martinez NM, Joachims M, Lloyd RE. 2002. Efficient cleavage of ribosome-associated poly(A)-binding protein by enterovirus 3C protease. *Journal of virology 76*:2062-2074.

Landsteiner K, Popper, c. 1909. Übertragung der Poliomyelitis acuta auf Affen. *Zeitschr Immunitätsforsch Orig 2*:377-390.

Le SY, Chen JH, Sonenberg N, Maizel JV. 1992. Conserved tertiary structure elements in the 5' untranslated region of human enteroviruses and rhinoviruses. *Virology 191*:858-866.

Learned RM, Cordes S, Tjian R. 1985. Purification and characterization of a transcription factor that confers promoter specificity to human RNA polymerase I. *Molecular and cellular biology 5*:1358-1369.

Learned RM, Learned TK, Haltiner MM, Tjian RT. 1986. Human rRNA transcription is modulated by the coordinate binding of two factors to an upstream control element. *Cell 45*:847-857.

Lee YF, Nomoto A, Detjen BM, Wimmer E. 1977. A protein covalently linked to poliovirus genome RNA. *Proceedings of the National Academy of Sciences of the United States of America 74*:59-63.

Lee YM, Chow M. 1992. Myristate modification does not function as a membrane association signal during poliovirus capsid assembly. *Virology 187*:814-820.

Leibowitz R, Penman S. 1971. Regulation of protein synthesis in HeLa cells. 3. Inhibition during poliovirus infection. *Journal of virology 8*:661-668.

Lenk R, Penman S. 1979. The cytoskeletal framework and poliovirus metabolism. *Cell 16*:289 301.

Li JP, Baltimore D. 1990. An intragenic revertant of a poliovirus 2C mutant has an uncoating defect. *Journal of virology 64*:1102-1107.

Lloyd RE, Grubman MJ, Ehrenfeld E. 1988. Relationship of p220 cleavage during picornavirus infection to 2A proteinase sequencing. *Journal of virology 62*:4216-4223.

Lo MK, Tilgner M, Bernard KA, Shi PY. 2003. Functional analysis of mosquito-borne flavivirus conserved sequence elements within 3' untranslated region of West Nile virus by use of a reporting replicon that differentiates between viral translation and RNA replication. *Journal of virology 77*:10004-10014.

Lobert PE, Escriou N, Ruelle J, Michiels T. 1999. A coding RNA sequence acts as a replication signal in cardioviruses. *Proceedings of the National Academy of Sciences of the United States of America 96*:11560-11565.

Lopez de Quinto S, Martinez-Salas E. 1997. Conserved structural motifs located in distal loops of aphthovirus internal ribosome entry site domain 3 are required for internal initiation of translation. *Journal of virology 71*:4171-4175.

Lyons T, Murray KE, Roberts AW, Barton DJ. 2001. Poliovirus 5'-terminal cloverleaf RNA is required in cis for VPg uridylylation and the initiation of negative-strand RNA synthesis. *Journal of virology 75*:10696-10708.

Macejak DG, Sarnow P. 1992. Association of heat shock protein 70 with enterovirus capsid precursor P1 in infected human cells. *Journal of virology 66*:1520-1527.

Mandl S, Sigal LJ, Rock KL, Andino R. 1998. Poliovirus vaccine vectors elicit antigen-specific cytotoxic T cells and protect mice against lethal challenge with malignant melanoma cells expressing a model antigen. *Proceedings of the National Academy of Sciences of the United States of America 95*:8216-8221.

Marc D, Drugeon G, Haenni AL, Girard M, van der Werf S. 1989. Role of myristoylation of poliovirus capsid protein VP4 as determined by site-directed mutagenesis of its N-terminal sequence. *The EMBO journal 8*:2661-2668.

Marc D, Masson G, Girard M, van der Werf S. 1990. Lack of myristoylation of poliovirus capsid polypeptide VP0 prevents the formation of virions or results in the assembly of noninfectious virus particles. *Journal of virology 64*:4099-4107.

Martinez-Salas E, Ramos R, Lafuente E, Lopez de Quinto S. 2001. Functional interactions in internal translation initiation directed by viral and cellular IRES elements. *The Journal of general virology 82*:973-984.

Mason PW, Bezborodova SV, Henry TM. 2002. Identification and characterization of a cis-acting replication element (cre) adjacent to the internal ribosome entry site of foot-and-mouth disease virus. *Journal of virology 76*:9686-9694.

McKnight KL, Lemon SM. 1998. The rhinovirus type 14 genome contains an internally located RNA structure that is required for viral replication. *RNA (New York, NY 4*:1569-1584.

Meerovitch K, Svitkin YV, Lee HS, Lejbkowicz F, Kenan DJ, Chan EK, Agol VI, Keene JD, Sonenberg N. 1993. La autoantigen enhances and corrects aberrant translation of poliovirus RNA in reticulocyte lysate. *Journal of virology 67*:3798-3807.

Melchers WJ, Hoenderop JG, Bruins Slot HJ, Pleij CW, Pilipenko EV, Agol VI, Galama JM. 1997. Kissing of the two predominant hairpin loops in the coxsackie B virus 3' untranslated region is the essential structural feature of the origin of replication required for negative-strand RNA synthesis. *Journal of virology 71*:686-696.

Melnick JL. 1996. Enteroviruses: polioviruses, coxsackieviruses, echoviruses, and newer enteroviruses. In: BN. Fields DK, PM. Howley, et al., ed. *Fields Virology*. Philadelphia, Pa.: Lippincott-Raven Publishers. pp 655-712.

Melnick JL, Agol VI, Bachrach HL, Brown F, Cooper PD, Fiers W, Gard S, Gear JH, Ghendon Y, Kasza L, LaPlaca M, Mandel B, McGregor S, Mohanty SB, Plummer G, Rueckert RR, Schaffer FL, Tagaya I, Tyrrell DA, Voroshilova M, Wenner HA. 1974. Picornaviridae. *Intervirology 4*:303-316.

Mendelsohn CL, Wimmer E, Racaniello VR. 1989. Cellular receptor for poliovirus: molecular cloning, nucleotide sequence, and expression of a new member of the immunoglobulin superfamily. *Cell 56*:855-865.

Michel YM, Poncet D, Piron M, Kean KM, Borman AM. 2000. Cap-Poly(A) synergy in mammalian cell-free extracts. Investigation of the requirements for poly(A)-mediated stimulation of translation initiation. *The Journal of biological chemistry 275*:32268-32276.

Minor PD. 1992. The molecular biology of poliovaccines. *The Journal of general virology 73 (Pt 12)*:3065-3077.

Modlin JF. 1995. Poliomyelitis and Poliovirus Immunization. In: Rotbart H, ed. *Human Enterovirus Infections*: ASM, Washington, DC.

Molla A, Paul AV, Wimmer E. 1991. Cell-free, de novo synthesis of poliovirus. *Science 254*:1647-1651.

Morasco BJ, Sharma N, Parilla J, Flanegan JB. 2003. Poliovirus cre(2C)-dependent synthesis of VPgpUpU is required for positive- but not negative-strand RNA synthesis. *Journal of virology 77*:5136-5144.

Morrison ME, Racaniello VR. 1992. Molecular cloning and expression of a murine homolog of the human poliovirus receptor gene. *Journal of virology 66*:2807-2813.

Morrow CD, Porter DC, Ansardi DC, Moldoveanu Z, Fultz PN. 1994. New approaches for mucosal vaccines for AIDS: encapsidation and serial passages of poliovirus replicons that express HIV-1 proteins on infection. *AIDS research and human retroviruses 10 Suppl 2*:S61-66.

Moscufo N, Chow M. 1992. Myristate-protein interactions in poliovirus: interactions of VP4 threonine 28 contribute to the structural conformation of assembly intermediates and the stability of assembled virions. *Journal of virology 66*:6849-6857.

Moscufo N, Simons J, Chow M. 1991. Myristoylation is important at multiple stages in poliovirus assembly. *Journal of virology 65*:2372-2380.

Murray KE, Barton DJ. 2003. Poliovirus CRE-dependent VPg uridylylation is required for positive-strand RNA synthesis but not for negative-strand RNA synthesis. *Journal of virology 77*:4739-4750.

Nayak A, Goodfellow IG, Belsham GJ. 2005. Factors required for the Uridylylation of the foot-and-mouth disease virus 3B1, 3B2, and 3B3 peptides by the RNA-dependent RNA polymerase (3Dpol) in vitro. *Journal of virology 79*:7698-7706.

Nicholson R, Pelletier J, Le SY, Sonenberg N. 1991. Structural and functional analysis of the ribosome landing pad of poliovirus type 2: in vivo translation studies. *Journal of virology 65*:5886-5894.

Nielsen PJ, McConkey EH. 1980. Evidence for control of protein synthesis in HeLa cells via the elongation rate. *Journal of cellular physiology 104*:269-281.

Nomoto A, Detjen B, Pozzatti R, Wimmer E. 1977a. The location of the polio genome protein in viral RNAs and its implication for RNA synthesis. *Nature 268*:208-213.

Nomoto A, Kitamura N, Golini F, Wimmer E. 1977b. The 5'-terminal structures of poliovirion RNA and poliovirus mRNA differ only in the genome-linked protein VPg. *Proceedings of the National Academy of Sciences of the United States of America 74*:5345-5349.

Novak JE, Kirkegaard K. 1991. Improved method for detecting poliovirus negative strands used to demonstrate specificity of positive-strand encapsidation and the ratio of positive to negative strands in infected cells. *Journal of virology 65*:3384-3387.

Nugent CI, Johnson KL, Sarnow P, Kirkegaard K. 1999. Functional coupling between replication and packaging of poliovirus replicon RNA. *Journal of virology 73*:427-435.

Nugent CI, Kirkegaard K. 1995. RNA binding properties of poliovirus subviral particles. *Journal of virology 69*:13-22.

Ohlmann T, Rau M, Pain VM, Morley SJ. 1996. The C-terminal domain of eukaryotic protein synthesis initiation factor (eIF) 4G is sufficient to support cap-independent translation in the absence of eIF4E. *The EMBO journal 15*:1371-1382.

Page GS, Mosser AG, Hogle JM, Filman DJ, Rueckert RR, Chow M. 1988. Three-dimensional structure of poliovirus serotype 1 neutralizing determinants. *Journal of virology 62*:1781-1794.

Parsley TB, Towner JS, Blyn LB, Ehrenfeld E, Semler BL. 1997. Poly (rC) binding protein 2 forms a ternary complex with the 5'-terminal sequences of poliovirus RNA and the viral 3CD proteinase. *RNA (New York, NY 3*:1124-1134.

Paul AV, Rieder E, Kim DW, van Boom JH, Wimmer E. 2000. Identification of an RNA hairpin in poliovirus RNA that serves as the primary template in the in vitro uridylylation of VPg. *Journal of virology 74*:10359-10370.

Paul AV, van Boom JH, Filippov D, Wimmer E. 1998. Protein-primed RNA synthesis by purified poliovirus RNA polymerase. *Nature 393*:280-284.

Paul AV, Yin J, Mugavero J, Rieder E, Liu Y, Wimmer E. 2003. A "slide-back" mechanism for the initiation of protein-primed RNA synthesis by the RNA polymerase of poliovirus. *The Journal of biological chemistry 278*:43951-43960.

Paul JR. 1971. *A History of Poliomyelitis.*: Yale University Press, New Haven, Conn.

Pause A, Methot N, Svitkin Y, Merrick WC, Sonenberg N. 1994. Dominant negative mutants of mammalian translation initiation factor eIF-4A define a critical role for eIF-4F in cap-dependent and cap-independent initiation of translation. *The EMBO journal 13*:1205-1215.

Pelletier J, Sonenberg N. 1988. Internal initiation of translation of eukaryotic mRNA directed by a sequence derived from poliovirus RNA. *Nature 334*:320-325.

Perez L, Carrasco L. 1993. Entry of poliovirus into cells does not require a low-pH step. *Journal of virology 67*:4543-4548.

Pestova TV, Hellen CU, Shatsky IN. 1996. Canonical eukaryotic initiation factors determine initiation of translation by internal ribosomal entry. *Molecular and cellular biology 16*:6859-6869.

Pfister T, Egger D, Bienz K. 1995. Poliovirus subviral particles associated with progeny RNA in the replication complex. *The Journal of general virology 76 (Pt 1)*:63-71.

Phillips BA, Emmert A. 1986. Modulation of the expression of poliovirus proteins in reticulocyte lysates. *Virology 148*:255-267.

Pilipenko EV, Blinov VM, Romanova LI, Sinyakov AN, Maslova SV, Agol VI. 1989. Conserved structural domains in the 5'-untranslated region of picornaviral genomes: an analysis of the segment controlling translation and neurovirulence. *Virology 168*:201-209.

Pilipenko EV, Gmyl AP, Maslova SV, Svitkin YV, Sinyakov AN, Agol VI. 1992a. Prokaryotic-like cis elements in the cap-independent internal initiation of translation on picornavirus RNA. *Cell 68*:119-131.

Pilipenko EV, Maslova SV, Sinyakov AN, Agol VI. 1992b. Towards identification of cis-acting elements involved in the replication of enterovirus and rhinovirus RNAs: a proposal for the existence of tRNA-like terminal structures. *Nucleic acids research 20*:1739-1745.

Pilipenko EV, Poperechny KV, Maslova SV, Melchers WJ, Slot HJ, Agol VI. 1996. Cis-element, oriR, involved in the initiation of (-) strand poliovirus RNA: a quasi-globular multi-domain RNA structure maintained by tertiary ('kissing') interactions. *The EMBO journal 15*:5428-5436.

Pincus SE, Wimmer E. 1986. Production of guanidine-resistant and -dependent poliovirus mutants from cloned cDNA: mutations in polypeptide 2C are directly responsible for altered guanidine sensitivity. *Journal of virology 60*:793-796.

Plotkin SA, A. Murdin, and E. Vidor. 1999. Inactivated polio vaccine. In: Plotkin S, W.A. Orenstein, ed. *Vaccines, 3rd ed.*: The W.B. Saunders Co., Philadelphia, Pa. pp 345-363.

Racaniello VR, Baltimore D. 1981a. Cloned poliovirus complementary DNA is infectious in mammalian cells. *Science 214*:916-919.

Racaniello VR, Baltimore D. 1981b. Molecular cloning of poliovirus cDNA and determination of the complete nucleotide sequence of the viral genome. *Proceedings of the National Academy of Sciences of the United States of America 78*:4887-4891.

Ren R, Racaniello VR. 1992. Human poliovirus receptor gene expression and poliovirus tissue tropism in transgenic mice. *Journal of virology 66*:296-304.

Ren RB, Costantini F, Gorgacz EJ, Lee JJ, Racaniello VR. 1990. Transgenic mice expressing a human poliovirus receptor: a new model for poliomyelitis. *Cell 63*:353-362.

Rieder E, Paul AV, Kim DW, van Boom JH, Wimmer E. 2000. Genetic and biochemical studies of poliovirus cis-acting replication element cre in relation to VPg uridylylation. *Journal of virology 74*:10371-10380.

Robertson ME, Seamons RA, Belsham GJ. 1999. A selection system for functional internal ribosome entry site (IRES) elements: analysis of the requirement for a conserved GNRA tetraloop in the encephalomyocarditis virus IRES. *RNA (New York, NY 5*:1167-1179.

Rodriguez PL, Carrasco L. 1993. Poliovirus protein 2C has ATPase and GTPase activities. *The Journal of biological chemistry 268*:8105-8110.

Rodriguez PL, Carrasco L. 1995. Poliovirus protein 2C contains two regions involved in RNA binding activity. *The Journal of biological chemistry 270*:10105-10112.

Roehl HH, Parsley TB, Ho TV, Semler BL. 1997. Processing of a cellular polypeptide by 3CD proteinase is required for poliovirus ribonucleoprotein complex formation. *Journal of virology 71*:578-585.

Roehl HH, Semler BL. 1995. Poliovirus infection enhances the formation of two ribonucleoprotein complexes at the 3' end of viral negative-strand RNA. *Journal of virology 69*:2954-2961.

Rubinstein SJ, Dasgupta A. 1989. Inhibition of rRNA synthesis by poliovirus: specific inactivation of transcription factors. *Journal of virology 63*:4689-4696.

Rubinstein SJ, Hammerle T, Wimmer E, Dasgupta A. 1992. Infection of HeLa cells with poliovirus results in modification of a complex that binds to the rRNA promoter. *Journal of virology 66*:3062-3068.

Rueckert RR. 1997. Picornaviridae: The Viruses and Their Replication. In: Fields B, D.M. Knipe, ed. *Virology*: Raven Press,New York. pp 609-654.

Sabin AB. 1955a. Characteristics and genetic potentialities of experimentally produced and naturally occurring variants of poliomyelitis virus. *Annals of the New York Academy of Sciences 61*:924-938; discussion, 938-929.

Sabin AB. 1955b. Immunity in poliomyelitis, with special reference to vaccination. *Monograph series 26*:297-334.

Sabin AB, Hennessen WA, Winsser J. 1954. Studies on variants of poliomyelitis virus. I. Experimental segregation and properties of avirulent variants of three immunologic types. *The Journal of experimental medicine 99*:551-576.

Salk JE. 1953a. Immunization against poliomyelitis. *Pediatric clinics of North America 1*:49-51.

Salk JE. 1953b. Recent studies on immunization against poliomyelitis. *Pediatrics 12*:471-482.

Salk JE. 1953c. Studies in human subjects on active immunization against poliomyelitis. I. A preliminary report of experiments in progress. *Journal of the American Medical Association 151*:1081-1098.

Sandoval IV, Carrasco L. 1997. Poliovirus infection and expression of the poliovirus protein 2B provoke the disassembly of the Golgi complex, the organelle target for the antipoliovirus drug Ro-090179. *Journal of virology 71*:4679-4693.

Sarnow P. 1989. Role of 3'-end sequences in infectivity of poliovirus transcripts made in vitro. *Journal of virology 63*:467-470.

Scheper GC, Voorma HO, Thomas AA. 1992. Eukaryotic initiation factors-4E and -4F stimulate 5' cap-dependent as well as internal initiation of protein synthesis. *The Journal of biological chemistry 267*:7269-7274.

Schlegel A, Giddings TH, Jr., Ladinsky MS, Kirkegaard K. 1996. Cellular origin and ultrastructure of membranes induced during poliovirus infection. *Journal of virology 70*:6576-6588.

Segall J, Matsui T, Roeder RG. 1980. Multiple factors are required for the accurate transcription of purified genes by RNA polymerase III. *The Journal of biological chemistry 255*:11986-11991.

Selinka HC, Zibert A, Wimmer E. 1991. Poliovirus can enter and infect mammalian cells by way of an intercellular adhesion molecule 1 pathway. *Proceedings of the National Academy of Sciences of the United States of America 88*:3598-3602.

Selinka HC, Zibert A, Wimmer E. 1992. A chimeric poliovirus/CD4 receptor confers susceptibility to poliovirus on mouse cells. *Journal of virology 66*:2523-2526.

Shafren DR, Bates RC, Agrez MV, Herd RL, Burns GF, Barry RD. 1995. Coxsackieviruses B1, B3, and B5 use decay accelerating factor as a receptor for cell attachment. *Journal of virology 69*:3873-3877.

Sharma N, O'Donnell BJ, Flanegan JB. 2005. 3'-Terminal sequence in poliovirus negative-strand templates is the primary cis-acting element required for VPgpUpU-primed positive-strand initiation. *Journal of virology 79*:3565-3577.

Shen Y, Igo M, Yalamanchili P, Berk AJ, Dasgupta A. 1996. DNA binding domain and subunit interactions of transcription factor IIIC revealed by dissection with poliovirus 3C protease. *Molecular and cellular biology 16*:4163-4171.

Shiroki K, Ishii T, Aoki T, Ota Y, Yang WX, Komatsu T, Ami Y, Arita M, Abe S, Hashizume S, Nomoto A. 1997. Host range phenotype induced by mutations in the internal ribosomal entry site of poliovirus RNA. *Journal of virology 71*:1-8.

Silvera D, Gamarnik AV, Andino R. 1999. The N-terminal K homology domain of the poly(rC)-binding protein is a major determinant for binding to the poliovirus 5'-untranslated region and acts as an inhibitor of viral translation. *The Journal of biological chemistry 274*:38163-38170.

Simoes EA, Sarnow P. 1991. An RNA hairpin at the extreme 5' end of the poliovirus RNA genome modulates viral translation in human cells. *Journal of virology 65*:913-921.

Skinner MA, Racaniello VR, Dunn G, Cooper J, Minor PD, Almond JW. 1989. New model for the secondary structure of the 5' non-coding RNA of poliovirus is supported by biochemical and genetic data that also show that RNA secondary structure is important in neurovirulence. *Journal of molecular biology 207*:379-392.

Sokolowski M, Schwartz S. 2001. Heterogeneous nuclear ribonucleoprotein C binds exclusively to the functionally important UUUUU-motifs in the human papillomavirus type-1 AU-rich inhibitory element. *Virus research 73*:163-175.

Sonenberg N. 1990. Poliovirus translation. *Current topics in microbiology and immunology 161*:23-47.

Sonenberg N. 1996. mRNA 5'cap-binding protein eIF4E and control of cell growth. In: JWB. Hershey MM, N. Sonenberg, ed. *Translational Control*. Plainview, N.Y.: Cold Spring Harbor Laboratory Press. pp 245-269.

Spagnolo JF, Hogue BG. 2000. Host protein interactions with the 3' end of bovine coronavirus RNA and the requirement of the poly(A) tail for coronavirus defective genome replication. *Journal of virology 74*:5053-5065.

Spector DH, Baltimore D. 1974. Requirement of 3'-terminal poly(adenylic acid) for the infectivity of poliovirus RNA. *Proceedings of the National Academy of Sciences of the United States of America 71*:2983-2987.

Stanway G, Tapani Hovi, Nick J. Knowles, Timo Hyypia. 2002. Molecular and Biological Basis of Picornavirus Taxonomy. In: Semler B, E. Wimmer, ed. *Molecular Biology of Picornaviruses*. Washington, DC: ASM Press. pp 17-24.

Summers DF, Maizel JV, Jr. 1968. Evidence for large precursor proteins in poliovirus synthesis. *Proceedings of the National Academy of Sciences of the United States of America 59*:966-971.

Sun XH, Baltimore D. 1989. Human immunodeficiency virus tat-activated expression of poliovirus protein 2A inhibits mRNA translation. *Proceedings of the National Academy of Sciences of the United States of America 86*:2143-2146.

Sutter RW, S.L. Cochi, and J.L. Melnick. 1999. Live attenuated poliovirus vaccine. In: Plotkin SA, W.A. Orenstein, ed. *Vaccines, 3rd ed.* : The W.B. Saunders Co., Philadelphia, Pa. pp 364-408.

Svitkin YV, Meerovitch K, Lee HS, Dholakia JN, Kenan DJ, Agol VI, Sonenberg N. 1994. Internal translation initiation on poliovirus RNA: further characterization of La function in poliovirus translation in vitro. *Journal of virology 68*:1544-1550.

Teterina NL, Kean KM, Gorbalenya AE, Agol VI, Girard M. 1992. Analysis of the functional significance of amino acid residues in the putative NTP-binding pattern of the poliovirus 2C protein. *The Journal of general virology 73 (Pt 8)*:1977-1986.

Todd S, Towner JS, Brown DM, Semler BL. 1997. Replication-competent picornaviruses with complete genomic RNA 3' noncoding region deletions. *Journal of virology 71*:8868-8874.

Towner JS, Ho TV, Semler BL. 1996. Determinants of membrane association for poliovirus protein 3AB. *The Journal of biological chemistry 271*:26810-26818.

Toyoda H, Nicklin MJ, Murray MG, Anderson CW, Dunn JJ, Studier FW, Wimmer E. 1986. A second virus-encoded proteinase involved in proteolytic processing of poliovirus polyprotein. *Cell 45*:761-770.

Troxler M, Egger D, Pfister T, Bienz K. 1992. Intracellular localization of poliovirus RNA by in situ hybridization at the ultrastructural level using single-stranded riboprobes. *Virology 191*:687-697.

van der Werf S, Bradley J, Wimmer E, Studier FW, Dunn JJ. 1986. Synthesis of infectious poliovirus RNA by purified T7 RNA polymerase. *Proceedings of the National Academy of Sciences of the United States of America 83*:2330-2334.

van Kuppeveld FJ, Galama JM, Zoll J, Melchers WJ. 1995. Genetic analysis of a hydrophobic domain of coxsackie B3 virus protein 2B: a moderate degree of hydrophobicity is required for a cis-acting function in viral RNA synthesis. *Journal of virology 69*:7782-7790.

Vance LM, Moscufo N, Chow M, Heinz BA. 1997. Poliovirus 2C region functions during encapsidation of viral RNA. *Journal of virology 71*:8759-8765.

Weidman MK, Yalamanchili P, Ng B, Tsai W, Dasgupta A. 2001. Poliovirus 3C protease-mediated degradation of transcriptional activator p53 requires a cellular activity. *Virology 291*:260-271.

Wessels E, Duijsings D, Niu TK, Neumann S, Oorschot VM, de Lange F, Lanke KH, Klumperman J, Henke A, Jackson CL, Melchers WJ, van Kuppeveld FJ. 2006. A viral protein that blocks Arf1-mediated COP-I assembly by inhibiting the guanine nucleotide exchange factor GBF1. *Developmental cell 11*:191-201.

Wimmer E. 1982. Genome-linked proteins of viruses. *Cell 28*:199-201.

Wimmer E, Hellen CU, Cao X. 1993. Genetics of poliovirus. *Annual review of genetics 27*:353-436.

Witwer C, Rauscher S, Hofacker IL, Stadler PF. 2001. Conserved RNA secondary structures in Picornaviridae genomes. *Nucleic acids research 29*:5079-5089.

World Health Organization. 2002. Progress towards the global eradication of poliomyelitis, 2001. . *Wkly. Epidemiol. Rec.* pp 98-107.

Xiang W, Cuconati A, Hope D, Kirkegaard K, Wimmer E. 1998. Complete protein linkage map of poliovirus P3 proteins: interaction of polymerase 3Dpol with VPg and with genetic variants of 3AB. *Journal of virology 72*:6732-6741.

Xiang W, Harris KS, Alexander L, Wimmer E. 1995. Interaction between the 5'-terminal cloverleaf and 3AB/3CDpro of poliovirus is essential for RNA replication. *Journal of virology 69*:3658-3667.

Yalamanchili P, Banerjee R, Dasgupta A. 1997a. Poliovirus-encoded protease 2APro cleaves the TATA-binding protein but does not inhibit host cell RNA polymerase II transcription in vitro. *Journal of virology 71*:6881-6886.

Yalamanchili P, Datta U, Dasgupta A. 1997b. Inhibition of host cell transcription by poliovirus: cleavage of transcription factor CREB by poliovirus-encoded protease 3Cpro. *Journal of virology 71*:1220-1226.

Yalamanchili P, Harris K, Wimmer E, Dasgupta A. 1996. Inhibition of basal transcription by poliovirus: a virus- encoded protease (3Cpro) inhibits formation of TBP-TATA box complex in vitro. *Journal of virology 70*:2922-2929.

Yalamanchili P, Weidman K, Dasgupta A. 1997c. Cleavage of transcriptional activator Oct-1 by poliovirus encoded protease 3Cpro. *Virology 239*:176-185.

Yang Y, Rijnbrand R, McKnight KL, Wimmer E, Paul A, Martin A, Lemon SM. 2002. Sequence requirements for viral RNA replication and VPg uridylylation directed by the internal cis-acting replication element (cre) of human rhinovirus type 14. *Journal of virology 76*:7485-7494.

Yin J, Paul AV, Wimmer E, Rieder E. 2003. Functional dissection of a poliovirus cis-acting replication element [PV-cre(2C)]: analysis of single- and dual-cre viral genomes and proteins that bind specifically to PV-cre RNA. *Journal of virology 77*:5152-5166.

Yogo Y, Wimmer E. 1972. Polyadenylic acid at the 3'-terminus of poliovirus RNA. *Proceedings of the National Academy of Sciences of the United States of America 69*:1877-1882.

Zawel L, Reinberg D. 1992. Advances in RNA polymerase II transcription. *Current opinion in cell biology 4*:488-495.

Zell R, Sidigi K, Bucci E, Stelzner A, Gorlach M. 2002. Determinants of the recognition of enteroviral cloverleaf RNA by coxsackievirus B3 proteinase 3C. *RNA (New York, NY 8*:188-201.

Zell R, Sidigi K, Henke A, Schmidt-Brauns J, Hoey E, Martin S, Stelzner A. 1999. Functional features of the bovine enterovirus 5'-non-translated region. *The Journal of general virology 80 (Pt 9)*:2299-2309.

Zell R, Stelzner A. 1997. Application of genome sequence information to the classification of bovine enteroviruses: the importance of 5'- and 3'-nontranslated regions. *Virus research 51*:213-229.

Zuker M, Mathews, DH., Turner, DH. 1999. Algorithms and thermodynamics for RNA secondary structure prediction: a practical guide. . In: Barciszewski J, Clark, BFC., ed. *RNA Biochemistry and Biotechnology*: Dordrecht: Kluwer. pp 11-43.

7. Publications / Abstracts

Dorothee Alatorre publishes under the name **Dorothee A. Vogt**.

Publications:

- van Ooij, M.J., **Vogt, D.A.**, Paul, A., Castro, C., Kuijpers, J., van Kuppeveld, F.J., Cameron, C.E., Wimmer, E., Andino, R. and Melchers, W.J. (2006) Structural and functional characterization of the coxsackievirus B3 CRE(2C): role of CRE(2C) in negative- and positive-strand RNA synthesis. *J Gen Virol*, **87:**103-113

- **Vogt, D.A.** & Andino, R. (2007) A ternary complex functions as a promoter for both negative- and positive-strand RNA synthesis in poliovirus. Manuscript in preparation.

Abstracts:

- **Vogt, D.A.** & R. Andino, The cloverleaf functions as a promoter for positive-strand RNA synthesis in poliovirus. July 17, 2006, 25th Annual Meeting of the American Society for Virology, Madison, Wisconsin, Oral presentation

- **Vogt, D.A.** & R. Andino, Determinants of Positive-Strand RNA synthesis in Poliovirus. , May 29, 2007, The Eighth Symposium on Positive-Strand RNA Viruses, Washington, DC, Poster